



Universität  
Bremen



**UNIS**  
The University Centre in Svalbard

# **Identification of key environmental drivers influencing macroalgal communities in high Arctic fjord coastal ecosystems**

**Master thesis submitted in fulfilment of the requirements for obtaining  
the degree of Master of Science (M.Sc.)**

Conducted at the department for **Arctic Biology**  
at the **University Centre in Svalbard (UNIS)**

&

the working group for **Marine Botany**  
at the **University of Bremen**  
(Faculty 02 – Biology/Chemistry)

Submitted by

**Milan Beck**

1st Supervisor: **Børge Damsgård, Professor for Marine Biology**  
(University Centre in Svalbard)

2nd Supervisor: **Kai Bischof, Professor for Marine Botany**  
(University of Bremen)

The following declarations are to be included in every exemplar of the Bachelor's and Master's Thesis

Name: MILAN BECK

Enrolment number: 4228311

#### Declaration of copyright

Hereby I declare that my Master's Thesis was written without external support and that I did not use any other sources and auxiliary means than those quoted. All statements which are literally or analogously taken from other publications have been identified as quotations.

Date: 11.03.2022

Signature 

#### Declaration with regard to publishing theses

Two years after the final degree, the thesis will be submitted to the University of Bremen archive and stored there permanently.

Storage includes:


- 1) Master's Theses with a local or regional reference, as well as 10 % of all theses from every subject and year
- 2) Bachelor's Theses: The first and last Bachelor degrees from every subject and year

I agree that for research purposes third parties can look into my thesis stored in the University archive.

I agree that for research purposes third parties can look into my thesis stored in the University archive after a period of 30 years (in line with §7 para. 2 BremArchivG).

I do not agree that for research purposes third parties can look into my thesis stored in the University archive.

Date: 11.03.2022

Signature 

# I. Table of Contents

1 Introduction.....	1
1.1 Role of High Arctic Fjord Ecosystems.....	1
1.2 Role of Macroalgal Communities in High Arctic Fjord Ecosystems.....	1
1.3 Effects of Climate Change on Arctic Coastal Ecosystems and Macroalgal Communities.....	3
1.4 Objectives and Justification of Study.....	6
2 Material and Methods.....	7
2.1 Study Site.....	7
2.2 Sampling Equipment.....	9
2.2.1 Unmanned Surface Vehicle.....	9
2.2.2 Split Beam Echosounder.....	10
2.2.3 Underwater Camera.....	11
2.2.4 CTD.....	12
2.3 Preliminary Measurements.....	14
2.4 Station Selection Process.....	14
2.5 Station Design.....	17
2.6 Station Work.....	18
2.6.1 Measurement of Sea Floor Bathymetry.....	18
2.6.2 Sea-Ice Station – ICE.....	21
2.6.3 Freshwater Station – FRE.....	22
2.6.4 Glacier Station – GLA.....	23
2.6.5 Measurement of Proximate Drivers.....	24
2.6.6 Measurement of Macroalgae.....	25
2.7 Data Management and Post-processing.....	27
2.7.1 Manual Editing of Echograms.....	27
2.7.2 Adjustments for Tides and Echosounder Depth.....	28
2.7.3 Statistical Analysis.....	29
3 Results.....	31
3.1 Differences in Plant Coverage between stations.....	31
3.2 Macroalgal Coverage per Depth and Station.....	32
3.3 Effect of Environmental Parameters on Macroalgal coverage.....	40
4 Discussion.....	43
4.1 Differences in Plant Coverage Between Stations.....	43
4.2 Macroalgal Coverage per Depth and Station.....	44
4.3 Effect of Environmental Parameters on Macroalgal Coverage.....	46
4.4 Conclusion.....	50
5 Acknowledgements.....	51
6 References.....	52
7 Appendix.....	58

## II. Tables

Table 1: SWIFT CTD Sensor characteristics.....	13
Table 2: CTD tide adjustment table.....	28
Table 3: Mean values for plant coverage per station.....	32
Table 4: Mean values for plant coverage per station and depth bin.....	33
Table 5: Spearman correlation results for the environmental parameters.....	40
Table 6: Anova results for plant coverage and parameter models.....	41
Table 7: Station selection segment with respective ranges for turbidity [NTU] and salinity [PSU]..	52
Table 8: Bottom depth grid report statistics.....	58
Table 8: Bottom depth grid report statistics from Visual Aquatics for each station.....	58
Table 9: Temperature, salinity, turbidity and plant coverage mean values, standard deviations and standard errors for every station and depth bin.....	59
Table 10: Tide predictions for the sea-ice station.....	67
Table 11: Tide predictions for the freshwater station.....	68
Table 12: Tide predictions for the glacier station.....	69
Table 13: Underwater camera validation table.....	72

### III. Figures

Figure 1: Topographic map of Svalbard. B) Satellite image of Billefjorden.....	8
Figure 2: Otter USV in the field in Billefjorden .....	9
Figure 3: Paralenz drop locations .....	11
Figure 4: Validation of the echosounder via drop camera samplings.....	12
Figure 5: Data transects from the preliminary bathymetric and CTD survey in Billefjorden.....	15
Figure 6: Location and GPS coordinates of sampling stations in Billefjorden.....	16
Figure 7: Schematic drawing of the general station design.....	17
Figure 8: Exemplary cross-hatched transect pattern for a station.....	18
Figure 9: Bottom detection settings for the post-processing of the echosounder data.....	19
Figure 10: Bathymetric sea-ice station grid.....	21
Figure 11: Bathymetric freshwater station grid.....	22
Figure 12: Bathymetric glacier station grid.....	23
Figure 13: Plant detection algorithm analysis parameters in Visual Aquatics.....	25
Figure 14: Parameter settings for the inverse distance weighting gridding method.....	26
Figure 15: Overall differences in plant coverage for the different sampling stations.....	31
Figure 16: Depth dependent plant coverage per station.....	32
Figure 17: Plant coverage at the sea-ice station (ICE) for the 5 depth bins.....	34
Figure 18: Plant coverage at the glacier station (GLA) for the 5 depth bins.....	35
Figure 19: Plant coverage at the freshwater station (FRE) for the 5 depth bins.....	36
Figure 20: Gridded plant coverage data for the freshwater station.....	37
Figure 21: Gridded plant coverage data for the sea-ice station.....	38
Figure 22: Gridded plant coverage data for the glacier station.....	39
Figure 23: GLM for the plant coverage in relation to temperature at the glacier station.....	41
Figure 24: GLM for the plant coverage in relation to temperature at the freshwater station.....	42
Figure 25: Rank of monthly sea-ice extent on Svalbard.....	58
Figure 27: Sea-ice chart for Isfjorden from the 15 January, 2021.....	59
Figure 28: Sea-ice chart for Isfjorden from the 15 February, 2021.....	60
Figure 29: Sea-ice chart for Isfjorden from the 15 March, 2021.....	61
Figure 30: Sea-ice chart for Isfjorden from the 15 April, 2021.....	62
Figure 31: Sea-ice chart for Isfjorden from the 14 May, 2021.....	63
Figure 32: Example for manual editing of the "crash-signal" of the echogram.....	67
Figure 33: Echogram example for false bottom and plant detection .....	68
Figure 34: Glacier fronts in 2020 and 2017 at the glacier station.....	70

## IV. Abbreviations

SBES	–	Split beam echosounder
USV	–	Unmanned surface vehicle
LIA	–	Little ice age
GLA	–	Glacier station
FRE	–	Freshwater station
ICE	–	Sea-ice station
VCS	–	Vehicle control station
LOS	–	Line of sight
SOG	–	Speed over ground
PC	–	Plant coverage
TVG	–	Time varied gain
IDW	–	Inverse distance weighting
LAT	–	Lowest astronomical tide
GLM	–	Generalized linear model

## Summary

Many Arctic coastal habitats such as kelp communities function as important hotspots for biodiversity by providing a stable food source, secondary settling substrate, shelter from wave action or nursing grounds for a plethora of different invertebrate and vertebrate species. Arctic environments are among the most affected by climate change in particular because of the rapid decline in its cryosphere due to global warming. Those changes include an increase in water temperature, precipitation, glacial melting rates, Arctic river discharge and sedimentation. This predicament emphasizes the need to study and predict the role of involved environmental parameters driving the systemic change in these regions. This will be essential to develop sustainable conservation and management plans for these endangered ecosystems. As part of the EU project FACE-IT, this study aimed at mapping the bathymetry and macroalgal distribution patterns of three distinct coastal stations in Billefjorden (Svalbard) while putting them into context with regional environmental differences in water temperature, salinity and turbidity. To study these spatial differences, sampling stations were established in front of the sea-terminating glacier in Adolfbukta (GLA), in Petuniabukta with high amounts of freshwater input (FRE) and near Kapp Scott with irregular winter sea-ice cover and little freshwater input (ICE). An unmanned surface vehicle (USV) equipped with an autonomous echosounder system and a CTD probe were used to assess plant coverage (PC) and the environmental conditions along a depth range of 5-30 metres. In decreasing order, macroalgal coverage was highest at the glacier (21.96%), sea-ice (9.54%) and freshwater station (0.64%). While no clear upper and lower distribution limits for macroalgae could be identified, statistically significant, positive relationships have been revealed for PC at the freshwater station and salinity ( $p < 3.817e-06$ ) as well as the glacier station and temperature ( $p < 2.07e-09$ ). Plant coverage at the ICE station did not exhibit any significant trends with respect to the same abiotic factors. Because measurements of the parameters were only covering a “snapshot” of the environmental conditions and macroalgal communities integrate changes of these parameters over time, ecological implications of these findings had to be made with care. However, distinct environmental differences between the stations seemed to be reflected by the strong differences in plant coverage, hinting at the negative effects of elevated sedimentation rates at the FRE station and positive effects of new potential settling substrates at the GLA station due to a recent landward retreat of the glacier. This study contributed to a better understanding of the links between environmental drivers and macroalgal communities. More research and validation of the results is needed in order to validate the echosounder data especially at greater depth (>20 m).

# 1 Introduction

## 1.1 Role of High Arctic Fjord Ecosystems

High Arctic fjords can be described as dynamic and highly stratified bodies of water connecting cold freshwater masses at the surface (originating from riverbeds or sea terminating glaciers) with the warm saline Atlantic waters typically entering the fjords at depths >200 m (Straneo *et al.*, 2012). The mixing of different water masses results in an exchange of heat, salt and nutrients creating complex spatial gradients (Mortensen *et al.*, 2014; Straneo & Cenedese, 2015). The calving and melting of sea terminating glaciers plays an important role in the buoyancy driven exchange between coastal shelf and glacial waters (Carroll *et al.*, 2015; Jackson *et al.*, 2017). The accompanying spatial modulation of parameters like salinity, turbidity and temperature can have a strong influence on marine productivity (Hopwood *et al.*, 2020; Meire *et al.*, 2016).

The high particle load of glacially discharged waters can for example result in an increased light attenuation and decrease in photosynthetically active radiation (PAR) throughout the water column (Lydersen *et al.*, 2014; Murray *et al.*, 2015). This in turn would affect the photosynthetic efficiency of associated algal communities. The higher particle concentration can also result in an increase in bioavailable macronutrients like nitrate, phosphate, iron or silicic acid with a potentially boosting effect on primary production in spring and summer (Chu *et al.*, 2012; Hopwood *et al.*, 2020). In contrast to Antarctic waters, where  $\text{Fe}^{2+}$  is the most limiting nutrient for primary production, Arctic primary producers are more limited by nitrate availability (Hopwood *et al.*, 2020).

To what extent this modulation takes place on a spatial and temporal scale is highly variable and dependent on fjord geometry as well as seasonal meteorological changes. Those changes include winter sea-ice cover, glacial discharge rates (e.g. through calving, abrasion or melting) as well as frequency and direction of katabatic winds (Hopwood *et al.*, 2020).

## 1.2 Role of Macroalgal Communities in High Arctic Fjord Ecosystems

Many Arctic ecosystems function as important refuges for biodiversity, that contribute to the establishment of diverse food webs, by providing a stable food source, secondary settling substrate, shelter from wave action or nursing grounds for a plethora of different invertebrate and vertebrate species (Hop *et al.*, 2016). Macroalgal communities, like those of the order Laminariales, form abundant Arctic habitats in the littoral to sublittoral fjord regions in Svalbard and entail all of these ecosystem functions (Al-Habahbeh *et al.*, 2020; Fredriksen *et al.*, 2015). Some of the most



frequently occurring species in Svalbard are *Saccharina latissima*, *Alaria esculenta* and “digitate kelps” (Filbee-Dexter *et al.*, 2019; Fredriksen & Kile, 2012). The latter term includes *Laminaria digitata* and *Hedophyllum nigripes*, which have recently been described as having the same phenotype (Dankworth *et al.*, 2020). These seaweeds typically settle on hard rocky substrates but can also adhere to glacial drop stones in otherwise soft bottom areas. They are perennial and capable of high biomass production, which can result in the formation of large macroalgal canopies (Steneck *et al.*, 2002).

In general about 193 marine macroalgal species have been described all around Svalbard, with 88 taxa found in Isfjorden alone (Fredriksen *et al.*, 2015). The zonation patterns of macroalgae along a coastal depth gradient is relatively well described for Svalbard, in particular Kongsfjorden (Wulff *et al.*, 2009). The intertidal is typically dominated by small brown (e.g. *Fucus distichus*.) and green algae (e.g. *Ulothrix spp.*). Beneath 2 m water depth, the number of species increases whereas the community between ca. 5 and 15 m is mainly dominated by kelp species. A relatively recent study in Kongsfjorden from 2017 showed, that kelp communities were especially dense within this depth region (Kruss *et al.*, 2017). Below that, a transition into more crustose red algae usually takes place.

Macroalgae are important primary producers and constitute to the oceanic blue carbon sink by fixating an estimated annual amount of 173 TgC (teragrams of carbon) world wide. This even exceeds estimated values for sequestration of carbon by angiosperms (111-131 TgC yr<sup>-1</sup>) (Bischof *et al.*, 2019; Krause-Jensen & Duarte, 2016). The fjord sediments in Svalbard are also supplied with macroalgal detritus as a primary source for organic matter (Zaborska *et al.*, 2018).

Biomass production of macroalgal communities is primarily governed by the availability of nitrate and light in the Arctic spring and summer months (Steneck *et al.*, 2002). Changing environmental factors like water temperature, salinity, the light regime and nutrient availability can have a direct impact on the growth and germination of different developmental stages and, thus, the spatial distribution of macroalgae (Bischof *et al.*, 2019). These effects are often species specific and depend on their respective regulatory and adaptive capacities to cope with dynamic environments (Bischof *et al.*, 2019; Karsten, 2007; Li *et al.*, 2020).

Combined with the high abundance of macroalgal species and their sedentary life style, they become valuable indicators of environmental change since they integrate the involved abiotic factors over time (Fredriksen *et al.*, 2015; Fredriksen & Kile, 2012).

### **1.3 Effects of Climate Change on Arctic Coastal Ecosystems and Macroalgal Communities**

Arctic coastal ecosystems are among the most affected areas by anthropogenic climate change when it comes to the effects of increasing air temperature and changing Arctic hydroclimatology (Box *et al.*, 2019; Pörtner *et al.*, 2019). Those changes include an increase in precipitation, glacial melting rates, river discharge and sedimentation (Bring *et al.*, 2016; Østby *et al.*, 2017; Rawlins *et al.*, 2010).

The decline in the cryosphere due to the rapid atmospheric warming of the oceans introduces a multitude of drivers, that have the potential to modify ecosystem functioning and biodiversity in littoral fjord areas and associated communities. These drivers comprise biogeochemical parameters like salinity, nutrients, turbidity and photosynthetically active radiation (PAR), which are all modulated temporally and spatially by the enhanced melting of sea-terminating glaciers and the steady decline in winter sea-ice formation. This makes studying the effects of those parameters especially important in order to document and predict changes in high Arctic communities.

Arctic sea-ice exhibited significant decreases in cover area, thickness, spatial distribution and temporal stability (Box *et al.*, 2019). A trend from perennial thick sea-ice cover to thinner ice sheets and longer open water periods could be observed (Comiso, 2002). Land ice masses began decreasing since the 1980s, corresponding strongly with increased precipitation and regional temperature rises. In particular for sea-terminating glaciers, this means, that by the end of this century, changes in fjord biogeochemistry are expected due to a steady retreat from water to land (Hopwood *et al.*, 2020). The overall decrease in sea-ice cover is also accompanied by a decrease in surface albedo, subsequently speeding up ocean warming in the Arctic even more (Box *et al.*, 2019). This effect is called the "ice albedo feedback".

It is not entirely clear how macroalgal distribution and community composition will react to this ecological development in the long run, especially since relatively little information is available on the actual spatial abundance patterns of macroalgae in the inner fjord systems of Svalbard. However, certain observations and assumptions based on their ecophysiology can still be made.

For example, since river and glacial discharge can increase sedimentation, an increase in algal biomass production could be the result of higher concentrations of dissolved bioavailable nutrients like nitrate. Conversely, the increased sediment load in the water column creates potentially unfavourable light regimes and reduced PAR (Hanelt *et al.*, 2001; Ronowicz *et al.*, 2020). This can cause a shift of the upper and lower depth distribution limits for macroalgae.

Another important aspect is the ongoing transition of sea-terminating or tidewater into land-terminating glaciers (Dowdeswell *et al.*, 1997; Hagen & Liestol, 1990). Tidewater glaciers play an important role in shaping the Arctic ecosystem dynamics and constitute an important food source for higher marine animals (e.g. mammals, seabirds) (Lydersen *et al.*, 2014).

A strong estuarine circulation fuelled by subsurface freshwater discharge modulates the environment in front of the glacier (Lydersen *et al.*, 2014). These currents can carry plankton and nutrient loaded sediments up to the surface waters and, therefore, build the basis for a diverse food web. The landward retreat of glaciers in Svalbard is most likely going to change these dynamics. The mixing of the vertical water column will decrease and stratification will increase, which in turn affects the fjords biogeochemistry (Torsvik *et al.*, 2019). These changing environmental framework conditions could also influence macroalgal distribution due to changes in the extent of the euphotic zone, salinity and sediment load.

The glacial landward retreat also means, that new substrate for settlement will be uncovered, potentially expanding the physical distribution limits for macroalgae. The decrease in littoral mechanical disturbances, due to less sea-ice scouring, poses a possibility for the establishment of novel intertidal macroalgal communities. In some regions of Isfjorden, Svalbard, a threefold increase in littoral macrophyte biomass within a 20 year time window (1988-2008) has already been recorded (Fredriksen *et al.*, 2015; Weslawski *et al.*, 2010). The shrinking period of annual sea-ice cover also widens the seasonal time window in which photosynthesis can effectively be conducted by primary producing organisms. This means that less sea-ice scouring and cover leads to increased production by macroalgae in some places in the Arctic (Al-Habahbeh *et al.*, 2020; Bartsch *et al.*, 2016; Ingvaldsen *et al.*, 2021; Krause-Jensen *et al.*, 2020).

The freshening of coastal waters via increased glacial and river run-off can also lead to overall lower levels of salinity. Since the Arctic is subject to high fluctuations in freshwater influx as a result of seasonal melting during the summer months, many species need to be adapted accordingly. While some algae species like *F. distichus* seem to have high tolerances for hyposaline conditions, other kelp species like *A. esculenta*, *S. latissima* and *L. solidungula* were shown to exhibit signs of stress in the form strong bleaching or loss of pigments (Karsten, 2007).

Climate change has contributed to an anomalously high inflow of Atlantic water masses to the Arctic Ocean. Besides the invasion of temperate species into Arctic ecosystems and the consequent modification of the Arctic food chain, there are a number of physical and ecological changes arising from this “Atlantification” (Assis *et al.*, 2016; Ingvaldsen *et al.*, 2021). The warm Atlantic currents

lead to a decrease in ocean sea-ice, which results in a less stratified water column. This is due to a more effective heat exchange between ocean and air leading to a weakening of the Arctic halocline (Ingvaldsen *et al.*, 2021). Positive feedback mechanisms like the melting of sea-ice are predicted to increase even further in the future (Ingvaldsen *et al.*, 2021). The reduction of the sea-ice coverage, warming waters and enhanced upper ocean mixing are driving a systemic change in the Arctic Ocean environment. Some of those changes can be observed through an increasingly connected food web and increased primary production in coastal zones due to a decrease in ice coverage and scouring (Ingvaldsen *et al.*, 2021).

## 1.4 Objectives and Justification of Study

To come up with effective management plans and accurately assess the effects of climate change on the ecosystem and community level in the Arctic, it is crucial to identify the relevant drivers of this change and their spatial and seasonal characteristics. At the same time, there still exists a significant gap in our knowledge with regards to how the environmental drivers affect macroalgal communities in coastal fjord ecosystems in a rapidly changing Arctic environment. Monitoring the spatial abundance, biomass and distribution of macroalgae can help to identify these proximate drivers of climate change and infer their effects on a temporal and spatial scale.

The following research questions were formulated in order to guide our fieldwork and shed light on the interactions between drivers and macroalgal distribution along the coast of a remote Arctic fjord in Svalbard.

### 1. How is macroalgae coverage affected by proximity to glaciers and riverbeds?

Hypothesis: We expect that macroalgae coverage will decrease with increasing proximity to sea-terminating glaciers and river deltas, mainly because of increased turbidity and subsequently lower amount of light in the water column, lower salinity and/or more frequent mechanical disturbances through ice scouring.

### 2. How is macroalgal depth distribution affected by proximity to glaciers and riverbeds?

Hypothesis: Macroalgae may exhibit a shallower depth distribution in areas with increased turbidity accounting for the increased light attenuation in the water column. On the other hand, areas affected less by turbidity but still within range of glacial nutrient upwelling plumes, could show an increase in biomass and macroalgal abundance, caused by elevated nutrient levels.

### 3. Which effects do the involved environmental parameters (temperature, salinity, turbidity) have on Arctic fjord coastal macroalgal communities?

Hypothesis: We expect, that all three variables have the potential to change depth distribution, coverage and even plant volume or biomass of macroalgae. It is unclear whether those effects can be observed and/or whether multiple variables might have a combined effect, which would make it difficult to isolate the individual cause and effect relationship between the drivers and macroalgal parameters.

## 2 Material and Methods

The spatial analysis included three sampling stations, subject to different degrees of winter sea-ice cover and freshwater input by rivers or the influence of a sea-terminating glacier. Each station represented distinct developmental stages and combinations of environmental parameters. The respective macroalgal distribution was monitored mainly by bio acoustic split-beam echosounder (SBES) measurements with the help of an unmanned surface vehicle (USV). Parallel underwater video footage served for validation of the echosounder plant detection algorithms and helped to gain a better overview of the stations' underwater characteristics. A CTD probe was used to identify differences between environmental factors in the water column for each station at different depths.

The data gathering included nine full days in the field taking place mainly during the summer of 2021 between 21 July and 20 October.

### 2.1 Study Site

As the inner central branch of Isfjorden, Billefjorden is located in the Norwegian archipelago of Svalbard between about 78.75° and 78.35°N, and between 15.90° and 17°E. Billefjorden is 32 km long and 5-8 km wide and has several glacial and river input sites but only one sea-terminating glacier in Adolfbukta called Nordenskiöldbreen (Fig. 1). Nordenskiöldbreen currently exhibits annual retreating rates of 12-35 m yr<sup>-1</sup> (Rachlewicz *et al.*, 2007; Szczuciński *et al.*, 2009). Petuniabukta lies in the northwestern end of the fjord and has a high amount of freshwater input sites due to the surrounding valley glaciers and mountains (Láska *et al.*, 2012). The fjords depth ranges from approximately 50 to 200 m at the deepest point and possesses a sill at the entrance of fjord. Warm Atlantic water masses enter the fjord via offshoots of the West Spitsbergen current. The annual mean temperature lies at about -6°C and has increased by approximately 4 °C since the end of the little ice age (LIA) circa 170 years ago. Temperature maxima of 6.5 to 8.5 °C occur between July and August. Winter sea-ice formation usually starts in November and lasts until July. Precipitation in this region is low with 200 mm yr<sup>-1</sup> but already increased by 2.5 % per decade since the end of the LIA and is still expected to rise in the future (Førland & Hanssen-Bauer, 2003; Rachlewicz *et al.*, 2007).

To test our hypotheses, three different stations with varying environmental framework conditions have been selected in Billefjorden (Fig. 6):

- Glacier station (**GLA**): a station where the littoral zone is affected by a sea-terminating glacier. This is not directly in front of the glaciers calving site, but in an area with close proximity to it, where the glacier has recently receded from (Fig. 12).
- Freshwater station (**FRE**): a station where the littoral zone has not been affected by a glacier in recent times but is affected by freshwater and sedimentation via river inputs (Fig. 11).
- Sea-ice station (**ICE**): a station where the littoral zone is influenced by irregular, winter sea-ice formation. The effects of glaciers and river deltas should be low here (Fig. 10).



**Figure 1:** A) Topographic map of Svalbard. B) Satellite image of Billefjorden. PT – Petuniabukta; AD – Adolfbukta; NB – Nordenskiöldbreen (Source: Norwegian Polar Institute)

## 2.2 Sampling Equipment

### 2.2.1 Unmanned Surface Vehicle

Our main tool for surveying the macroalgal habitats with echosounder technology, CTD and drop camera, was the unmanned surface vehicle manufactured by Maritime Robotics AS from Trondheim, Norway (Fig. 2). The USV model "Otter" is a small catamaran with two identical pontoons and Torqeedo Ultralight 403 motors. With a footprint of 200×108×106.5 cm the Otter was quite small and relatively easy to handle logistically. The deployment and retrieval of the USV from our boat could be accomplished with two to three people which made it possible to design our fieldwork much more flexibly since we were able to use a small and fast boat to carry the USV from one station to the other.



**Figure 2:** Otter USV in the field in Billefjorden . Parts of the DT-X and its cable were located in the rear (right). The camera as well as the various radio/wifi antennae are mounted to the top of the USV's OBS control box on the left.

A forward-facing camera was installed on the USV which was used to steer the Otter in more difficult waters and to avoid collisions. The camera's live feed could be accessed via the vehicle control stations (VCS).



The on-board system (OBS) control box contained the onboard computer, GNSS receiver and the automatic identification AIS transmitter as well as the ethernet port necessary for communication with the payload.

The USV was remotely controlled via wifi (802.11ac WiFi hotspot with ~400m range and 4G LTE modem) or broadband radio (Direct link 5150 – 5875 MHz radio with 2km+ Line of sight (LOS) range) from a nearby Polarcirkel boat with a laptop configured with Maritime Robotics' VCS or from an android app on our mobile phone for close quarter maneuvers in immediate sight range. The VCS allowed us to plot and change the course of the USV in real time on a preloaded map (openstreetmaps tile server) while receiving and using dGPS and bathymetric depth data from the Otter and the echosounder's transducer as a reference to hold the correct course.

The VCS has several control modes to maneuver the USV either autonomously or manually. For the preliminary transect measurements along the coastline, we used the "waypoint mode", which gave us the highest amount of flexibility by adjusting the directional heading with respect to the bottom depth. The daily operation time was mainly limited by the two Torqeedo lithium-ion batteries (2×915 Wh) that powered the USV's 2 geared electric motors and the DT-X for up to 5 hours in the field at a mean speed over ground (SOG) of 3 knots.

### **2.2.2 Split Beam Echosounder**

A downward facing split-beam echosounder (BioSonics DT-X Digital Scientific Echosounder by BioSonics, Seattle, USA) mounted to the autonomous, remotely controlled USV was used to gather echosounder data. The echosounder's transducer had a submersion depth of 40 cm, was mounted towards the rear of the USV and was connected to the OBS via a sensor payload box. The echosounder has a beam angle of 6.5×6.5 degrees and was set to a ping rate of 5 Hz and a depth range of 0-15 m for the preliminary survey. The DT-X has a very high temporal (precise time stamping of the pings) and spatial resolution (accurate internal dGPS measurements).

To keep the echosounder's spatial resolution as even as possible during data measurements, the USV was driven with a constant SOG of 3 knots, with minor deviations caused by the wind and wave conditions. Except for the ping rate and depth range, all other settings (e.g. detection thresholds for the sea floor and macroalgae) could be changed and edited during post-processing.

### 2.2.3 Underwater Camera

To validate the plant detection algorithm of the DT-X, an underwater camera (model: Vaquita by Paralenz, Rødovre, Denmark) has been used for ground truthing of the acoustic plant signal with actual underwater footage. The camera has been set to a recording depth trigger of 3 m, a frame rate of 30 fps and a video resolution of 1080p. The camera was rigged to the Otters AutoCast SVP winch system which is designed for static casts of equipment in the water column.

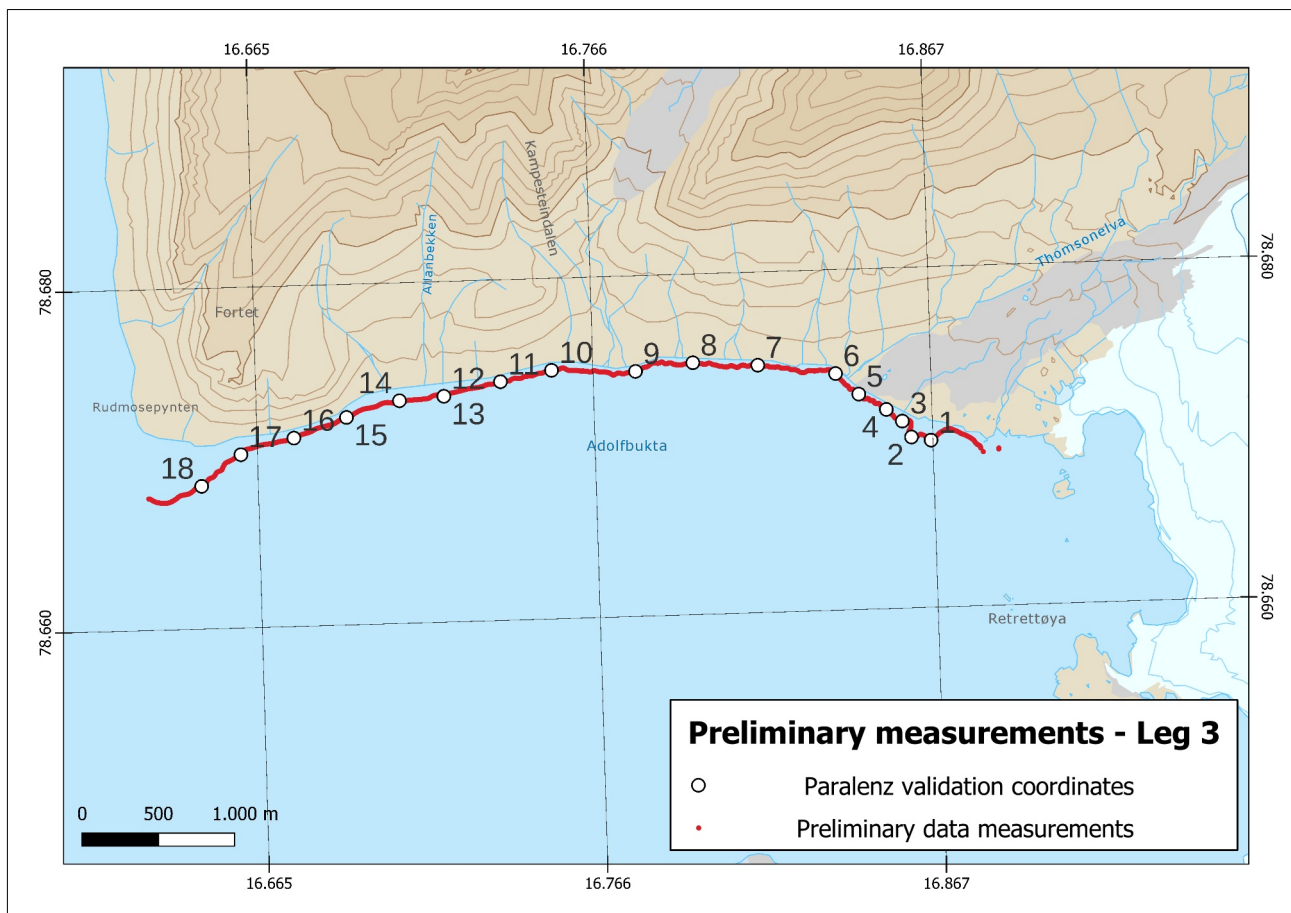


**Figure 3:** Paralenz drop locations along the preliminary data gathering course of the USV/DT-X. The upper and lower axis are showing the longitude while the left and right are displaying the latitudinal coordinates. (Basemap: Norwegian Polar Institute – Svalbard topography WMS dynamic mapserver, EPSG: 32633)

A total of 18 drops have been used to validate the DT-Xs plant detection algorithm. The footage has been gathered along the northern coast of Adolfbukta between 4 and 9 m (Fig. 3).

Via the VCS GUI it was possible to set a desired drop depth above the sea floor. The distance to the ground was usually set to around 1.5 m but could vary depending on the wave conditions. The bottom time for the camera was set to 10 s to ensure that enough footage could be taken of the bottom to assess whether significant plant coverage (PC) by macroalgae was present or not.

This footage was then cross referenced with the echosounder's echograms at the same locations. The correlation of camera footage to the correct segments of seafloor in the echogram has been done by comparing the time stamps of the two devices and allocating the individual camera drops in the echogram, since the descending camera has been picked up by the echosounder and was visible as a straight, continuous line with a strong backscattering signal in the open water (Fig. 4).

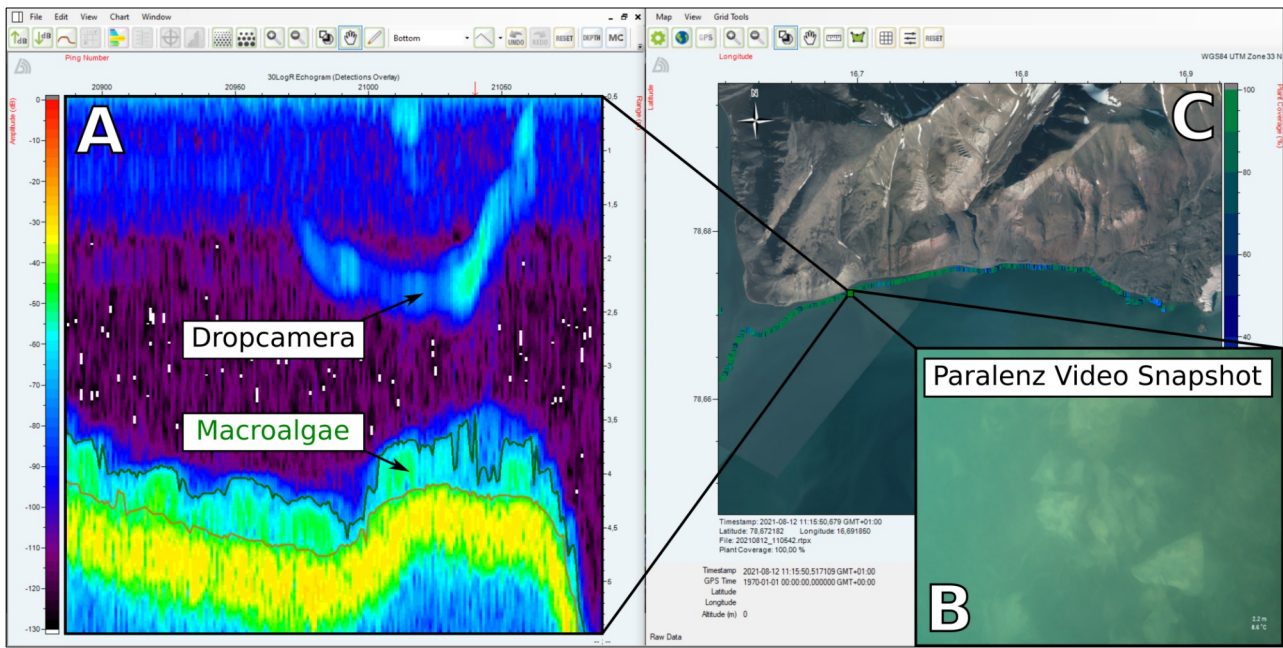


**Figure 4:** Process of validation of the echosounder via drop camera samplings. A – Echogram with the dropcamera, bottom and macroalgae signal all visible, B – Paralenz video snapshot of a dense macroalgae canopy at the same location, C – Location of this respective cast.

This way a positive or negative validation of the plant signals detected by the DT-X could be conducted by checking if algae was actually growing where the algorithm picked them up. The validation was done in parallel to the process of obtaining the preliminary fjord data at different segments of the coastline – mostly in Adolf- and Petuniabukta. In total, 17 out of 18 drops verified plant growth picked up by the DT-X and one camera drop confirmed no plant coverage where the algorithm did not detect plants either.

The full account of validation footage is attached in the digital appendix. The validation table is attached in the written appendix of this document (Appendix: Tab. 10).

## 2.2.4 CTD

A Valeport SWiFT Turbidity CTDplus (Valeport Ltd., Totnes, UK) probe aided in measuring environmental parameters such as temperature, salinity and turbidity in the water column.

Its temperature sensor is a thermally-sensitive resistor (thermistor) that measures temperature via an electrical resistance that's proportional to the environmental temperature. The output salinity values are calculated based on the integrated conductivity, temperature and pressure sensors using standard EOS80 formulas. The calculated practical salinity is based on the distribution of ions in the seawater rather than its density as is the case for absolute salinity (Tab. 1).

**Table 1:** SWiFT CTD Sensor characteristics.

Sensor	Type	Range	Accuracy	Resolution	Response
Salinity	Calculated	-	±0.01 PSU	0.001 PSU	-
Conductivity	Inductive conductivity sensor	0 to 80 mS/cm	±0.01 mS/cm	0.001 mS/cm	31.25 ms
Temperature	Fast response Thermistor	-5 °C to +35 °C	±0.01 °C	0.001 °C	<100 ms

The turbidity measurement system of the Valeport Swift CTD combines two sensors. A nephelometer with a 90° beam angle for turbidity levels between 0 and 1000 NTU with a linear response and an optical backscattering sensor with a ~120° beam angle for levels higher than 6000 NTU and a non-linear response. Their minimum detection level lies at 0.03 NTU and both sensors are rated for full ocean depth.

The CTD was mounted at the front of the Otter and the sensors were submersed to about 40 cm below the waterline, so that surface measurements could be taken in parallel to the echosounder pinging. The CTD was set to continuous recording mode at an interval of 1 Hz for all the sensors. The start and stop of the recording in continuous mode could be controlled by an app installed on a Bluetooth capable android device (mobile phone or laptop).

Both the CTD and the DT-X could later be correlated with each other via the GPS tagged echosounder pings to create an idea of the fjords' coastal characteristics with respect to different environmental ranges for salinity, temperature and turbidity. Since the CTD's GPS transmitter did not work while deployed under water, the internal clock of the CTD was used to link the CTD measurements to the georeferenced echosounder pings.

## **2.3 Preliminary Measurements**

The sampling stations have been selected based on geographic fjord characteristics and preliminary bathymetric as well as CTD data, gathered along the coastline of Billefjorden. The baseline measurements for the selection of sampling stations have been conducted over the course of four separate days in July and August (21 & 27 July; 12 & 18 August, 2021). This culminated in four separate legs worth of CTD and echosounder data. The CTD files were saved and exported as tabular VP2 files for later analysis in Libre Office Calc (v7.1.3.2, x64), whereas the echosounder data was exported into RTPX files that were read and edited in BioSonics' Visual Aquatic software (v1.0.0.13146).

The bathymetry measurements were done at approximately 5 m bottom depth below the surface along the coastline. Because of varying weather conditions – essentially wind and wave action – between the sampling days, the actual depth could vary between 3 m and 12 m when it became difficult for the USV to hold the course. In total, around 50 kilometers of coastline have been measured in this phase of data acquisition.

The measurements started near Phantomodden and ended at the southern part of Mimerbukta. This means most of Billefjordens eastern coastline and the two main bays (Adolfbukta and Petuniabukta) have been covered with the survey. Due to difficulties in maneuvering the heterogenous and unpredictable moraine underwater landscape, only some parts of the coastline in front of Nordenskiöldbreen could be measured. Directly in front of the sea-terminating glacier section, the depth of the sea floor was consistently deeper than 30 m, which meant that those regions were left out since they would be unsuitable for monitoring macroalgal growth.

## **2.4 Station Selection Process**

To avoid a biased selection of the stations towards homogeneously structured sites with abundant macroalgal coverage, only the CTD and GPS data have been involved in the actual selection process combined with a randomized approach to determine the geographical centre of each station within a larger, suitable region of the fjord.

Three separate larger segments of the coastal echosounder transects in Billefjorden were determined as the areas for the selection of each station (GLA, ICE and FRE). Each cluster of 5 pings in the respective echosounder files had a unique GPS location. Every cluster was then assigned to a whole

number in ascending order. Subsequently, with the help of a random number generator, one of these GPS positions has been chosen as the cross-sectional centre of each station.

The segment for the freshwater station was located on the western side of Petuniabukta. The region for the selection of the glacier station was situated in the northern part of Adolfbukta in front of a land-terminating strip surrounded by sea-terminating calving sites of the glacier. The selection region for the sea-ice station was located between Kapp Scott and Kapp Napier on the eastern coast of Billefjord in a coastal sector where there was no significant river deltas or direct influence by glacial fronts (Fig. 5). The ranges in turbidity and salinity in addition to the GPS coordinates of these segments can be found in the appendix (Appendix: Tab. 7).

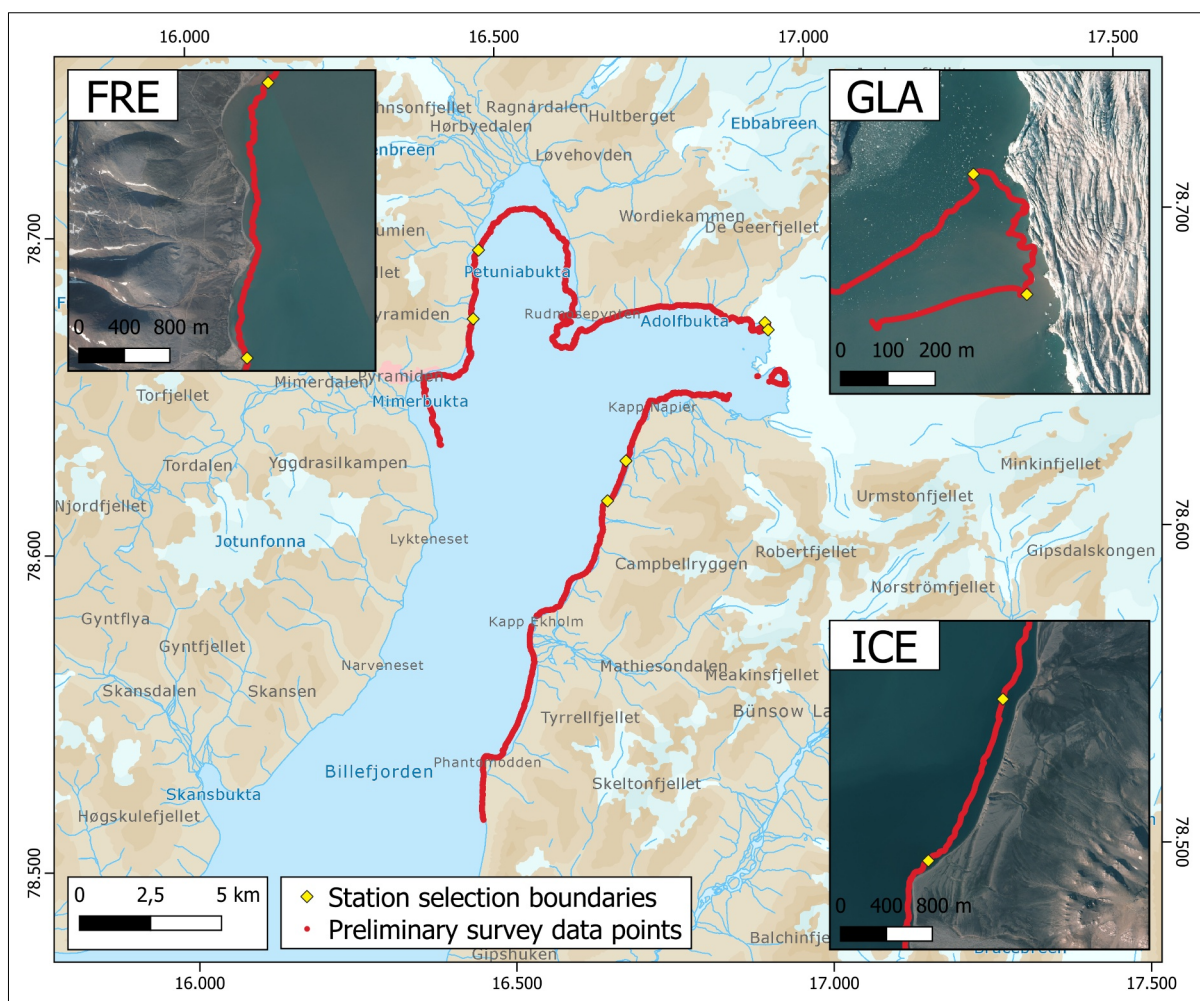


**Figure 5:** Data transects from the preliminary bathymetric and CTD survey in Billefjorden. The yellow rectangles show the chosen selection boundaries for all three stations (FRE, GLA, ICE). Basemaps are from the Norwegian Polar Institutes Map Services: middle – Svalbard topography WMS dynamic mapserver, stations - Svalbard Orthophoto WMTS mapserver

The central coordinates of the freshwater station were 78.692758°N and 16.463854°E at roughly two to three km distance to the main exiting river delta (Fig. 6). The glacier station was positioned at 78.667902°N and 16.928750°E. The sea-ice station was located at 78.617678°N and 16.678655°E close to Kapp Scott circa 3.5 km away from the opening of Adolfbukta (Fig. 6).

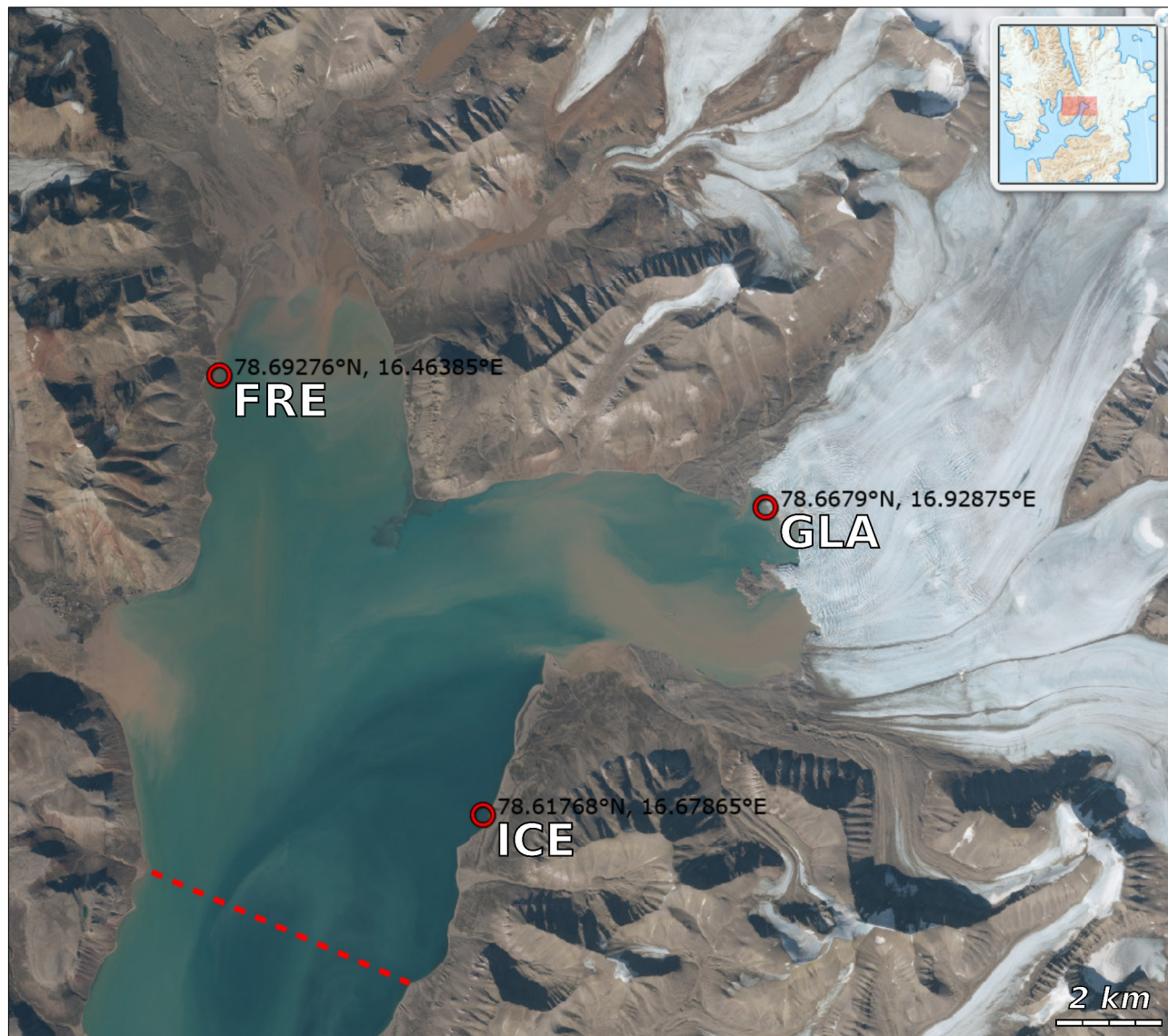


**Figure 6:** Location and GPS coordinates of sampling stations in Billefjorden. The dashed red line roughly illustrates the maximum sea-ice extend of the period between December and March 2020/2021. For a more detailed overview of the winter sea-ice extent in Billefjorden see the attached ice charts from the Norwegian Meteorological Institute in the appendix (Fig. 25-31). Basemap: Norwegian Polar Institute's geological map services.

## 2.5 Station Design

The stations were 150 m wide ( $\pm 10$  m on each side as a buffer) while the length that the stations would reach into the fjord was determined by a maximum depth of 30 m for each transect. That means the steeper the incline of the slope, the shorter the transect. The stations were then divided into transects that were oriented approximately at a 90 degree angle to the coast with a variable length depending on the slope of each station (Fig. 7 & 8).

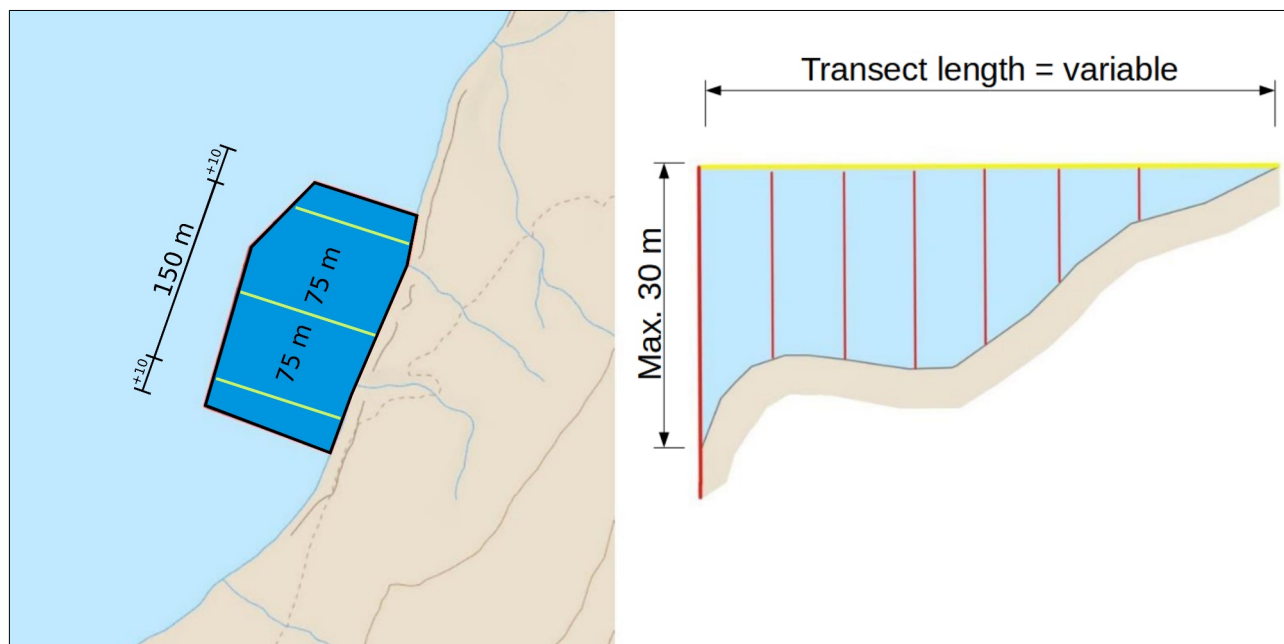


**Figure 7:** Schematic drawing of the general station design. Red lines illustrate potential drop samplings along a station's transect (yellow lines) e.g. for CTD drop samplings. The outer yellow lines illustrate the lateral station boundaries for data that will be processed. The area outside the yellow lines is designed as a buffer. Basemap: Norwegian Polar Institute's geological map services.

For later analysis, the stations were separated into depth bins of 5 m. The shallowest bin was from 5 to 10 metres and the deepest one from 25-30 metres. The shallow intertidal and littoral zone between 0-5 metres depth was excluded from the analysis, since data acquisition with the echosounder was not consistently possible below 5 m depth as a result of the coastal slopes and station characteristics. At the glacier station for example a very steep slope and heterogenous coastline, characterised by large boulders or land strips reaching into the fjord, prevented us from monitoring the full range of the 5-10 m depth bin for some transects.



## 2.6 Station Work

### 2.6.1 Measurement of Sea Floor Bathymetry

Bathymetric measurements for the stations were conducted along a cross-hatched pattern following the stations' transects (Fig. 8). The pattern was pre-drawn and saved in the VCS prior to the field work using the "chart planner" function. Centre coordinates of the stations were taken from the station selection process and each cross-hatched pattern was moved as close to the coastline as possible to assure that most of the slope was included into the echosounder measurements.

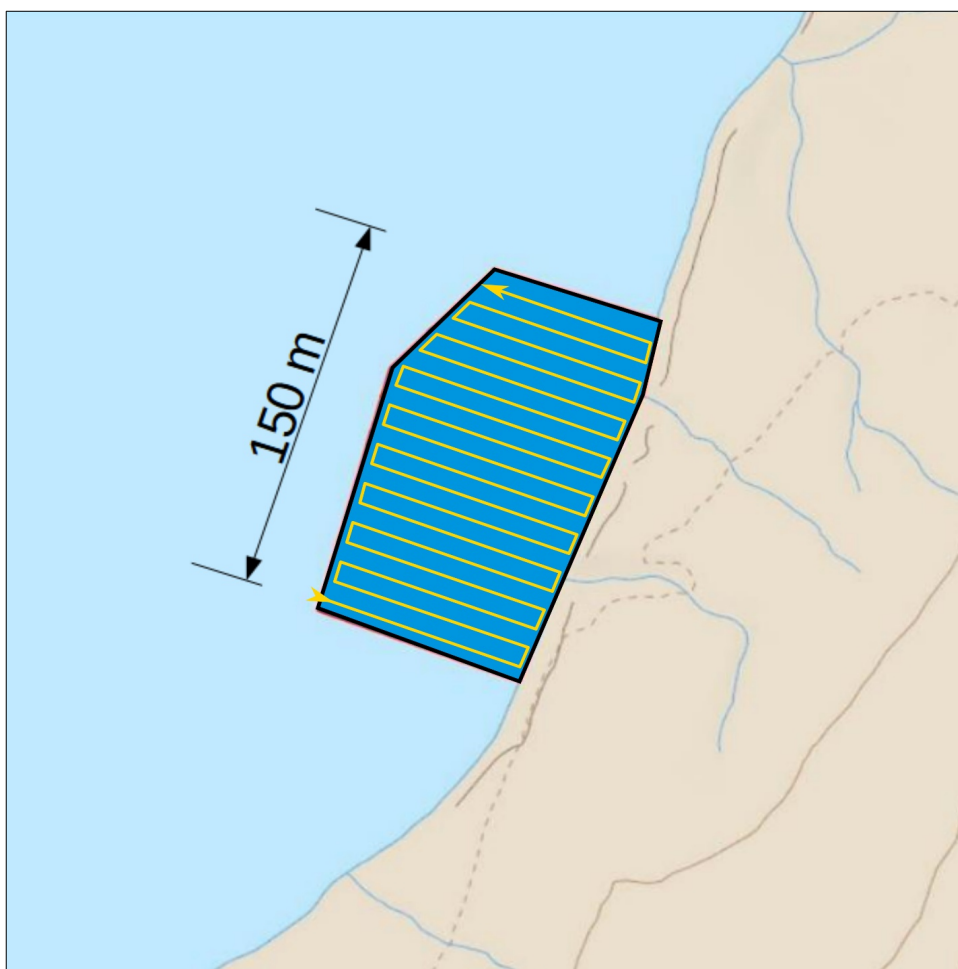


**Figure 8:** Exemplary cross-hatched transect pattern for a station. Bathymetric measurements were continuously taken along these transect lines (yellow).

Each station was divided into 16 transects with a distance of circa 10 m between each other, covering a total width of 150 m. Two additional transects were added to create some buffer on each side of the station when conducting the fieldwork. For the later analysis of the echosounder data only the central 16 transects were included.

To make sure, that the maximum depth of 30 m was covered by each echosounder transect line, the real time depth was observed via the VCS and if necessary the Otters course had to be manually edited by extending the respective transect line until the DT-X reported a depth  $\geq 30$  m. The DT-X's recording depth range was set to 0-40 m. This way we created room for a 10 m depth measuring buffer. Every value below 40 m was excluded. The echosounder was set to split-beam mode and a ping rate of 5 Hz.

A Rising Edge Threshold of -55 dB was chosen for the bottom detection settings in Visual Aquatics (Fig. 9). The threshold varies from the recommended -30 dB and was chosen through a process of trial and error during post-processing of the echograms to optimise the correct bottom line detection. The minimum and maximum depth was set from 0 to 35 m in post processing to restrict the data regions to the predefined depth bins (plus or minus a margin of 5 m). The recommended domain of 30LogR, as the time varied gain (TVG) for the echogram, was applied. The TVG is a signal compensation mechanism, which accounts for transmission loss effects, that can be caused by spreading and absorption of the acoustic signal.

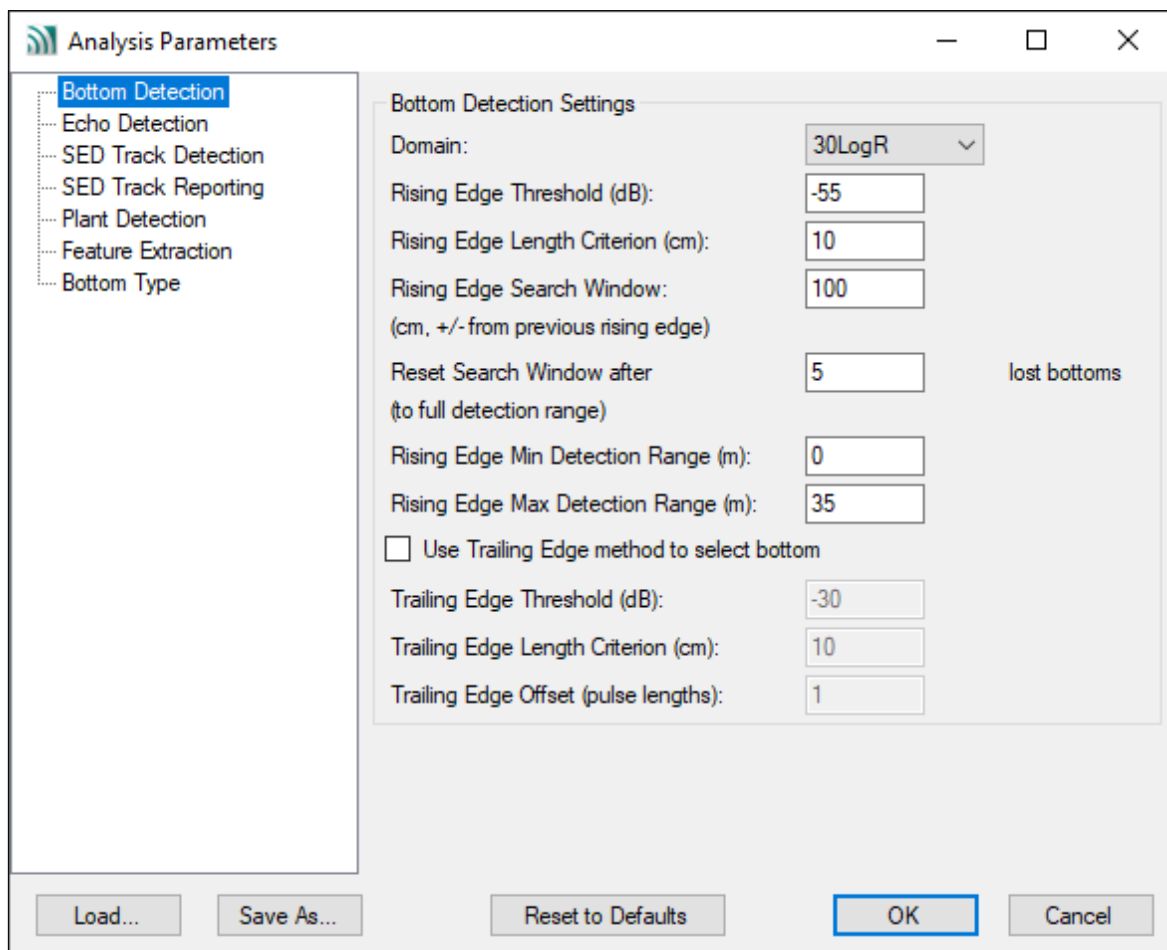


**Figure 9:** Bottom detection settings for the post-processing of the echosounder data in Visual Aquatics.

The bathymetric map for each station was calculated with the help of Visual Aquatics' Gridding and Contouring function. To grid the depth data with the individual transects, we used the triangulated linear method. This way we received bathymetric data maps for each station with predefined contour line intervals for every 5 m. The grid cell size was set to 0.6 m as the highest equal resolution for every station.

The "Set Survey Region" tool was used to select the station regions containing the desired transects and depth ranges. The survey region included the maximum and minimum contours and was cut off on the sides directly parallel to the outer transects. The survey area has been trimmed along the contour line and the echosounder values closest to the maximum and minimum depth value (i.e. 5 m and 30 m). The report interval was set to 10 pings per second, which means that ping clusters of 10 pings each have been used for the gridding of the data. The USV was driven at a speed of 3 knots during the pinging process of the DT-X.

For the basemaps of all the gridded data, a WMTS map server with orthorectified aerial imagery (Orthophoto) of Svalbard was used and provided by the geological map services of the Norwegian Polar Institute. The pictures for the map were taken between mid-July and mid-August of 2009 at a minimum scale of 1:625 for the highest zoom level. The "EPSG:32633 WGS84 Geographic, Equiarectangular"-projection was set as a spatial coordinate reference system for the projection of the map.

## 2.6.2 Sea-Ice Station – ICE

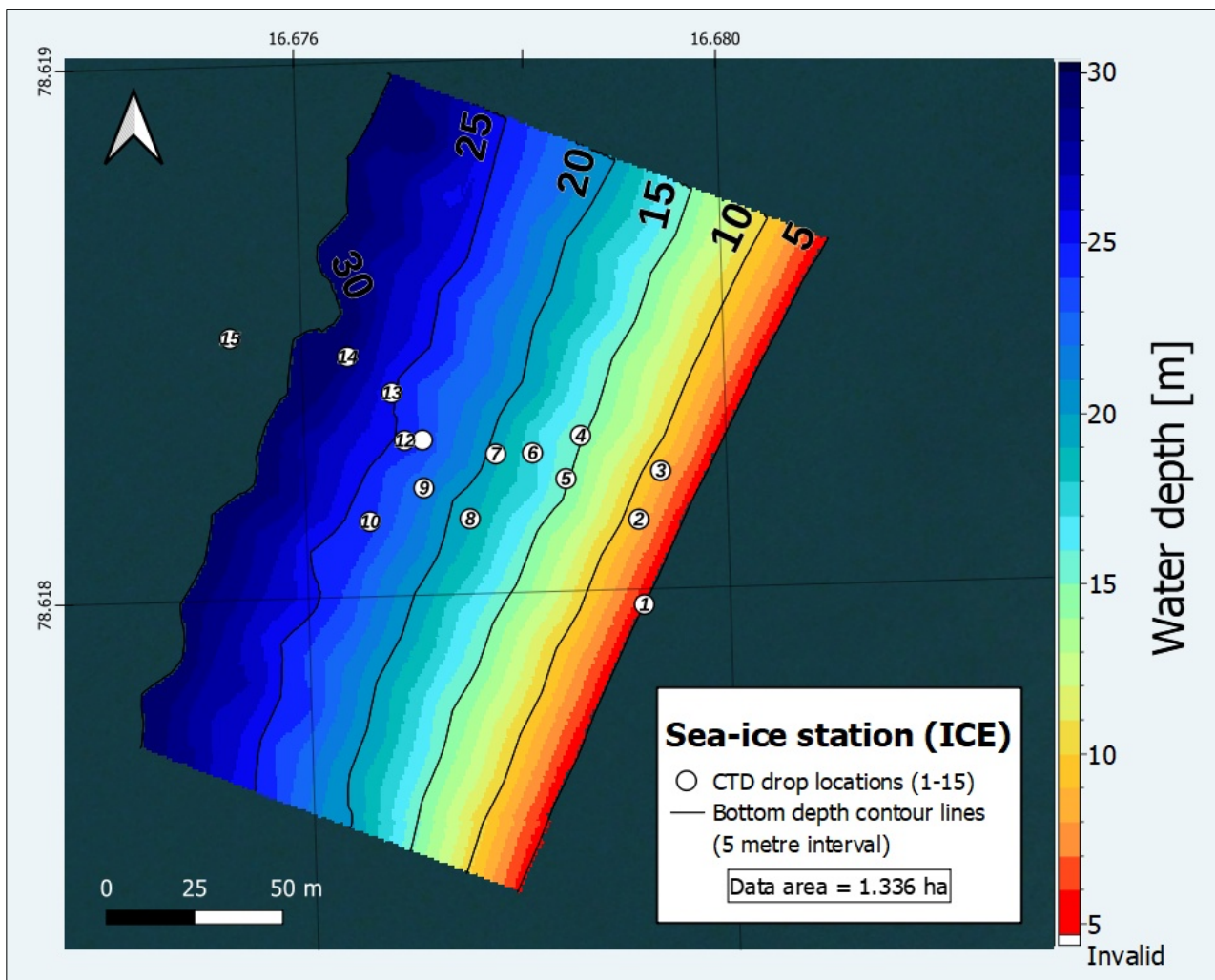


**Figure 10:** Bathymetric sea-ice station grid with contour lines at 5 m intervals, starting at 5 and ending at 30 m. Upper and left axes show the longitude and latitude, respectively. The colour graded scale on the right shows the respective water depth values. The colour graded scale on the right shows the respective depth values. White circles illustrate the location of the CTD drops (1-15) for measurements of the environmental parameters. The detailed grid report statistics can be found in the appendix (Tab. 8). Basemap data from the Norwegian Polar Institutes geological map services (Orthophoto from 2009).

Data for the sea-ice station was obtained on the 24 August, 2021 and the sampling lasted for approximately 1 hour and 20 minutes (11:40 to 13:00 (GMT+2)). The wave conditions were calm that day (waves < 20 cm). The survey area enclosed by the central 16 transects and between 5 to 30 m water depth had a size of approximately 1.34 ha (Fig. 10).

### 2.6.3 Freshwater Station – FRE

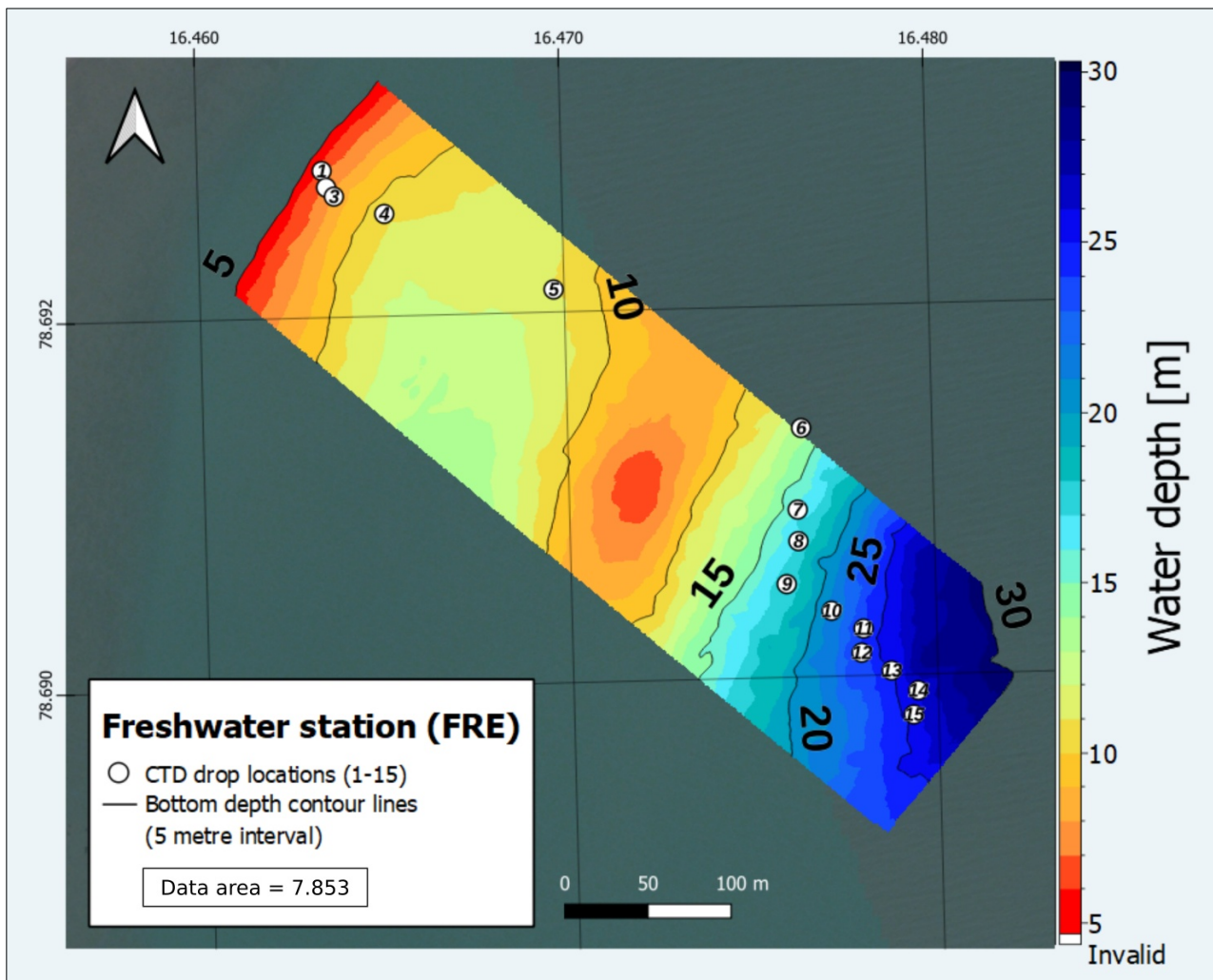


**Figure 11:** Bathymetric freshwater station grid with contour lines at 5 m intervals, starting at 5 and ending at 30 m. Upper and left axes show the longitude and latitude, respectively. The colour graded scale on the right shows the respective depth values. The colour graded scale on the right shows the respective depth values. White circles illustrate the location of the CTD drops for measurements of the environmental parameters. The detailed grid report statistics can be found in the appendix (Tab. 8). Basemap data from the Norwegian Polar Institutes geological map services (Orthophoto from 2009).

The bathymetric data for the freshwater station was gathered on the same day as the sea-ice station between 13:40 and 16:00 (GMT+2) and under similar weather conditions. Due to a shallow incline of the sea floor at the freshwater station, the total survey area and length of the transects was significantly higher compared to the other stations (Fig. 11). Not all the transects reached 30 m depth and due to the time limitation in the field, the missing parts of the transects could not be measured at another time.

## 2.6.4 Glacier Station – GLA

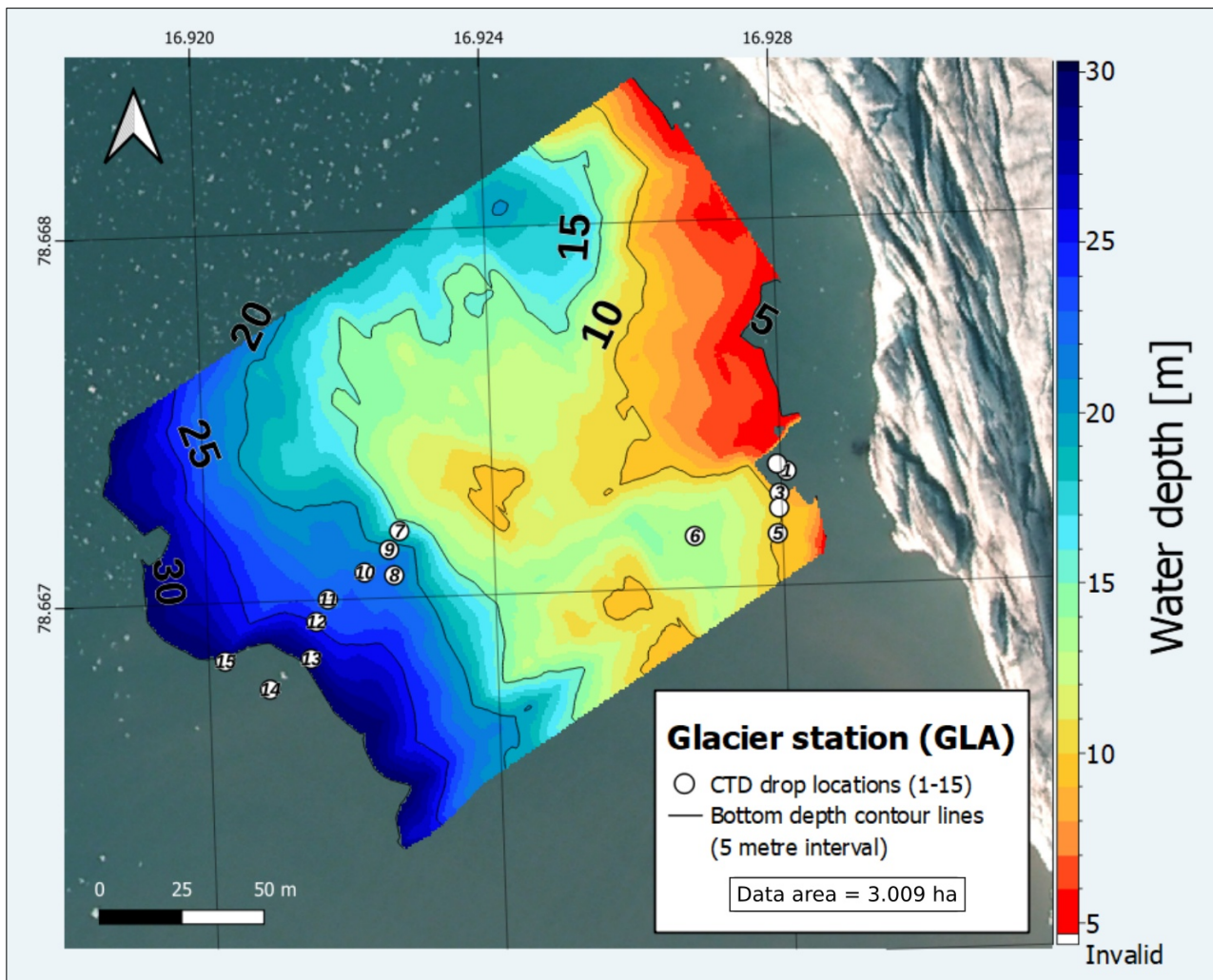


**Figure 12:** Bathymetric glacier station grid with contour lines at 5 m intervals (labelled in metres by the bold black numbers on the lines), starting at 5 and ending at 30 m. Upper and left axes show the longitude and latitude, respectively. The colour graded scale on the right shows the respective depth values. White circles illustrate the location of the CTD drops for measurements of the environmental parameters. The detailed grid report statistics can be found in the appendix (Tab. 8). Basemap data from the Norwegian Polar Institutes geological map services (Orthophoto from 2009).

The survey of the glacier station has been conducted on a separate day (25 August, 2021) after the other two stations due to time limitation in the field. The measuring process took one and a half hours (11:30 to 13:00) with calm sea (waves <20 cm) but slightly rainy conditions. Since the aerial base map data is from 2009, the map depicts the station as being situated directly in front of the sea-terminating glacial calving front (Fig. 12). At the time when the station was sampled, the glacier was already retreated to land in that particular region. The whole 5 to 10 m depth bin could not be measured with the echosounder, because the slope close to the shore was too steep. The contour lines emphasize the much more heterogeneous and irregular sea floor structure compared to the other two stations, where most of the contour lines are more or less parallel to the coastline.

### 2.6.5 Measurement of Proximate Drivers

**Temperature, salinity** and **turbidity** profiles have been measured with the Valeport CTD.

Due to technical difficulties of the USV remote control connection towards the end of the field period and bad weather, the CTD drops had to be delayed to the 20<sup>th</sup> of October and were not done with the Otter AutoCast winch nor at the same time as the bathymetric station survey.

For the station work, the down-cast configuration was used to gather environmental data along vertical depth profiles. The trigger depth at which the CTD would start measurements was set to 40 cm and the depth measuring increment to 10 cm. The CTDs trigger step, which defines the amount of upward vertical movement after which the measurement would automatically stop, was set to 1 m. The drop samplings were performed by hand along the middle transect of the station with a depth labelled rope.

The casts were performed to the approximate bottom depth (reference from the boats echosounder) at each respective sampling location. Once the desired maximum depth for the respective bin could be read from the boats echosounder, a CTD cast could be conducted. For every station a total of 15 down-casts were made from shallow to deeper water (i.e. three for each depth bin) (Fig. 10, 11, 12). The drops have also been georeferenced by the integrated GPS.

QGIS (version 3.22.3-Białowieża), was used to depict the coordinates of the vertical drop samplings in relation to the stations' bins (Fig. 10-12). The maps are projected in EPSG:32633 over a WMS map service of the Norwegian Mapping Authorities. They show, that even though the CTD profiles were conducted to the correct depths that day according to the boats echosounder, the drop coordinates were not always accurately placed within the boundaries of the respective bins. This was partly due to the lesser maneuverability of the vessel in use and strong currents on the sampling day.

## 2.6.6 Measurement of Macroalgae

To quantify macroalgae, plant coverage has been calculated with the help of Visual Aquatics plant detection algorithms.

Plant coverage was defined via a certain backscattering signal strength set by the plant detection threshold of -70 dB. This means, that the upper detection limit for plants in the echogram was set by this threshold, while the lower detection border was set by the rising edge threshold of the bottom detection (Fig. 13).

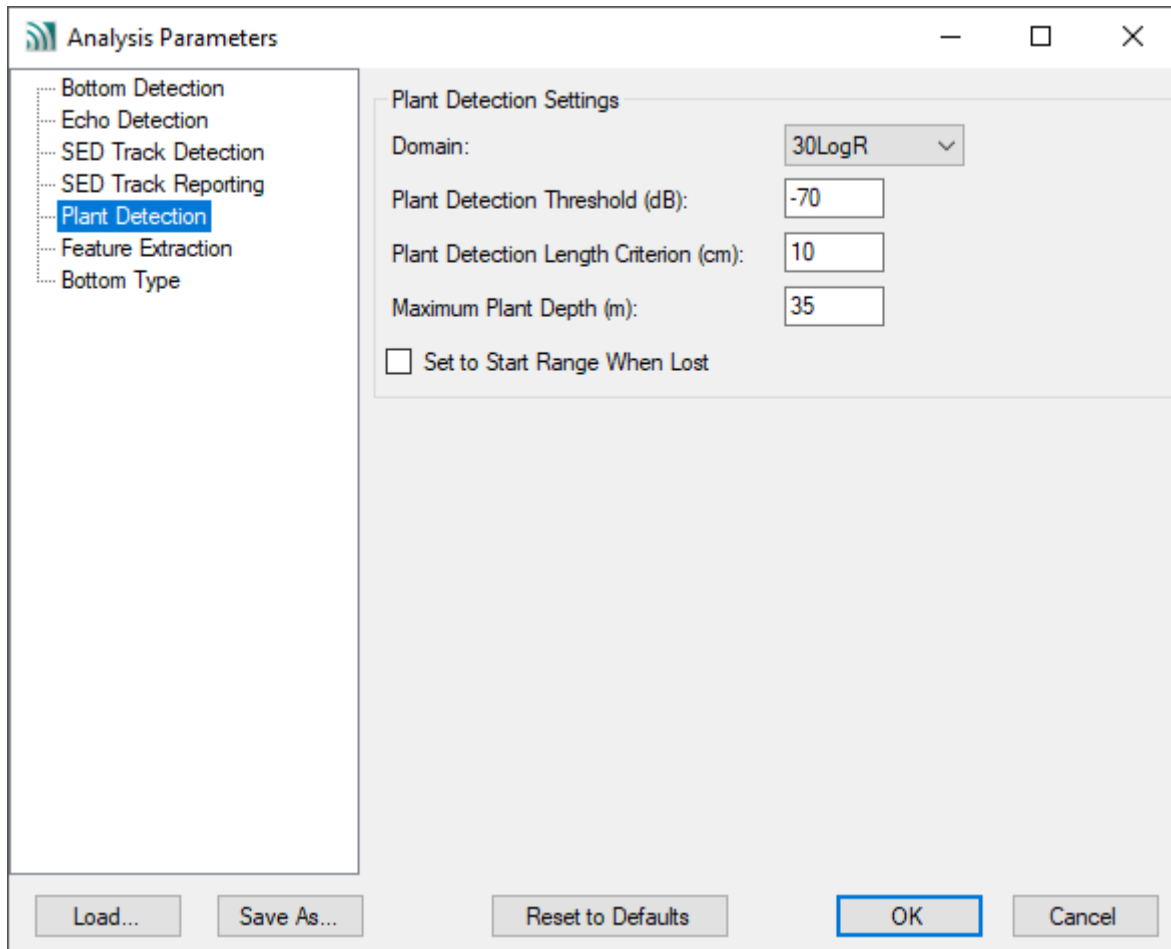


**Figure 13:** Plant detection algorithm analysis parameters in Visual Aquatics. The settings were the same for each station.

For the plant coverage data gridding, a more complicated method called inverse distance weighting (IDW) was used to extrapolate the more complex and irregular plant data between the transects. IDW allows the fine-tuning of several other parameters like the "statistical weight" of the data which in this case is proportional to the inverse distance raised to the "Power" value ( $P$ ). Essentially, changing the power value changes how much or fast the weights decrease over distance. A higher  $P$  means a quick decrease and vice versa. In this case  $P = 2$  was chosen (Fig. 14).



A smoothing factor could be set to reduce an overly strong influence of some data points on others during the gridding process. The search neighbourhood shape for each extrapolated data point within the gridded area was set to 30 m at each station and to the "suggested minor axis direction" (Fig. 14).

The Axis ratio was left at 1 to ensure a symmetrical search neighbourhood shape. Advanced search parameters, the Power value and the smoothing factor were all set to the values recommended by the DT-X's user guide. Except for the axis ratio, the search neighbourhood shape settings were different for each station, because minor sampling differences (e.g. exact distance between transects) affected the "Transect Analysis" results.

The screenshot shows the 'Inverse Distance Weighting' dialog box with the following settings:

- Interpolation:**
  - Grid Cell Size (m, >0): 0.6
  - Power (≥0): 2
  - Smoothing Factor (≥0): 2
- Search Neighborhood Shape:**
  - Semi-Major Axis Length (m, >0): 30
  - Minor Axis Direction (deg): -47.4
  - Axis Ratio (≥1): 1
- Transect Analysis:**
  - Minimum Suggested Semi-Major Axis Length (m): 6.2
  - Suggested Minor Axis Direction (deg): -46.0
  - Direction is degrees clockwise from vertical
- Advanced Search Parameters:**
  - Number of Sectors (>0): 1
  - Sector Offset Angle (deg): 0
  - Number of Points Required Per Sector (>0): 1

**Figure 14:** Parameter settings for the inverse distance weighting gridding method in Visual Aquatic. This figure shows the exemplary settings for the freshwater station.

## 2.7 Data Management and Post-processing

### 2.7.1 Manual Editing of Echograms

There were several instances where the automatic bottom and plant detection algorithms had to be aided by some selective manual editing of the bottom and plant canopy in the echograms. This could be done with the "Edit Tool" in Visual Aquatics.

For manual editing of the bottom and plant lines, the "linear line" mode has been used to trace the respective lines along the actual -55 and -70 dB detection thresholds as closely as possible.

Reasons for an inaccurate bottom line detection by the algorithm can be very dense plant canopies and schools of demersal or pelagic fish. The case of fish schools causing a false bottom line detection could for example be observed at the sea-ice station (Appendix: Fig. 33).

The area at the glacier station was quite difficult to maneuver with the USV. Some manual editing had to be done at an instance, where the USV collided with an iceflow in the open water and another time when it came too close to land due to a malfunction in the radio connection to the VCS control unit. The affected regions have been cut out in Visual Aquatics 50 pings before and after the apparent crash to make sure it was excluded from the analysis (Appendix: Fig. 32).

After adjusting the detection thresholds for bottom and plant canopy, a more or less continuous false-positive plant signal could be observed above the bottom line, which we attempted to filter out by setting the plant report height threshold to 20 cm. This means, that no plant signals smaller than 20 cm were included in the plant coverage report, effectively focusing on bigger macroalgal species like kelp.

Manual editing has been done within the depth range of interest (5 to 30 m). Before and after pictures of the manually edited parts of each transect's echogram can be found in the digital appendix.

Another problem were the pronounced differences in the plant detection with respect to the course of the USV while pinging up or down the coastal slope. A higher plant backscattering echo was produced whenever the DT-X was measuring down the slope. This is why the semi major axis length of the search neighbourhood had been adjusted to 30 m (as a significantly higher value than the minimum required) which means, that the impact by this artificial difference between the slopes on the gridded illustration of plant coverage has been reduced, since the calculated values were using a bigger reference area.

## 2.7.2 Adjustments for Tides and Echosounder Depth

Because the fjords water depth is subject to tidal fluctuations and the bathymetric survey took usually at least one hour, we attempted to correct the depth measurements for the respective astronomical tidal predictions during each sampling time. The submersion depth of 40 cm of the echosounders transducer had to be taken into account as well to produce accurate depth data.

Tidal charts for each location and time frame have been obtained from the Norwegian Mapping Authority's Hydrographic Service at a temporal resolution of 600 seconds. For the positional data, the centre coordinates from each station have been used.

The station specific tidal charts were generated from the hydrographic service's tide system Application Programming Interface (Appendix: Tab. 10, 11, 12). Mean water levels over the chart datum – in this case the lowest astronomical tide (LAT) – were calculated within each station-specific sampling time frame. This includes the start to finish time of the entire operational period of the DT-X at each station. Since the tidal charts are given in UTC+1 and the DT-X was logging data in GMT+1, no time conversion had to be conducted.

The transducer depth has been added to the depth reading and the water level above the chart datum has been subtracted to standardize the depth data of all stations to the same zero reference depth.

The CTD depth referenced data was tide corrected in the same manner and with reference to the chart datum. The following table shows the depth correction values in metre above chart datum for each stations sampling time frame. About an hour was spent for drop sampling each station. The mean value for tide predictions of every 10 minutes within that hour was calculated (Tab. 2).

**Table 2:** CTD tide adjustment table. Mean tidal height predictions above chart datum within each sampling time frame and each station. (Source for tidal data: Norwegian Mapping Authority's Hydrographic Service). FRE – freshwater station, GLA – glacier station, ICE – sea-ice station.

Station	Tide predictions (cm) above chart datum					Mean (cm)	
ICE	95.7	101.4	107.3	113.4	119.7	<b>107.5</b>	
GLA	180.2	181.9	182.9	183.3	183.1	<b>182.3</b>	
FRE	162.8	159.2	155.4	151.4	147.2	142.7	<b>153.1</b>

### 2.7.3 Statistical Analysis

For the in depth statistical analysis of the environmental CTD and plant coverage data, RStudio (version: 2021.09.2+382 "Ghost Orchid" Release (fc9e2179, 2022-01-04)) has been used as the main tool. In addition to the system library, R packages that were used throughout the script were "car", "ggplot2", "ggsignif", "plotly", "dplyr" and "sciplot". Basic tabular calculus was done with Libre Office Calc (v7.1.3.2, x64).

The raw bottom depth and plant coverage data for the statistical analysis was exported from Visual Aquatics as shapefiles for the map visualization in QGIS and as CSV files to compile the data sheets for R. Shapefiles and gridding results are attached in the digital appendix. Plant coverage data has been calculated at 10 percent intervals ranging from 0 to 100 %. To achieve this percentual resolution of plant coverage, a report interval of 10 pings per second was chosen. Depth and coverage data was combined into a single spreadsheet via the respective latitudinal and longitudinal GPS coordinates. Due to the apparent false positive plant detection by the algorithm, a plant report threshold of 20 cm was set as a minimum signal height over the bottom line to count as plant canopy. This false positive detection was even stronger on downward measured slopes which is the reason they were excluded from the statistical analysis.

To prepare the statistical analysis of the environmental parameters, CTD raw data was exported from the Valeport Ocean software (version. 1.1.0.18) into VP2 files that could be read into Libre Office Calc. Every station had 15 profiles ranging from 40 cm submersion depth to the bottom depth with 3 drops designated for each depth bin ( $n = 3$ ). To calculate mean values for the different bins and stations, every CTD profile was trimmed to include measurements within the respective bottom depth range of each bin. For example for the 5 to 10 m bin, only values from drop 1 to 3 were included, that were measured within the same bottom depth range. For the drops 4 to 6, only measurements between 10 and 15 m were analysed, and so on. The only exception was made for the turbidity values when correlating them with the plant coverage since turbidity has a cumulative effect over the whole height of the water column.

To compare and combine the CTD and PC data, they were grouped into 5 m depth bins. Mean values for each station as a whole and bins were calculated in R.

With the help of the R package "car", generalized linear models (GLM) were run for the station and bin dependent plant coverage as well as environmental data to find out significant differences and trends between the respective variables.

The plant data was further tested for normal distribution using the shapiro test, which resulted in a non-gaussian distribution. Type F quasibinomial Anovas were chosen for the station and depth dependent plant coverage models because of dispersion coefficients being lower than 0.5 (Type Chi for binomial is chosen if dispersion coefficient falls between 0.5 and 2). The packages "ggplot2" and "ggsignif" were used to create boxplots for the station PC data and the jittered scatterplot for the depth related plant coverage. Regression line parameters for the equations in the scatterplot were taken from the model summary. The binned PC data was plotted in the form of violin plots using the "plotly" package for R.

To conduct the correlative analysis between the environmental drivers with the purpose of revealing potential codependent influences of these variables, their data distribution had to be examined. Therefore, histograms for the trimmed environmental parameters were plotted and showed a non-normal distribution for all of them. Spearman correlation coefficients were calculated for temperature, salinity, turbidity and depth.

To analyse the effect of the environmental on macroalgal coverage, the CTD and PC data were merged via a matching index of station and depth. To achieve this, the depth values of both data sets' measurements were adjusted to one metre intervals by rounding the respective depths to a whole number. This also served the purpose of increasing the n of plant coverage data points for each CTD data point and strengthen the validity of the model results. This would not have been the case if the 5 m depth bins were used, since that would have resulted in a loss of n by grouping multiple values into a mean. Type F Anovas were done for the three stations, looking for statistically significant ( $p < 0.001$ ) relationships between the coverage and drivers. Significant trends were then visualized in scatterplots with their respective trend lines. The minimal adequate model approach with backwards stepwise selection of parameters by p-value was used to extract p-values.

For reference, the raw data tables as well as the R script are placed in the digital appendix.

### 3 Results

#### 3.1 Differences in Plant Coverage between stations

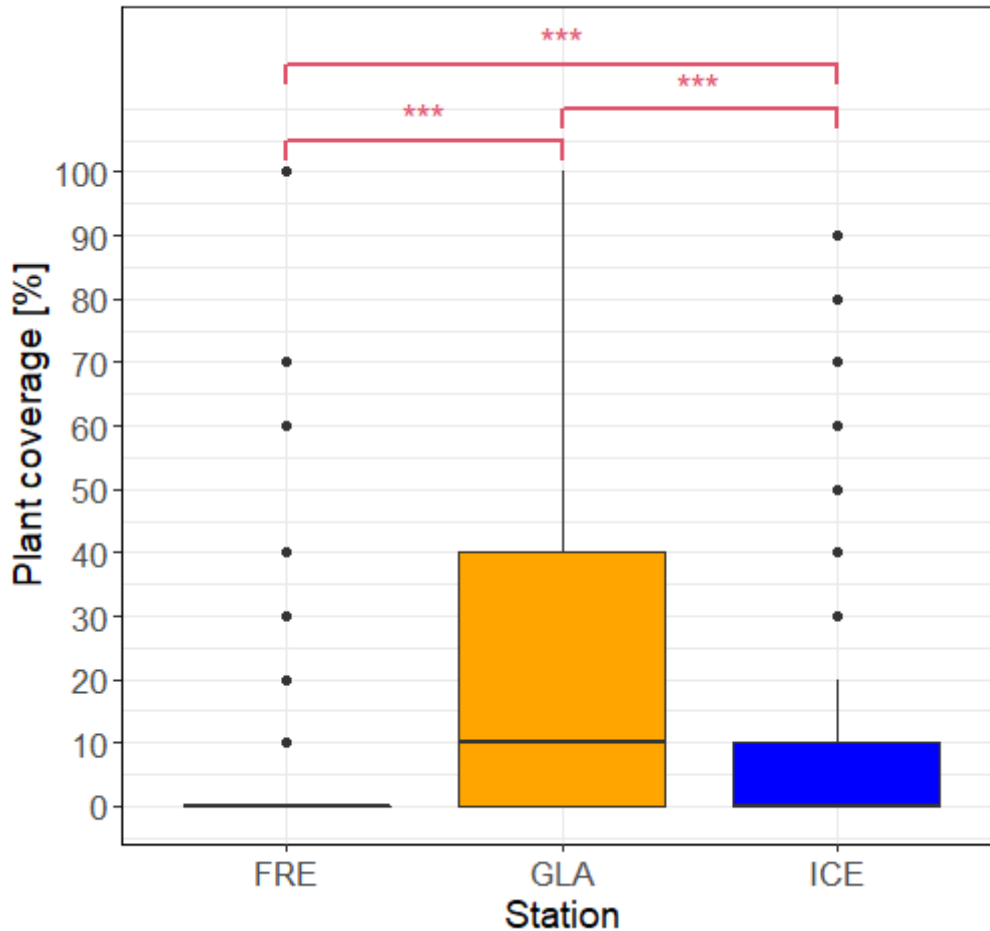


**Figure 15:** Overall differences in plant coverage for the different sampling stations. Plant coverage data is given over the whole depth range of 5 to 30 m. P-value significance codes: 0 '\*\*\*' 0.001 '\*\*' 0.01 '\*' 0.05 '.' 0.1 ' ' 1. FRE – freshwater station, GLA – glacier station, ICE – sea-ice station.

Macroalgal coverage was significantly different between the stations ( $p < 0.001$ ) (Fig. 15). It was lowest at the freshwater station and highest at the glacier station while the sea-ice station placed in between. There were several outliers for the sea-ice and freshwater station, ranging from 10 to 100% and 30 to 90%, respectively. Corresponding maximum, minimum and mean values for plant coverage are in table 3. The range of plant coverage values was highest for GLA and lowest for FRE as indicated by the height of the boxplots (i.e. the upper and lower quartiles).

**Table 3:** Mean values (PCmean), median (PCmed), standard error (PCse) and deviation (PCsd) for plant coverage from each station in %. FRE – freshwater station, GLA – glacier station, ICE – sea-ice station.

Station	PCmean	PCmed	PCsd	PCse	PCmax	PCmin
FRE	0.64	0	5.05	0.14	100	0
GLA	21.96	10	28.63	1.19	100	0
ICE	9.54	0	16.25	1.05	90	0

### 3.2 Macroalgal Coverage per Depth and Station

Depth showed a distinct influence on plant coverage in this study. The depth dependent plant coverage exhibited significantly different trends for all three stations ( $p < 2.2 \times 10^{-16}$ ) (Fig. 16). Whereas a steady decline of plant coverage with increasing depth was the case for the ICE station, plant coverage seemed to be increasing with depth in front of the glacier. The freshwater station in Petuniabukta averaged consistently low plant coverage values between 5 to 20 m water depth. A slight increase over the last two bins to approximately 10% was observed.

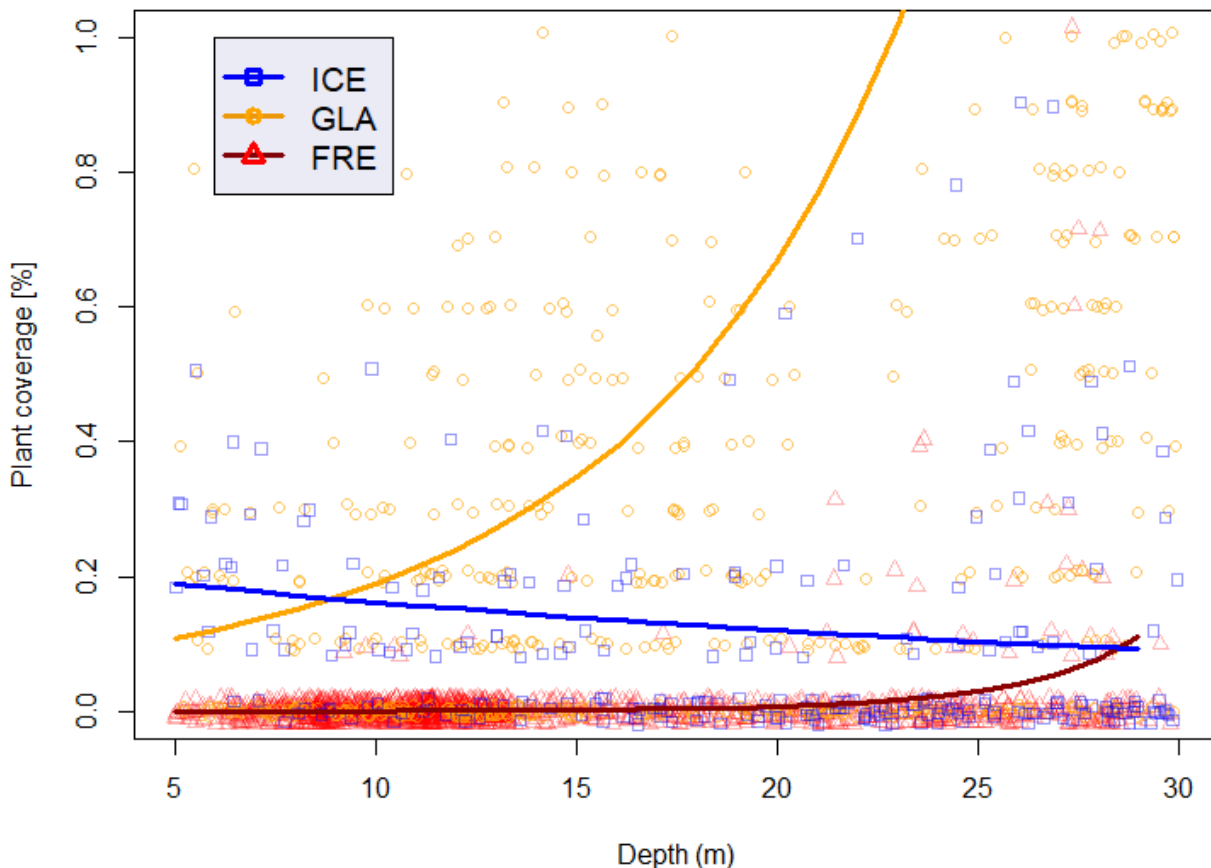


**Figure 16:** Depth dependent plant coverage per station. The blue, orange and red regression lines represent the relationship of plant coverage and depth for the sea-ice, glacier and freshwater station, respectively. The coloured data points are the corresponding jittered plant coverage percentage values. FRE – freshwater station, GLA – glacier station, ICE – sea-ice station.

The violin plots portray the data as boxplots for each bin with additional bell shaped areas on top of them to depict the respective quantity of plant coverage percentage measurements (Fig. 17, 18, 19).

With a few exceptions (ICE: 5-10 m, 10-15 m & GLA: 25-30 m bin) the violin plots revealed a mostly zero inflated data distribution across all bins and stations. This becomes especially apparent when looking at the coverage median values in table 4 and even more so in the case of the freshwater station, where median values are consistently at 0%, despite mean plant coverage values increasing from 1.56 to 4.05% between 20 and 30 m (Tab. 4, Fig. 19). The trends in coverage are better represented by the mean values.

The bins of the ICE and GLA station followed the same trend as in figure 16 but some differences could be observed. The 20 to 25 m depth bin at the sea-ice station for instance showed a slightly increased mean plant coverage compared to the previous bin (6.09 to 6.18%) and a further increase for the last bin from 6.18 to 11.08% (Fig. 17, Tab. 4). Such a "dip" in plant coverage also occurred at the glacier station for the same depth bin (Fig. 18, Tab. 4). Here, the mean plant coverage transitioned from 24.91 to 12.00 and ultimately 44.67% over the 3rd, 4th and 5th depth bin, respectively.

**Table 4:** Mean (*PCmean*), median (*PCmed*), standard deviations (*PCsd*) and errors (*PCse*) for each station and depth bin. *FRE* – freshwater station, *GLA* – glacier station, *ICE* – sea-ice station. (1: 5-10m, 2: 10-5m, 3: 15-20m, 4: 20-25m, 5: 25-30m).

Station	Bin	PCmean [%]	PCmed [%]	PCsd [%]	PCse [%]
<i>FRE</i>	1	0.05	0	0.73	0.04
	2	0.09	0	1.13	1.61
	3	0.08	0	0.89	2.67
	4	1.56	0	5.99	0.05
	5	4.05	0	14.02	1.78
<i>GLA</i>	1	9.70	0	16.11	1.81
	2	15.79	0	23.71	0.08
	3	24.91	20	25.84	2.55
	4	12.00	0	21.87	1.57
	5	44.67	45	35.33	0.47
<i>ICE</i>	1	16.67	10	15.34	2.53
	2	9.75	10	11.43	2.27
	3	6.09	0	10.64	1.23
	4	6.18	0	16.83	3.20
	5	11.08	0	20.47	2.54



The standard deviations in addition to the height of the boxplots as well as their whiskers (representing standard deviation) in the violin plots emphasize how differently the data is spread around the mean values at each station and bin (Tab. 4, Fig. 17, 18, 19). In total, the data is spread furthest for the glacier station, least for the freshwater station and intermediate for the sea-ice station.

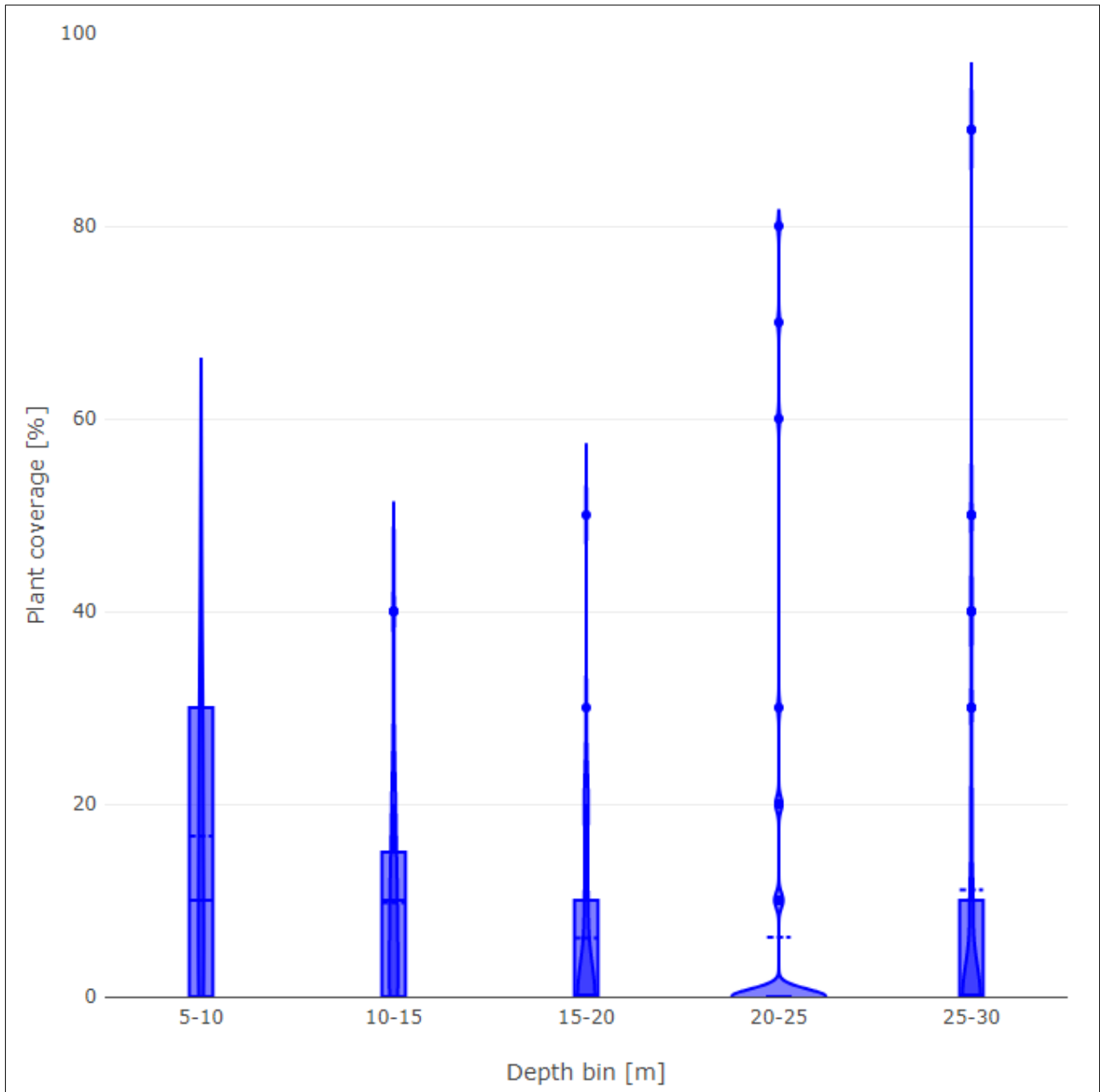


**Figure 17:** Plant coverage at the sea-ice station (ICE) for the 5 depth bins. Binned data is portrayed as boxplots with violin plots to illustrate the quantitative distribution of plant coverage values. Dots are outliers, the dashed line shows the mean values and the solid line represents the median. The central vertical lines show the standard deviation and the boxes the upper and lower central quartile where 50 percent of the data is located.

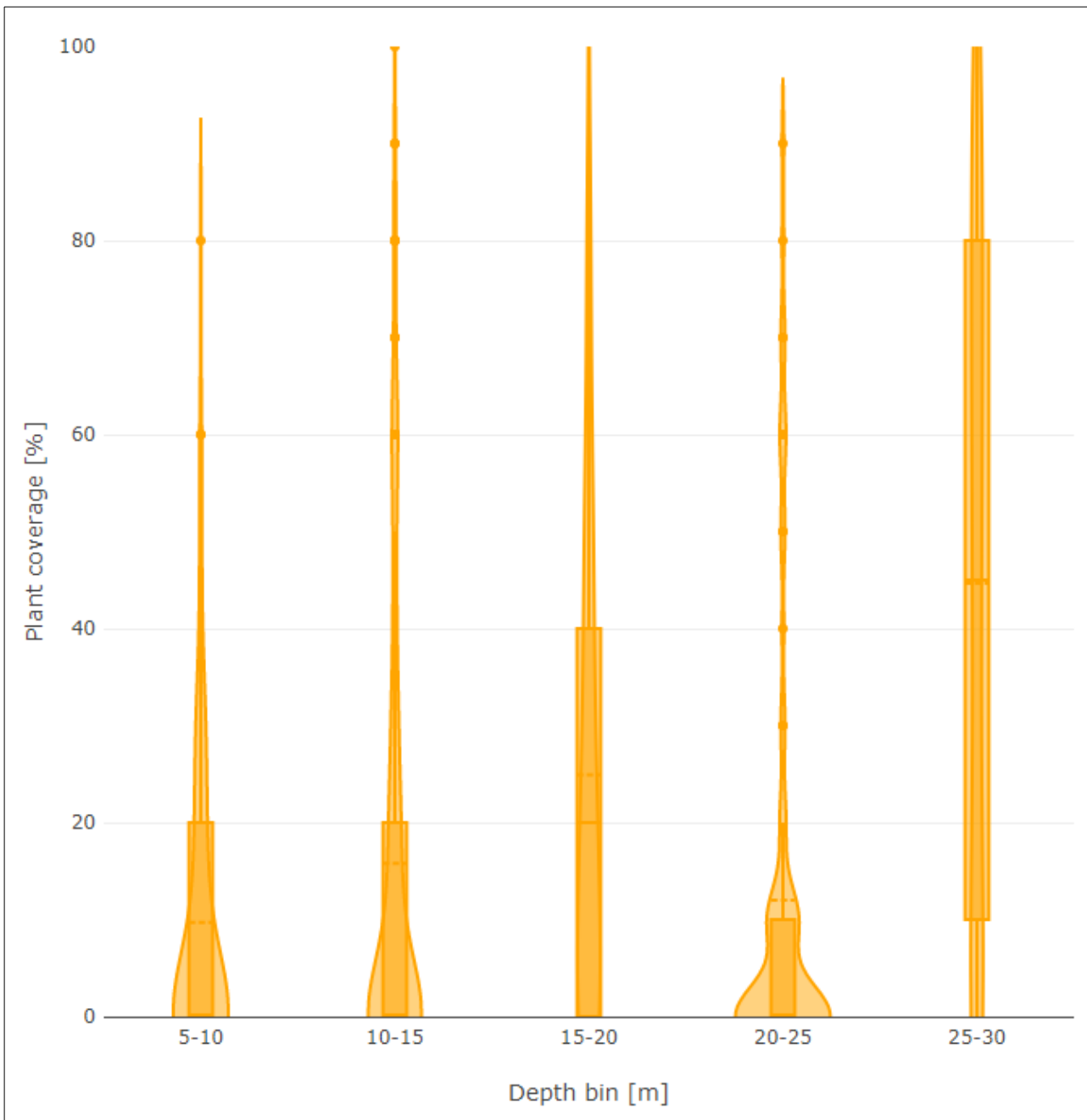


**Figure 18:** Plant coverage at the glacier station (GLA) for the 5 depth bins. Binned data is portrayed as boxplots with violin plots to illustrate the quantitative distribution of plant coverage values. Dots are outliers, the dashed line shows the mean values and the solid line represents the median. The central vertical lines show the standard deviation and the boxes the upper and lower central quartile where 50 percent of the data is located.

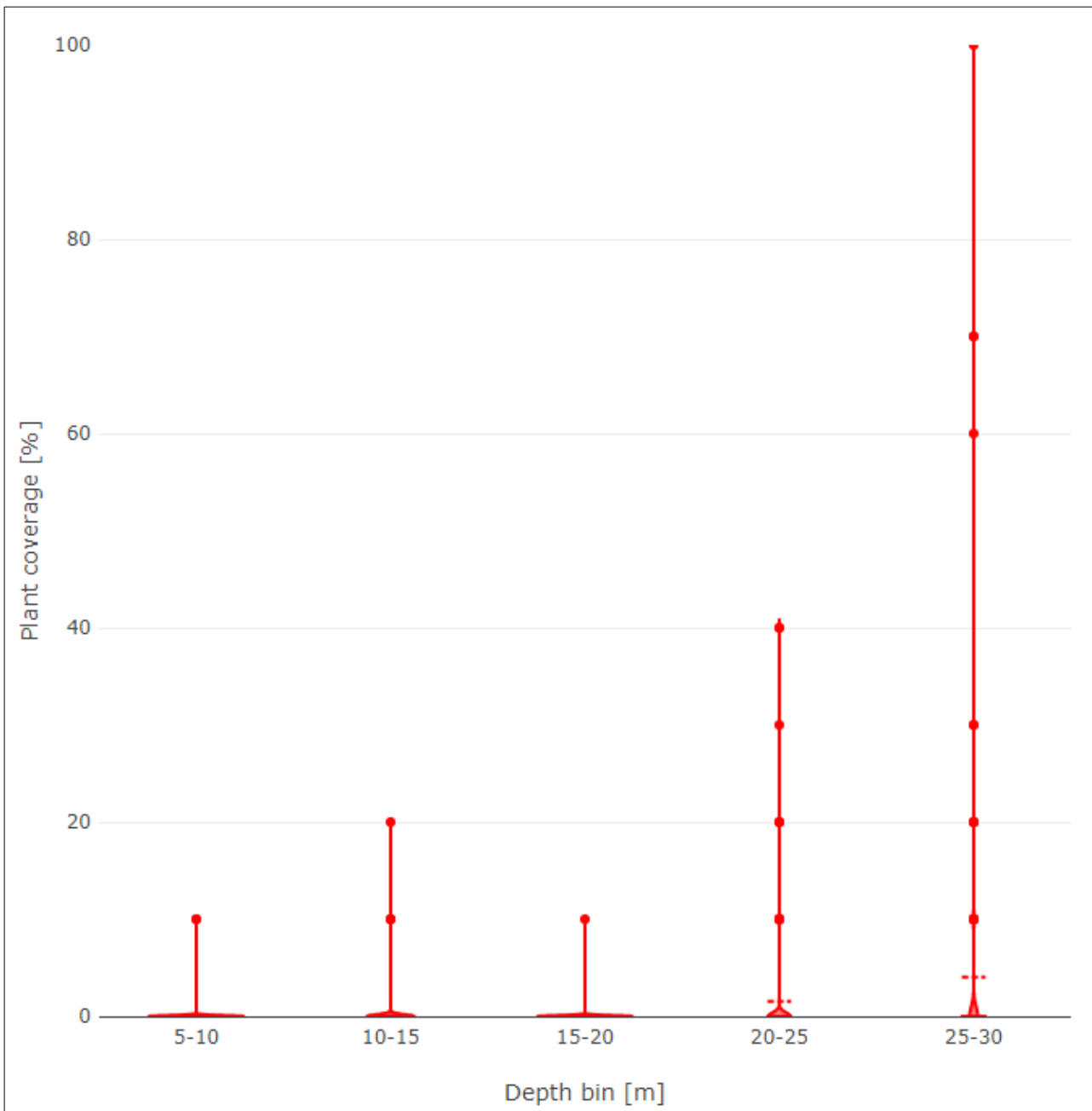


**Figure 19:** Plant coverage at the freshwater station (FRE) for the 5 depth bins. Binned data is portrayed as boxplots with violin plots to illustrate the quantitative distribution of plant coverage values. Dots are outliers, the dashed line shows the mean values and the solid line represents the median. The central vertical lines show the standard deviation and the boxes the upper and lower central quartile where 50 percent of the data is located.

The maps confirm that the ICE and FRE station did have fewer overall plant coverage and a seemingly less heterogenous coverage pattern compared to the GLA station. The plant coverage was higher with increasing distance to the shoreline at the freshwater and glacier station within the surveyed depth range, contrasting the maximum values in shallower depths at the sea-ice station (Fig. 20, 21, 22). Another observable feature across stations was the "striped" pattern caused by the alternatingly higher (measured up the slope) and lower (measured down the slope) plant coverage values across neighbouring transects.

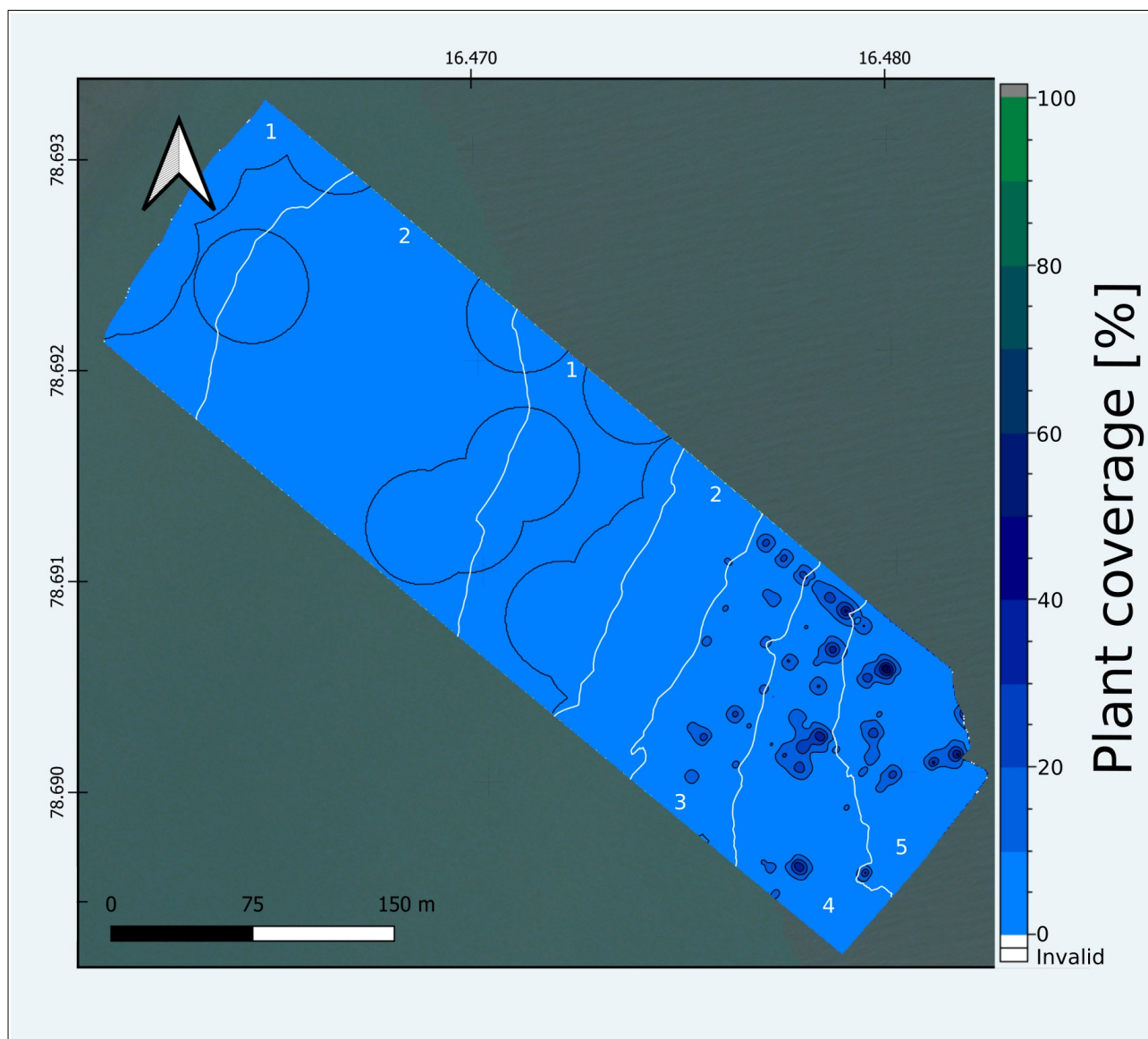


**Figure 20:** Gridded plant coverage data for the freshwater station. The white lines represent the bottom depth contour lines numbered from 1-5 (1: 5-10m, 2: 10-5m, 3: 15-20m, 4: 20-25m, 5: 25-30m). The large circular contours in the first two depth bins were an artefact of the plant detection algorithm. Plant coverage in these regions equals 0. Upper and left axes show the longitude and latitude, respectively. The colour graded scale on the right shows the respective plant coverage values. Basemap data from the Norwegian Polar Institute geological map services (Orthophoto from 2009).

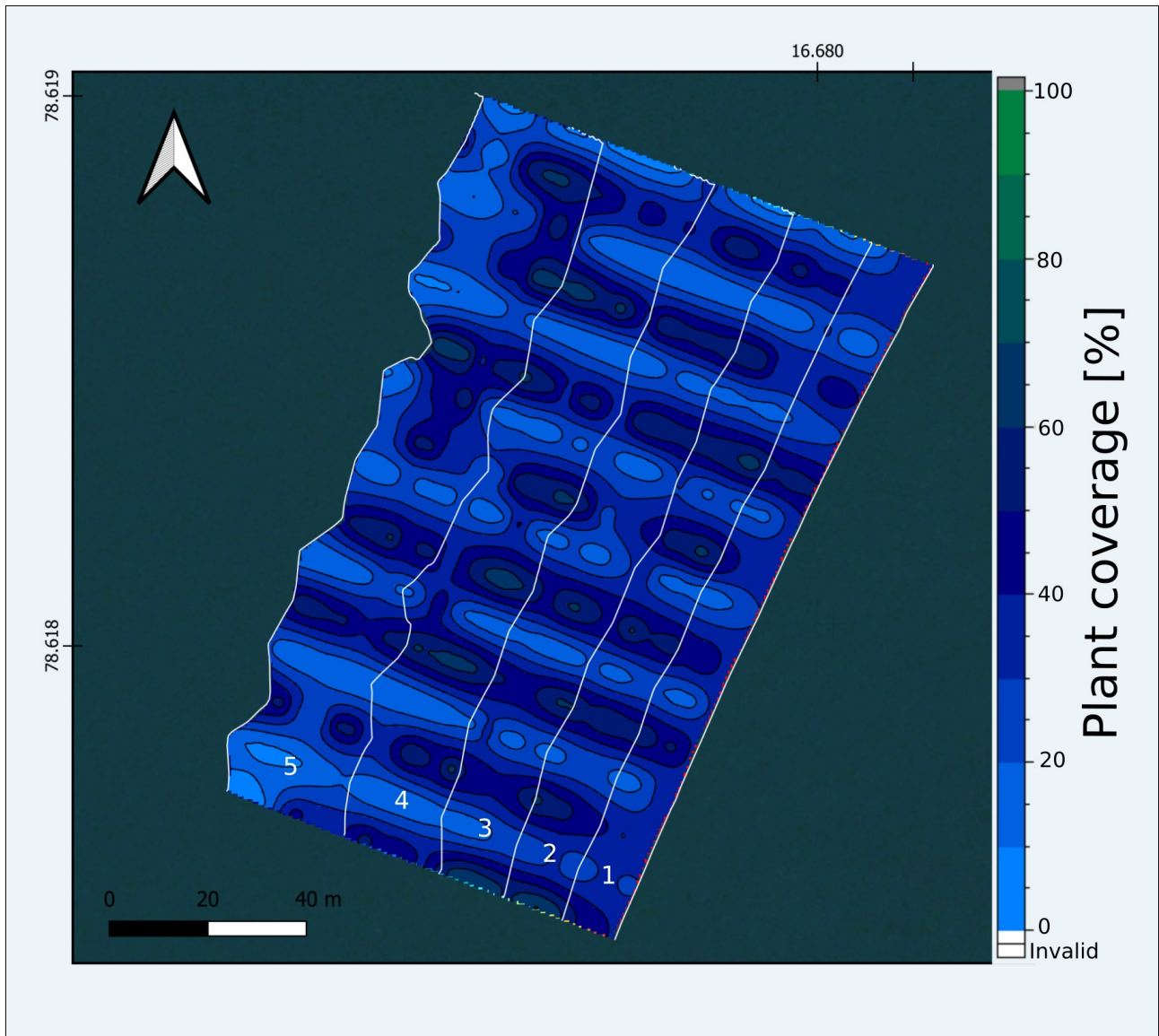


**Figure 21:** Gridded plant coverage data for the sea-ice station. The white lines represent the bottom depth contour lines numbered from 1-5 (1: 5-10m, 2: 10-5m, 3: 15-20m, 4: 20-25m, 5: 25-30m). Upper and left axes show the longitude and latitude, respectively. The colour graded scale on the right shows the respective plant coverage values. Basemap data from the Norwegian Polar Institute geological map services (Orthophoto from 2009).

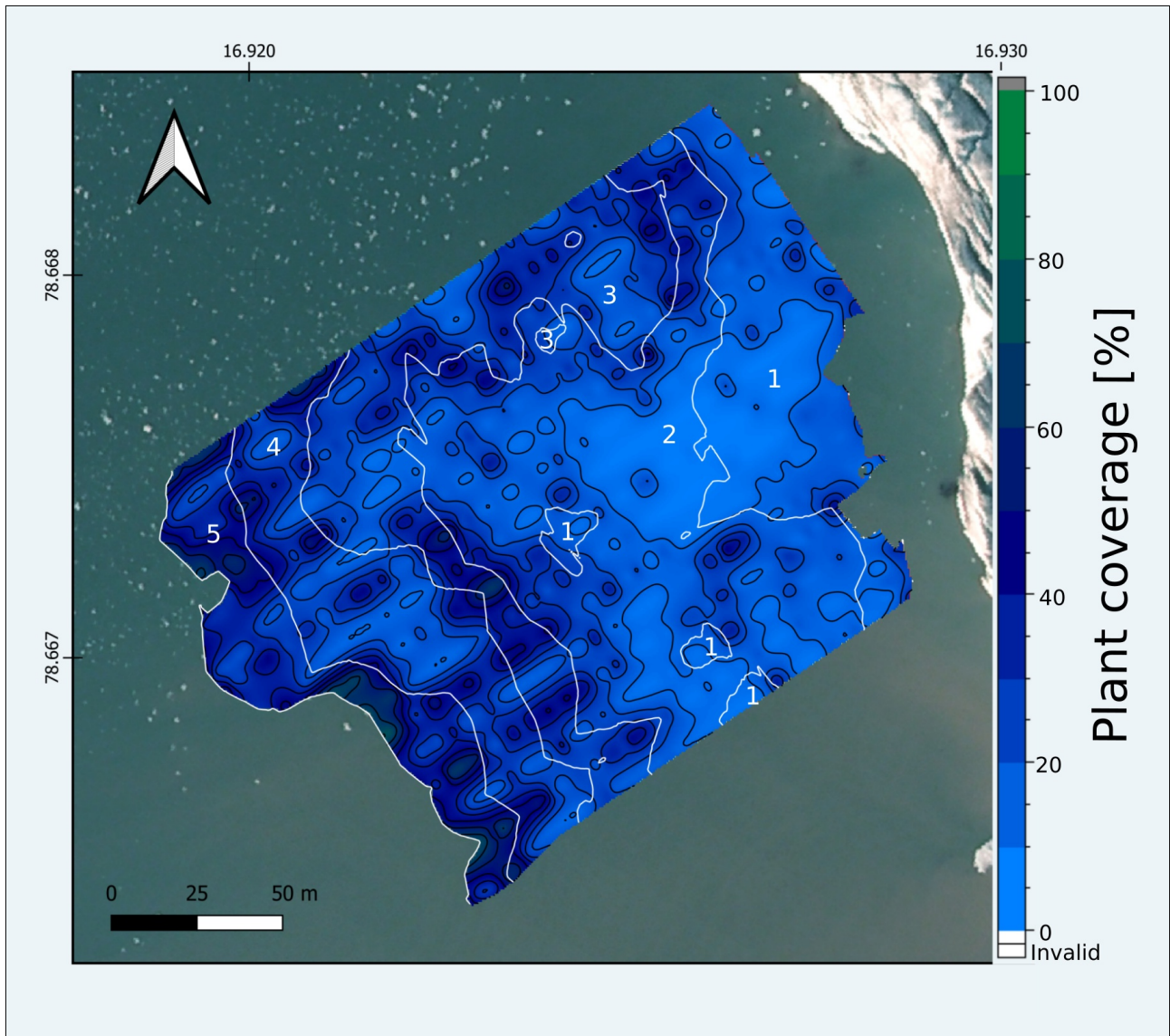


**Figure 22:** Gridded plant coverage data for the glacier station. The white lines represent the bottom depth contour lines numbered from 1-5 (1: 5-10m, 2: 10-5m, 3: 15-20m, 4: 20-25m, 5: 25-30m). Upper and left axes show the longitude and latitude, respectively. The colour graded scale on the right shows the respective plant coverage values. Basemap data from the Norwegian Polar Institute geological map services (Orthophoto from 2009).

### 3.3 Effect of Environmental Parameters on Macroalgal coverage

To determine which factors should be modeled with plant coverage for the different stations, a spearman correlation analysis has been conducted (Tab. 5). A sufficiently strong correlation between factors to conclude a statistically similar effect of the correlated drivers on plant coverage would have been assumed at values higher than 0.80. This was only the case for the relation of depth and salinity. In the generalized linear models of each stations' plant coverage, the relation to every single driver was still explored. More detailed values of plant coverage and the CTD data can be found in the appendix (Tab. 9). The raw CTD data is attached in the digital appendix.

*Table 5: Spearman correlation coefficient results for the three observed abiotic factors (temperature, salinity, turbidity) and water depth across all stations.*

	Temperature	Salinity	Turbidity	Depth
Temperature	1	0.65	-0.52	0.63
Salinity	0.65	1	-0.14	0.83
Turbidity	-0.52	-0.14	1	-0.25
Depth	0.63	0.83	-0.25	1

The only significant results were produced for temperature at the glacier station ( $p < 2.07e-09$ ) and salinity at the freshwater station ( $p < 3.817e-06$ ) (Fig. 23, 24). All of the p-values for the models of the other parameters have been calculated and listed (Tab. 6).

The relation between temperature and plant coverage at the glacier station was positive, which means, that increasing values of temperature correlated with higher values for plant coverage (Fig. 23). The relation between salinity and coverage at the freshwater station was also positive but less significant (Fig. 24). Positive trends between coverage and temperature or turbidity at the freshwater station were statistically insignificant (Tab. 6). At the sea-ice station no significant relations between plant coverage and temperature, salinity or turbidity could be proven.

Mean values for salinity at the different bins at the freshwater station ranged from 31.3 to 34.1 psu, while temperature at the glacier station ranged from 1.6 to 1.9 °C (Appendix: Tab. 9). The range of binned plant coverage values was also higher for the glacier station with mean values ranging from 9.7 to 44.7% opposed to 0.05 to 4.05% at the freshwater station (Appendix: Tab. 9).

**Table 6:** P-values for Anovas (Type F) of the GLM's. Values are given for plant coverage (PC) at each station and for all potential drivers. FRE – freshwater station, GLA – glacier station, ICE – sea-ice station. Signif. codes: 0 ‘\*\*\*’ 0.001 ‘\*\*’ 0.01 ‘\*’ 0.05 ‘.’ 0.1 ‘ ’ 1

Station	PC:Temperature	PC:Salinity	PC:Turbidity
FRE	0.064151 .	3.817e-06 ***	0.07383 .
GLA	2.07e-09 ***	0.4962736	0.980796
ICE	0.5663	0.7169	0.2201

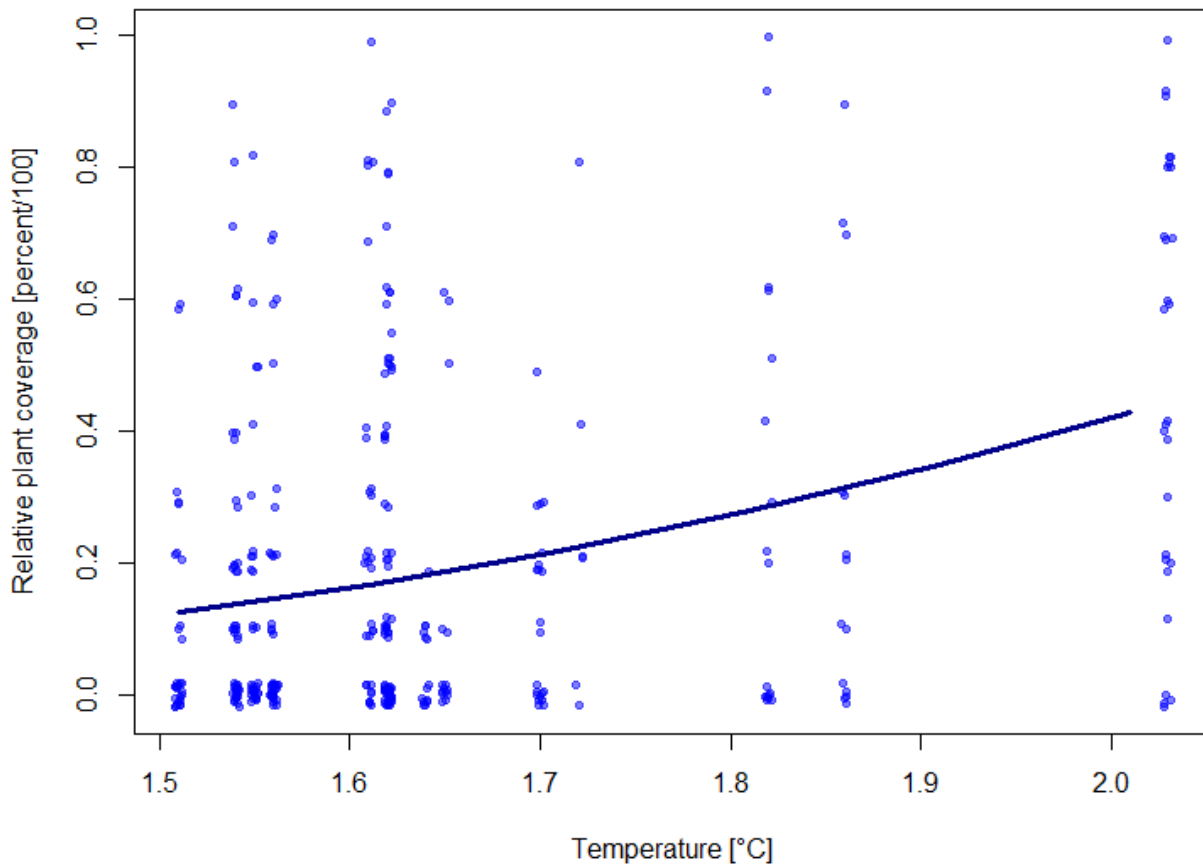


**Figure 23:** GLM for the plant coverage in relation to temperature at the glacier station. The blue data points are the jittered plant coverage percentage values.  $P < 2.07e-09$  \*\*\*, P-value significance codes: 0 ‘\*\*\*’ 0.001 ‘\*\*’ 0.01 ‘\*’ 0.05 ‘.’ 0.1 ‘ ’ 1.



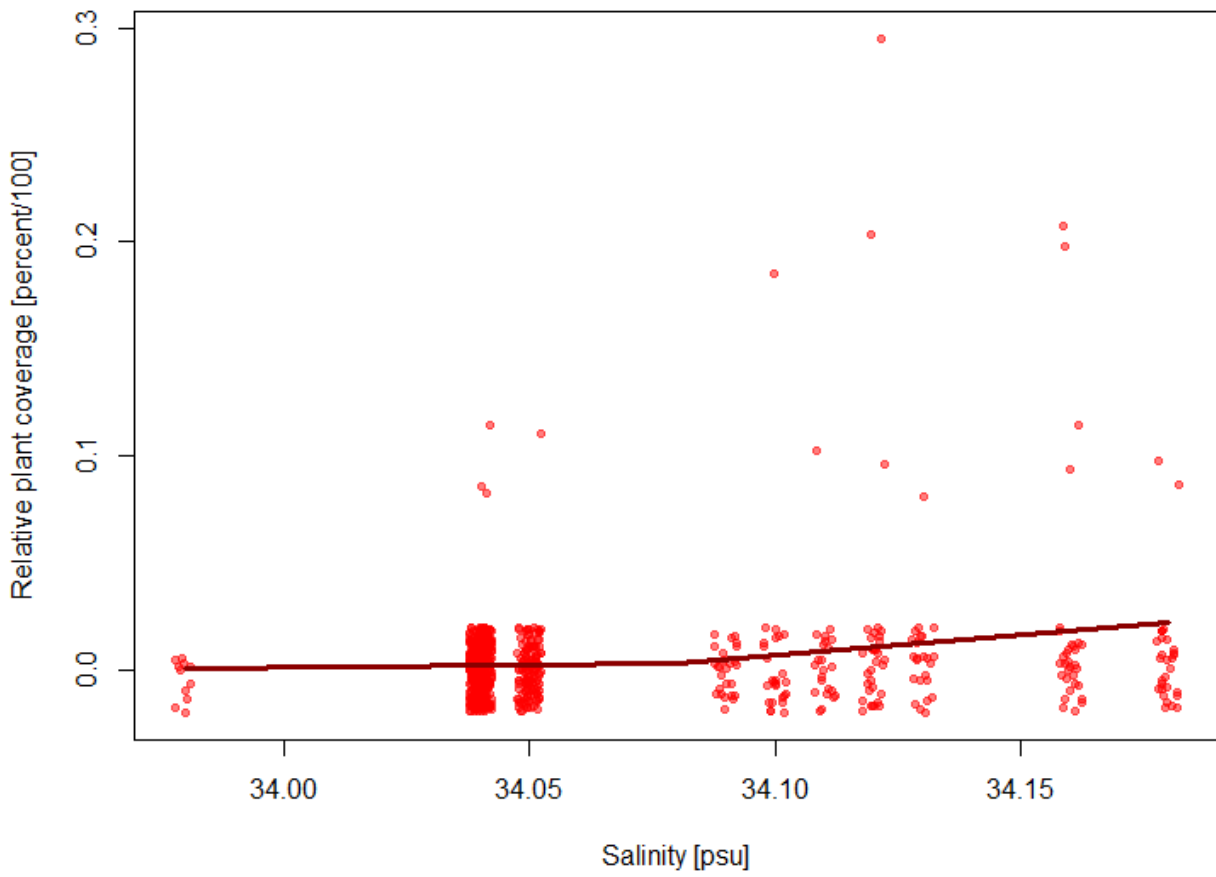


**Figure 24:** GLM for the plant coverage in relation to temperature at the freshwater station. The red data points are the jittered plant coverage percentage values.  $P < 3.817e-06$  \*\*\*, P-value significance codes: 0 '\*\*\*' 0.001 '\*\*' 0.01 '\*' 0.05 '.' 0.1 ' ' 1.

## 4 Discussion

### 4.1 Differences in Plant Coverage Between Stations

The results of this study have shown clear differences of mean macroalgal coverage between the three sampling stations (Fig. 15). In decreasing order, coverage was highest at the glacier (21.96%), sea-ice (9.54%) and freshwater station (0.64%) (Tab. 3). These differences may be explained by the varying environmental framework conditions at each station.

The freshwater station is located in an estuarine bay with a large tidal flat and overall high input of freshwater and sediments via fluvial streams and rivers that are fed by 170 km<sup>2</sup> of drainage area (Søreide *et al.*, 2021; Strzelecki, 2012). Sediments entering the fjord via rivers typically settle on the seafloor within a few hundred metres of the exit point. When they are released directly from a sea-terminating glacier front, they are typically dispensed in the water column for a longer time and settle down at ca. 2-3 km distance (Szczeniński *et al.*, 2009).

Coastal classifications by Søreide *et al.* (2021) characterised the coast in Petuniabukta as a predominantly soft bottom type. A soft bottom seafloor created by high rates of sedimentation could explain the strikingly low amount of kelp growth, since they often rely on rocky substrates to adhere to (Steneck *et al.*, 2002; Wulff *et al.*, 2009). Similarly, the sedimentation may increase turbidity in the water column which in turn has a negative effect on macroalgae by reducing the euphotic zone and decreasing the photosynthetically active radiation available at the seafloor. Other studies have also found clear negative effects of sedimentation on the germination rates of kelps, altering the successful recruitment of sporophytes (Traiger & Konar, 2018; K. Zacher *et al.*, 2016). For example, an experiment from 2012 demonstrated that "suspended particles, settled sediment covering the substratum and smothering of attached spores" all had a negative effect on the spore attachment of two kelp species of the order Laminariales (Deiman *et al.*, 2012). Specifically, they showed a 90% decrease in spore attachment at a treatment of 420 mg of sediment per liter.

The relatively high plant coverage at the glacier station may seem counterintuitive at first, since high sedimentation rates and freshwater input are typical for sea-terminating glacier fronts as well (Lydersen *et al.*, 2014; Szczeniński *et al.*, 2009). With 265 km<sup>2</sup> the drainage area for Adolfbukta is also higher than for Petuniabukta and dominated by Nordenskiöldbreen (Strzelecki, 2012). However, the fact that sediments usually travel further before settling on the seafloor when emitted from tidewater glacier fronts combined with a mostly rocky substrate in front of the glacier, might constitute to more favourable conditions for macroalgal communities to establish (Strzelecki, 2012).

Since the LIA, Nordenskiöldbreen retreated about 3.5 km revealing approximately 17 km<sup>2</sup> of rocky para-periglacial landscape (Strzelecki, 2012). This means, that novel potential settling substrate for macroalgae has been exposed. The station was located near a section of the shore, where the glacier has already retreated to land, implying less mechanical disturbances from calving events. An increase of Arctic kelp abundance due to less sea-ice scouring has already been proposed by Weslawski *et al.* (2010) who discovered a threefold increase of littoral macrophyte biomass over the last 20 years in Sorkapland (Svalbard). The high plant coverage values at the glacier station in comparison to the two other stations could certainly be the result of recent landward glacial retreat, leading to the development of new habitat space for macroalgal communities. These findings also deliver important information on the time it takes macroalgal communities to populate such habitats once they have been exposed. Judging from data by the Norwegian Polar Institute's geological mapping services, the glacier front of Nordenskiöldbreen has ceased to be sea-terminating in that area around 2017, which suggests a potential repopulation time of at least 4 years in front of the glacier (Fig. 34).

The sea-ice station is located near Kapp Scott on the east coast of Billefjorden and has comparatively little to no big river deltas exiting at its coastal section. Comparisons with sea-ice charts for the winter 2020/21 indicate a coastal winter sea-ice coverage with mostly "very open drift ice" to "fast ice" between January and March (Fig. 26-31). Therefore, the environmental conditions in terms of ice-scouring and freshwater input should be less extreme than at the other two stations, which appear to be covered by continuous fast sea-ice for a longer period during winter (February to May, 2021). Therefore, it seems plausible that plant coverage is higher than at the freshwater station which is subjected to stronger seasonal changes of fluvial and sediment inputs and also, that it is decreasing with depth, while it seemingly increases with depth at the other two stations. The pronounced differences in coverage between the glacier and sea-ice station are mainly caused by the anomalously high plant coverage between 25 and 30 metres at the glacier station. A possible explanation might be differences in settling substrate or a false-positive detection of plants on steeper slopes.

## **4.2 Macroalgal Coverage per Depth and Station**

Macroalgal coverage strongly increased with depth at the glacier station and slightly at the freshwater station while it decreased with depth at the sea-ice station (Fig. 16). No clear upper and lower distribution limits could be identified for any station within the given depth range. Patterns and trends in the gridded maps and binned violin plots hint at a lower distribution limit for

macroalgae between 20 and 25 m for the ICE station and possibly an upper limit within the littoral range outside of the survey depth range (Fig. 17-22).

Comparisons with previous studies in Svalbard suggest an approximate depth distribution range of 5 to 15 m for kelp with peak biomass values around 5 m (Bartsch *et al.*, 2016; Wulff *et al.*, 2009). A study comparing macroalgal depth distribution at Hansneset (Kongsfjorden) between 1996/1998 and 2012/2013 even discovered a shift in peak kelp biomass from 5 to 2.5 m proposing a "lack of ice-scouring, elongation of the open-water period and deterioration of the underwater irradiance climate" as the most likely reasons (Bartsch *et al.*, 2016). Peak plant coverage values for the ICE, GLA and FRE station were in the 5-10 m, 25-30 m and 25-30 m bin, respectively. While these values align with the expected depth distribution at the ICE station, they diverge quite strongly from the expected pattern at the other two stations.

At the glacier station, higher turbidity in the water column through sediment discharge should expectedly modulate the euphotic zone and restrict kelp growth to shallower regions while mechanical disturbances by annual winter sea-ice formation should dictate the upper limit for plant growth (Hop *et al.*, 2012; Wulff *et al.*, 2009). At the freshwater station, the depth distribution is most likely dictated by turbidity and salinity in the water column because of the high amounts of freshwater and sediment discharge in the immediate vicinity. Plant coverage should, therefore, be highest in shallower depth bins than observed in this study.

A possible explanation for the coverage maxima in the 25-30 m bins could be a higher incidence angle of the seafloor in those areas. This is indeed the case for the deepest bins at the glacier and freshwater station. At the sea-ice station the slope was much more even in terms of steepness over the entire length of the transects. The backscattering signal strength is modulated by the angle at which it hits the seafloor and may have had an effect on the plant coverage signal strength (Kruss *et al.*, 2017; Lurton *et al.*, 2018). A steeper slope can result in a weaker backscattering signal. As a consequence, the plant detection algorithm might have detected unusually high plant coverage in those areas. Disregarding the deepest depth bin at the glacier station and looking only at the range of 5-25 m, would shift the plant coverage maximum to 15-20 m for the glacier station, which seems more reasonable. The freshwater station would have close to 0% plant coverage over the entire sampling range.

Another factor potentially contributing to the anomalously deep distribution limits of macroalgae at the glacier station might be connected to the echosounder settings and developmental stages of macroalgae in shallower depths. Considering, that the coastal section in front of the glacier station

was still largely covered by the glacier until about 2017 (Appendix: Fig. 34) and that Adolfbukta is usually covered by fast sea-ice in winter (Appendix: Fig. 26-31), the macroalgae that establish these new and shallower settling substrates may predominantly be young specimen that could be too small for the set plant report height threshold of 20 cm. This becomes an even more important aspect, when assuming that most of the kelp is not standing erect in the water column but rather laying on the substrate. This is hypothetical at this point and needs to be verified to make a definitive statement.

The general differences in plant coverage between the stations could be partly validated and confirmed by baited remote underwater video (BRUV) drop camera observations that were conducted in parallel to this study for assessment of fish communities at the stations. These were done at an approximate depth of 10 m and showed no plant coverage at the freshwater station, very little at the glacier station and a very thick canopy of mostly *Saccharina latissima* at the sea-ice station. To conquer the uncertainties for plant coverage at greater depth (>20 m), a more comprehensive in situ ground truthing of the plant coverage via a standardised approach of underwater camera validation would be expedient.

### **4.3 Effect of Environmental Parameters on Macroalgal Coverage**

Potential effects of the environmental parameters on the plant coverage at the three stations have been observed (Fig. 23, 24, Tab. 6). Statistically significant, positive relationships have been revealed for the freshwater station and salinity ( $p < 3.817e-06$ ) as well as the glacier station and temperature ( $p < 2.07e-09$ ). Plant coverage at the ICE station did not exhibit any significant trends with respect to the same abiotic factors.

The conclusion, that low salinity at the freshwater station affects plant coverage seems plausible due to the high amount of freshwater input. A study on some of the most common Arctic kelp species (*L. digitata*, *A. esculenta*, *S. latissima*, and *L. solidungula*) showed signs of stress in the form of strong bleaching, loss of pigments or even elevated mortality rates when exposed to hyposaline (5 psu) conditions (Karsten, 2007). Their Effective quantum yields were measured at salinities ranging from 5 to 60 psu with two or five day treatments and then compared to their maximum quantum yields (control). *A. esculenta*, *S. latissima* and *L. solidungula* showed strongly reduced effective quantum yields (< 25% of control) and bleaching under hyposaline conditions of 5 psu after both 2 and 5 days. *L. digitata* seemed to be more resilient and only decreased its photosynthetic performance by approximately 40% at hypo- and hypersaline conditions (Karsten, 2007).

Overall, hypersaline conditions were much better tolerated than hyposaline treatments among the tested species. Other studies demonstrated, how lower salinity levels of around 20 psu already have the potential to inhibit germination and photosynthesis in spores of *A. esculenta*, while reduced growth and bleaching occurred in an experiment of prolonged hyposaline exposure to *S. latissima* (Fredersdorf *et al.*, 2009; Li *et al.*, 2020). Severe pigment bleaching in *S. latissima* occurred after 18 days in a treatment of 20 psu and at 0°C (Li *et al.*, 2020).

However, the correlation between an increasing salinity and plant coverage at the freshwater station is based on a rather low range of salinity and overall little plant coverage in this study. Therefore, the small salinity range is not sufficient to conclude a causal relationship. This is especially true, since the focus was put on the station wide comparison of parameters and macroalgal coverage and did not take into account the seasonal variations, which play an important role in modulating environmental parameters (Wulff *et al.*, 2009). Discharge rates are for instance usually much higher at river deltas and tidewater glaciers during summer (Karsten, 2007).

Given the fact, that measurements of the parameters were only contributing to the establishment of a "snapshot" of the environmental framework at each station and the macroalgal communities integrate changes of these parameters over time, conclusions should be made carefully from these findings. A specific spearman correlation of parameters at the freshwater station also revealed a strong correlation (coefficient > 0.8) of salinity and depth, hinting, that plant coverage might rather be dependent on depth judging from this data.

The positive relation of plant coverage and increasing temperature at the glacier station is prone to the same uncertainties caused by seasonal and depth dependent dynamics of the environmental parameters. However, the analysis of depth and temperature at the glacier station did not show a very strong correlation (coefficient = 0.71). Rising temperatures are considered to be one of the major environmental drivers influencing macroalgal communities in a steadily warming Arctic and a negative effect of temperatures on kelp abundance or coverage is to be expected when physiological thresholds are outpaced by rising temperature levels (Smale, 2020). These effects contain "increased mortality, decreased abundance, altered size structure, local extirpation and range contractions" (Smale, 2020).

The upper survival temperatures (UST) for abundant Arctic kelp gametophytes were tested (*A. esculenta*, *S. latissima* and *L. solidungula*, *S. latissima*) and ranged from 20 to 25 °C while being lowest for the endemic *Laminaria solidungula* (tom Dieck, 1993). This means, they are generally capable of tolerating temperatures much higher than the ambient water temperatures. However, the

gradual predicted increase in global sea surface temperatures may still have the potential to restructure coastal kelp communities in Arctic fjords because of species specific optimum temperature ranges and environmental temperature niches (Smale, 2020). This could for example be due to differences in successful growth and developmental or stage specific survival of the different cold-temperate macroalgal species in the Arctic.

A study published in 2019 investigated the temperature effects on the interactions of different early life-history stages of *A. esculenta* and *Laminaria digitata* in co-culture (Zacher *et al.*, 2019). In both species, an increase in physiological activity was observed when temperatures were raised by 5°C from their respective environmental summer temperatures of 4 – 5°C to the global warming scenario of 9 - 10°C in the Arctic. At 15°C the formation of sporophytes and gametes was impaired strongly in the monoculture of *A. esculenta* compared to *L. digitata*. In coculture with digitate kelps at 9°C, an interactive effect of competition and temperature on *A. esculenta* was observed, effectively boosting its germination rates in comparison to the monoculture treatment. Similarly, sporophyte growth was accelerated greatly for *A. esculenta* in coculture at 9°C. *L. digitata* showed no significant differences of such sort between treatments, proposing a competitive and physiological advantage for *A. esculenta* in a global warming scenario of 10°C water temperature for the Arctic (Zacher *et al.*, 2019).

Some studies suggest that productivity and biodiversity of macroalgae already has and may increase further in the near future with rising ambient water temperatures (Krause-Jensen & Duarte, 2014). This is mostly due to decreased sea-ice cover and longer open water periods (Smale, 2020). A study focusing on the transcriptomic responses of *Saccharina latissima* under elevated temperature treatments also showed, that the kelp was increasing its physiological performance at a temperature of 8 - 15°C hinting at its capability to successfully adapt to increasing temperature regimes (Li *et al.*, 2020).

At the time, negative effects of rising water temperatures and climate warming might be more visible on a level of geographical macroalgal distribution instead of the local depth zonation pattern in Arctic ecosystems. A poleward shift of kelp communities due to temperatures exceeding their physiological tolerances at the low latitudinal range limits is an ongoing process (Beas-Luna *et al.*, 2020; Smale, 2020). The large-scale shift in populations of *S. latissima* to mostly filamentous brown and red algae communities in the rocky sublittoral of southern Norway for instance is largely attributed to elevated water temperatures as one of the major drivers together with nutrient and particle pollution (Moy & Christie, 2012).

Furthermore, a more immediate and indirect effect of rising temperatures in Arctic coastal ecosystems will probably take effect through the elevated freshwater and sediment inputs caused by increased melting rates of sea- and land-terminating glaciers (Li *et al.*, 2020).

The sea-ice station did not show any significant trends of the drivers affecting plant coverage (Tab. 6). The environmental parameter influencing plant coverage the most seemed to be depth in this region. This difference to the results from the other stations might be due to the absence of large river deltas or glaciers in the immediate surroundings of the ICE station. Therefore, turbidity and salinity should be less of a driver. Depth and mechanical disturbances by winter sea-ice formation should be more important in structuring the macroalgal distribution pattern and setting the limits for upper and lower distribution. This would concur with the finding, that plant coverage decreased with increasing depth, most likely because of decreasing levels of light availability.

In order to derive ecological implications from this spatial analysis to predict future changes in plant coverage in Arctic fjord ecosystems, it may be useful to evaluate the three different stations as representing different developmental stages of the Arctic environment with respect to the effects of climate change.

Consequently, the freshwater station with high amounts of fluvial and sediment input may provide insights into how other regions in Arctic fjords might develop in the long term future with respect to increasing rates of sedimentation and freshwater discharge, resulting in very low plant coverage rates. The glacier station may represent a more immediate scenario where reduced mechanical disturbances by winter sea-ice or calving and the expansion of suitable coastal settling substrate for kelp increase plant biomass and coverage. The sea-ice station presumably represents an area less affected by rising temperatures or river discharge, where communities are still majorly modified by winter sea-ice formation and depth dependent light attenuation. A long-term gradual transition of ICE and GLA type stations into FRE type regions driven by changes in salinity, turbidity and temperature could be likely.

The complex spatially and temporally modified interactions of environmental parameters in the Arctic make it difficult to make large-scale assumptions and the actual manifestation of these changes will probably vary to some extent between Arctic fjords and their environment.



## 4.4 Conclusion

The experimental set up of USV, DT-X and CTD proved to be a highly effective and non invasive tool for surveying Arctic macroalgal habitats. Significant differences in plant coverage between the stations have been revealed, while simultaneously providing a potential explanation with respect to the overall differences of the environmentally distinct conditions. However, the monitoring of environmental drivers at a specific point in time introduces certain limitations for the interpretation of plant coverage data. A conflict between the spatial and temporal component of the data exists, meaning that the environmental data is more suitable in highlighting overall differences between the stations rather than revealing causal relationships between the drivers and macroalgal coverage. The differences in trends and relationships between the stations seemed plausible when comparing the findings with relevant literature. This "space-for-time" substitution can be a valid approach trading off the seasonal resolution of environmental parameters for a spatially comparative and large-scale assessment of plant coverage, that still allows to infer the effect of these parameters via distinct regional settings of the sampling stations and the inherent environmental differences between them.

To further strengthen or verify the approach and findings of this study, a combination of these remote sampling techniques and in situ methods for detailed validation of the echosounder data in the future would be expedient and desirable. The spatial study could also be complemented with a time series of CTD measurements at the different stations to better understand the relation of plant coverage and environmental drivers in Arctic kelp communities. The exact extent to which kelp distribution and abundance will be affected in Arctic coastal ecosystems, differs with respect to species specific physiological tolerance levels. An analysis of species composition at the different stations would contribute to a better understanding of the zonation patterns and might allow better conclusions from the respective environmental framework conditions to the patterns of plant coverage. A detailed classification of bottom type and the inclusion of the littoral zone and a more "Atlantic" station in Isfjorden would also help to build a better fundament for the discussion of these findings.

Isolating the effects of single environmental drivers on macroalgal communities is made difficult by the complex spatial and temporal interactions of parameters and their combined effects. Fundamental differences in plant coverage at the different stations could still be observed and should be developed further by studies focusing on the in situ validation of the echosounder data and seasonal aspects of the drivers.

## 5 Acknowledgements

Thank you to Børge Damsgård and Kai Bischof as my main supervisors for making this collaboration possible in the first place as well as their continuous support and help in planning, undertaking and realizing this project as my thesis.

Special thanks go out to Victor Gonzalez Triginer as my project colleague at UNIS throughout the entire planning process and field work of this study.

I would like to thank Ben Thomsson, Cheshtaa Chitkara, Snorre Flo & Samira Terzenbach for their crucial assistance during fieldwork in Billefjorden.

Thanks to Benedikt Merk for his substantial help with the statistical analysis as well as moral and critical support throughout the process of writing this thesis.

A warm thank you also belongs to my family, close friends and studying colleagues who made my stay on Svalbard an unforgettable and rewarding experience in my life and career as a becoming scientist.

Thanks to the "Departement of Arctic Biology" at UNIS for accepting me as a guest master student during my stay on Svalbard and welcoming me into their team.

This project has received funding from the European Union's Horizon 2020 research and innovation programme in the frame of the FACE-IT project under grant agreement No 869154.

## 6 References

- Al-Habahbeh, A. K., Kortsch, S., Bluhm, B. A., Beuchel, F., Gulliksen, B., Ballantine, C., Cristini, D., & Primicerio, R. (2020). Arctic coastal benthos long-term responses to perturbations under climate warming: Climate change impact on Arctic benthos. *Philosophical Transactions of the Royal Society A: Mathematical, Physical and Engineering Sciences*, 378(2181).  
<https://doi.org/10.1098/rsta.2019.0355>
- Assis, J., Lucas, A. V., Bárbara, I., & Serrão, E. Á. (2016). Future climate change is predicted to shift long-term persistence zones in the cold-temperate kelp *Laminaria hyperborea*. *Marine Environmental Research*, 113, 174–182. <https://doi.org/10.1016/j.marenvres.2015.11.005>
- Bartsch, I., Paar, M., Fredriksen, S., Schwanitz, M., Daniel, C., Hop, H., & Wiencke, C. (2016). Changes in kelp forest biomass and depth distribution in Kongsfjorden, Svalbard, between 1996–1998 and 2012–2014 reflect Arctic warming. *Polar Biology*, 39(11), 2021–2036.  
<https://doi.org/10.1007/s00300-015-1870-1>
- Beas-Luna, R., Micheli, F., Woodson, C. B., Carr, M., Malone, D., Torre, J., Boch, C., Caselle, J. E., Edwards, M., Freiwald, J., Hamilton, S. L., Hernandez, A., Konar, B., Kroeker, K. J., Lorda, J., Montaña-Moctezuma, G., & Torres-Moye, G. (2020). Geographic variation in responses of kelp forest communities of the California Current to recent climatic changes. *Global Change Biology*, 26(11), 6457–6473. <https://doi.org/10.1111/gcb.15273>
- Bischof, K., Buschbaum, C., Fredriksen, S., Gordillo, F. J. L., Heinrich, S., Jiménez, C., Lütz, C., Molis, M., Roleda, M. Y., Schwanitz, M., & Wiencke, C. (2019). *Kelps and Environmental Changes in Kongsfjorden: Stress Perception and Responses* (pp. 373–422).  
[https://doi.org/10.1007/978-3-319-46425-1\\_10](https://doi.org/10.1007/978-3-319-46425-1_10)
- Box, J. E., Colgan, W. T., Christensen, T. R., Schmidt, N. M., Lund, M., Parmentier, F. J. W., Brown, R., Bhatt, U. S., Euskirchen, E. S., Romanovsky, V. E., Walsh, J. E., Overland, J. E., Wang, M., Corell, R. W., Meier, W. N., Wouters, B., Mernild, S., Mård, J., Pawlak, J., & Olsen, M. S. (2019). Key indicators of Arctic climate change: 1971-2017. In *Environmental Research Letters* (Vol. 14, Issue 4, p. 045010). Institute of Physics Publishing.  
<https://doi.org/10.1088/1748-9326/aafc1b>
- Bring, A., Fedorova, I., Dibike, Y., Hinzman, L., Mård, J., Mernild, S. H., Prowse, T., Semenova, O., Stuefer, S. L., & Woo, M. K. (2016). Arctic terrestrial hydrology: A synthesis of processes, regional effects, and research challenges. In *Journal of Geophysical Research G: Biogeosciences* (Vol. 121, Issue 3, pp. 621–649). Blackwell Publishing Ltd.  
<https://doi.org/10.1002/2015JG003131>
- Carroll, D., Sutherland, D. A., Shroyer, E. L., Nash, J. D., Catania, G. A., & Stearns, L. A. (2015). Modeling turbulent subglacial meltwater plumes: Implications for fjord-scale buoyancy-driven circulation. *Journal of Physical Oceanography*, 45(8), 2169–2185.  
<https://doi.org/10.1175/JPO-D-15-0033.1>

- Chu, V. W., Smith, L. C., Rennermalm, A. K., Forster, R. R., & Box, J. E. (2012). Hydrologic controls on coastal suspended sediment plumes around the Greenland Ice Sheet. *Cryosphere*, 6(1), 1–19. <https://doi.org/10.5194/tc-6-1-2012>
- Comiso, J. C. (2002). A rapidly declining perennial sea ice cover in the Arctic. *Geophysical Research Letters*, 29(20), 17–1. <https://doi.org/10.1029/2002GL015650>
- Dankworth, M., Heinrich, S., Fredriksen, S., & Bartsch, I. (2020). DNA barcoding and mucilage ducts in the stipe reveal the presence of *Hedophyllum nigripes* (Laminariales, Phaeophyceae) in Kongsfjorden (Spitsbergen). *Journal of Phycology*, 56(5), 1245–1254. <https://doi.org/10.1111/jpy.13012>
- Deiman, M., Iken, K., & Konar, B. (2012). Susceptibility of *Nereocystis luetkeana* (Laminariales, Ochrophyta) and *Eualaria fistulosa* (Laminariales, Ochrophyta) spores to sedimentation. *ALGAE*, 27(2), 115–123. <https://doi.org/10.4490/algae.2012.27.2.115>
- Dowdeswell, J. A., Hagen, J. O., Björnsson, H., Glazovsky, A. F., Harrison, W. D., Holmlund, P., Jania, J., Koerner, R. M., Lefauconnier, B., Ommanney, C. S. L., & Thomas, R. H. (1997). The Mass Balance of Circum-Arctic Glaciers and Recent Climate Change. *Quaternary Research*, 48(1), 1–14. <https://doi.org/10.1006/qres.1997.1900>
- Filbee-Dexter, K., Wernberg, T., Fredriksen, S., Norderhaug, K. M., & Pedersen, M. F. (2019). Arctic kelp forests: Diversity, resilience and future. In *Global and Planetary Change* (Vol. 172, pp. 1–14). <https://doi.org/10.1016/j.gloplacha.2018.09.005>
- Førland, E. J., & Hanssen-Bauer, I. (2003). Past and future climate variations in the Norwegian Arctic: Overview and novel analyses. *Polar Research*, 22(2), 113–124. <https://doi.org/10.1111/j.1751-8369.2003.tb00102.x>
- Fredersdorf, J., Müller, R., Becker, S., Wiencke, C., & Bischof, K. (2009). Interactive effects of radiation, temperature and salinity on different life history stages of the Arctic kelp *Alaria esculenta* (Phaeophyceae). *Oecologia*, 160(3), 483–492. <https://doi.org/10.1007/s00442-009-1326-9>
- Fredriksen, S., Gabrielsen, T. M., Kile, M. R., & Sivertsen, K. (2015). Benthic algal vegetation in Isfjorden, Svalbard. *Polar Research*, 34(1), 25994. <https://doi.org/10.3402/polar.v34.25994>
- Fredriksen, S., & Kile, M. R. (2012). The algal vegetation in the outer part of Isfjorden, Spitsbergen: Revisiting Per Svendsen's sites 50 years later. *Polar Research*, 31(SUPPL.). <https://doi.org/10.3402/polar.v31i0.17538>
- Hagen, J. O., & Liestol, O. (1990). Long-term glacier mass-balance investigations in Svalbard 1950–88. *Annals of Glaciology*, 14, 102–106. <https://doi.org/10.3189/s0260305500008351>
- Hanelt, D., Tüg, H., Bischof, K., Groß, C., Lippert, H., Sawall, T., & Wiencke, C. (2001). Light regime in an Arctic fjord: A study related to stratospheric ozone depletion as a basis for determination of UV effects on algal growth. *Marine Biology*, 138(3), 649–658. <https://doi.org/10.1007/s002270000481>

- Hop, H., Kovaltchouk, N. A., & Wiencke, C. (2016). Distribution of macroalgae in Kongsfjorden, Svalbard. *Polar Biology*, 39(11), 2037–2051. <https://doi.org/10.1007/s00300-016-2048-1>
- Hop, H., Wiencke, C., Vögele, B., & Kovaltchouk, N. A. (2012). Species composition, zonation, and biomass of marine benthic macroalgae in Kongsfjorden, Svalbard. *Botanica Marina*, 55(4), 399–414. <https://doi.org/10.1515/bot-2012-0097>
- Hopwood, M. J., Carroll, D., Dunse, T., Hodson, A., Holding, J. M., Iriarte, J. L., Ribeiro, S., Achterberg, E. P., Cantoni, C., Carlson, D. F., Chierici, M., Clarke, J. S., Cozzi, S., Fransson, A., Juul-Pedersen, T., Winding, M. H. S., & Meire, L. (2020). Review article: How does glacier discharge affect marine biogeochemistry and primary production in the Arctic? In *Cryosphere* (Vol. 14, Issue 4, pp. 1347–1383). Copernicus GmbH. <https://doi.org/10.5194/tc-14-1347-2020>
- Ingvaldsen, R. B., Assmann, K. M., Primicerio, R., Fossheim, M., Polyakov, I. V., & Dolgov, A. V. (2021). Physical manifestations and ecological implications of Arctic Atlantification. *Nature Reviews Earth & Environment*, 1–16. <https://doi.org/10.1038/s43017-021-00228-x>
- Jackson, R. H., Shroyer, E. L., Nash, J. D., Sutherland, D. A., Carroll, D., Fried, M. J., Catania, G. A., Bartholomaeus, T. C., & Stearns, L. A. (2017). Near-glacier surveying of a subglacial discharge plume: Implications for plume parameterizations. *Geophysical Research Letters*, 44(13), 6886–6894. <https://doi.org/10.1002/2017GL073602>
- Karsten, U. (2007). Research note: Salinity tolerance of Arctic kelps from Spitsbergen. *Phycological Research*, 55(4), 257–262. <https://doi.org/10.1111/j.1440-1835.2007.00468.x>
- Krause-Jensen, D., Archambault, P., Assis, J., Bartsch, I., Bischof, K., Filbee-Dexter, K., Dunton, K. H., Maximova, O., Ragnarsdóttir, S. B., Sejr, M. K., Simakova, U., Spiridonov, V., Wegeberg, S., Winding, M. H. S., & Duarte, C. M. (2020). Imprint of Climate Change on Pan-Arctic Marine Vegetation. *Frontiers in Marine Science*, 7, 1129. <https://doi.org/10.3389/FMARS.2020.617324/BIBTEX>
- Krause-Jensen, D., & Duarte, C. M. (2014). Expansion of vegetated coastal ecosystems in the future Arctic. *Frontiers in Marine Science*, 1(DEC). <https://doi.org/10.3389/fmars.2014.00077>
- Krause-Jensen, D., & Duarte, C. M. (2016). Substantial role of macroalgae in marine carbon sequestration. *Nature Geoscience*, 9(10), 737–742. <https://doi.org/10.1038/ngeo2790>
- Kruss, A., Tęgowski, J., Tatarek, A., Wiktor, J., & Blondel, P. (2017). Spatial distribution of macroalgae along the shores of Kongsfjorden (West Spitsbergen) using acoustic imaging. *Polish Polar Research*, 38(2), 205–229. <https://doi.org/10.1515/popore-2017-0009>
- Láska, K., Witoszová, D., & Prošek, P. (2012). Weather patterns of the coastal zone of Petuniabukta, central Spitsbergen in the period 2008-2010. *Polish Polar Research*, 33(4), 297–318. <https://doi.org/10.2478/v10183-012-0025-0>
- Li, H., Monteiro, C., Heinrich, S., Bartsch, I., Valentin, K., Harms, L., Glöckner, G., Corre, E., & Bischof, K. (2020). Responses of the kelp *Saccharina latissima* (Phaeophyceae) to the warming

Arctic: from physiology to transcriptomics. *Physiologia Plantarum*, 168(1), 5–26.  
<https://doi.org/10.1111/ppl.13009>

- Lurton, X., Eleftherakis, D., & Augustin, J. M. (2018). Analysis of seafloor backscatter strength dependence on the survey azimuth using multibeam echosounder data. *Marine Geophysical Research*, 39(1–2), 183–203. <https://doi.org/10.1007/s11001-017-9318-3>
- Lydersen, C., Assmy, P., Falk-Petersen, S., Kohler, J., Kovacs, K. M., Reigstad, M., Steen, H., Strøm, H., Sundfjord, A., Varpe, Ø., Walczowski, W., Weslawski, J. M., & Zajaczkowski, M. (2014). The importance of tidewater glaciers for marine mammals and seabirds in Svalbard, Norway. In *Journal of Marine Systems* (Vol. 129, pp. 452–471). Elsevier.  
<https://doi.org/10.1016/j.jmarsys.2013.09.006>
- Meire, L., Mortensen, J., Rysgaard, S., Bendtsen, J., Boone, W., Meire, P., & Meysman, F. J. R. (2016). Spring bloom dynamics in a subarctic fjord influenced by tidewater outlet glaciers (Godthåbsfjord, SW Greenland). *Journal of Geophysical Research: Biogeosciences*, 121(6), 1581–1592. <https://doi.org/10.1002/2015JG003240>
- Mortensen, J., Bendtsen, J., Lennert, K., & Rysgaard, S. (2014). Seasonal variability of the circulation system in a west Greenland tidewater outlet glacier fjord, Godthåbsfjord (64°N). *Journal of Geophysical Research: Earth Surface*, 119(12), 2591–2603.  
<https://doi.org/10.1002/2014JF003267>
- Moy, F. E., & Christie, H. (2012). Large-scale shift from sugar kelp (*Saccharina latissima*) to ephemeral algae along the south and west coast of Norway. *Marine Biology Research*, 8(4), 309–321. <https://doi.org/10.1080/17451000.2011.637561>
- Murray, C., Markager, S., Stedmon, C. A., Juul-Pedersen, T., Sejr, M. K., & Bruhn, A. (2015). The influence of glacial melt water on bio-optical properties in two contrasting Greenlandic fjords. *Estuarine, Coastal and Shelf Science*, 163(PB), 72–83.  
<https://doi.org/10.1016/J.ECSS.2015.05.041>
- Østby, T. I., Vikhamar Schuler, T., Ove Hagen, J., Hock, R., Kohler, J., & Reijmer, C. H. (2017). Diagnosing the decline in climatic mass balance of glaciers in Svalbard over 1957–2014. *Cryosphere*, 11(1), 191–215. <https://doi.org/10.5194/tc-11-191-2017>
- Pörtner, H.-O., Roberts, D. C., Alegría, A., Nicolai, M., Okem, A., Petzold, J., Rama, B., & Weyer, N. M. (2019). *The Ocean and Cryosphere in a Changing Climate: A Special Report of the Intergovernmental Panel on Climate Change*.
- Rachlewicz, G., Szczuciński, W., & Ewertowski, M. (2007). Post-"Little Ice Age" retreat rates of glaciers around Billefjorden in central Spitsbergen, Svalbard. In *Polish Polar Research* (Vol. 28, Issue 3).
- Rawlins, M. A., Steele, M., Holland, M. M., Adam, J. C., Cherry, J. E., Francis, J. A., Groisman, P. Y., Hinzman, L. D., Huntington, T. G., Kane, D. L., Kimball, J. S., Kwok, R., Lammers, R. B., Lee, C. M., Lettenmaier, D. P., Mcdonald, K. C., Podest, E., Pundsack, J. W., Rudels, B., ... Zhang, T. (2010). Analysis of the Arctic system for freshwater cycle intensification:

Observations and expectations. *Journal of Climate*, 23(21), 5715–5737.  
<https://doi.org/10.1175/2010JCLI3421.1>

- Ronowicz, M., Włodarska-Kowalczyk, M., & Kukliński, P. (2020). Glacial and depth influence on sublittoral macroalgal standing stock in a high-Arctic fjord. *Continental Shelf Research*, 194(December 2019), 1–9. <https://doi.org/10.1016/j.csr.2019.104045>
- Smale, D. A. (2020). Impacts of ocean warming on kelp forest ecosystems. In *New Phytologist* (Vol. 225, Issue 4, pp. 1447–1454). Blackwell Publishing Ltd. <https://doi.org/10.1111/nph.16107>
- Søreide, J. E., Pitusi, V., Vader, A., Damsgård, B., Nilsen, F., Skogseth, R., Poste, A., Bailey, A., Kovacs, K. M., Lydersen, C., Gerland, S., Descamps, S., Strøm, H., Renaud, P. E., Christensen, G., Arvnes, M. P., Graczyk, P., Moiseev, D., Singh, R. K., ... Węślawski, J. M. (2021). Environmental status of Svalbard coastal waters: coastscapes and focal ecosystem components (SvalCoast). In *State of Environmental Science in Svalbard (SESS) report 2020* (pp. 143–174). <https://doi.org/10.5281/zenodo.4293849>
- Steneck, R. S., Graham, M. H., Bourque, B. J., Corbett, D., Erlandson, J. M., Estes, J. A., & Tegner, M. J. (2002). Kelp forest ecosystems: Biodiversity, stability, resilience and future. *Environmental Conservation*, 29(4), 436–459. <https://doi.org/10.1017/S0376892902000322>
- Straneo, Fiamma, & Cenedese, C. (2015). The dynamics of greenland’s glacial fjords and their role in climate. *Annual Review of Marine Science*, 7, 89–112. <https://doi.org/10.1146/annurev-marine-010213-135133>
- Straneo, Fiammetta, Sutherland, D. A., Holland, D., Gladish, C., Hamilton, G. S., Johnson, H. L., Rignot, E., Xu, Y., & Koppes, M. (2012). Characteristics of ocean waters reaching greenland’s glaciers. *Annals of Glaciology*, 53(60), 202–210. <https://doi.org/10.3189/2012AoG60A059>
- Strzelecki, M. C. (2012). High Arctic Paraglacial Coastal Evolution in Northern Billefjorden, Svalbard. In *Department of Geography*. Durham University.
- Szczuciński, W., Zajaczkowski, M., & Scholten, J. (2009). Sediment accumulation rates in subpolar fjords - Impact of post-Little Ice Age glaciers retreat, Billefjorden, Svalbard. *Estuarine, Coastal and Shelf Science*, 85(3), 345–356. <https://doi.org/10.1016/j.ecss.2009.08.021>
- tom Dieck, I. (1993). Temperature tolerance and survival in darkness of kelp gametophytes (Laminariales, Phaeophyta): ecological and biogeographical implications Inka tom Dieck (Bartsch). *Marine Ecology Progress Series*, 100, 253–264.
- Torsvik, T., Albretsen, J., Sundfjord, A., Kohler, J., Sandvik, A. D., Skarðhamar, J., Lindbäck, K., & Everett, A. (2019). Impact of tidewater glacier retreat on the fjord system: Modeling present and future circulation in Kongsfjorden, Svalbard. *Estuarine, Coastal and Shelf Science*, 220, 152–165. <https://doi.org/10.1016/j.ecss.2019.02.005>
- Traiger, S. B., & Konar, B. (2018). Mature and developing kelp bed community composition in a glacial estuary. *Journal of Experimental Marine Biology and Ecology*, 501, 26–35. <https://doi.org/10.1016/j.jembe.2017.12.016>

- Weslawski, J. M., Wiktor, J., & Kotwicki, L. (2010). Increase in biodiversity in the arctic rocky littoral, Sorkapland, Svalbard, after 20 years of climate warming. *Marine Biodiversity*, 40(2), 123–130. <https://doi.org/10.1007/s12526-010-0038-z>
- Wulff, A., Iken, K., Quartino, M. L., Al-Handal, A., Wiencke, C., & Clayton, M. N. (2009). Biodiversity, biogeography and zonation of marine benthic micro- and macroalgae in the Arctic and Antarctic. In *Botanica Marina* (Vol. 52, Issue 6, pp. 491–507). <https://doi.org/10.1515/BOT.2009.072>
- Zaborska, A., Włodarska-Kowalczyk, M., Legeżyńska, J., Jankowska, E., Winogradow, A., & Deja, K. (2018). Sedimentary organic matter sources, benthic consumption and burial in west Spitsbergen fjords – Signs of maturing of Arctic fjordic systems? *Journal of Marine Systems*, 180, 112–123. <https://doi.org/10.1016/j.jmarsys.2016.11.005>
- Zacher, K., Bernard, M., Bartsch, I., & Wiencke, C. (2016). Survival of early life history stages of Arctic kelps (Kongsfjorden, Svalbard) under multifactorial global change scenarios. *Polar Biology*, 39(11), 2009–2020. <https://doi.org/10.1007/s00300-016-1906-1>
- Zacher, Katharina, Bernard, M., Daniel Moreno, A., & Bartsch, I. (2019). Temperature mediates the outcome of species interactions in early life-history stages of two sympatric kelp species. *Marine Biology*, 166(12), 1–16. <https://doi.org/10.1007/s00227-019-3600-7>



## 7 Appendix

**Table 7:** Station selection segment with respective ranges for turbidity [NTU] and salinity [PSU]

	Lat_range	Long_range	ntu_range	psu_range
<b>FRE</b>	78.693926 – 78.672289	16.467522 – 16.456322	5 – 70	29.8 – 31.5
<b>GLA</b>	78.668447 – 78.666135	16.924123 – 16.928887	3 – 35	29.5 – 30.75
<b>ICE</b>	78.626224 – 78.613778	16.694833 – 16.663501	0 – 12	32.4 – 32.7

**Table 8:** Bottom depth grid report statistics from Visual Aquatics for each station.

	ICE	FRE	GLA
<b>Projection</b>	WGS84 UTM Zone 33 N	WGS84 UTM Zone 33 N	WGS84 UTM Zone 33 N
<b>Max Distortion</b>	1.000097	1.000193	1.000096
<b>Survey area (hectares)</b>	1.355777	7.912503	3.054389
<b>Data area (hectares)</b>	1.336248	7.85268	3.008916
<b>Water volume (m3)</b>	258109.77	1109293.39	513047.69
<b>Min Depth (m)</b>	5.1	5.03	5.02
<b>Max Depth (m)</b>	30.02	29.98	43.58
<b>Avg Depth (m)</b>	19.32	14.13	17.05
<b>Contour Interval (m)</b>	5	5	5
<b>Report Interval (pings)</b>	10	10	10
<b>Grid Cell Size (m)</b>	0.6	0.6	0.6
<b>Grid Method</b>	Triangulated Linear	Triangulated Linear	Triangulated Linear

**Table 9:** Temperature, salinity, turbidity and plant coverage mean values, standard deviations and standard errors for every station and depth bin.

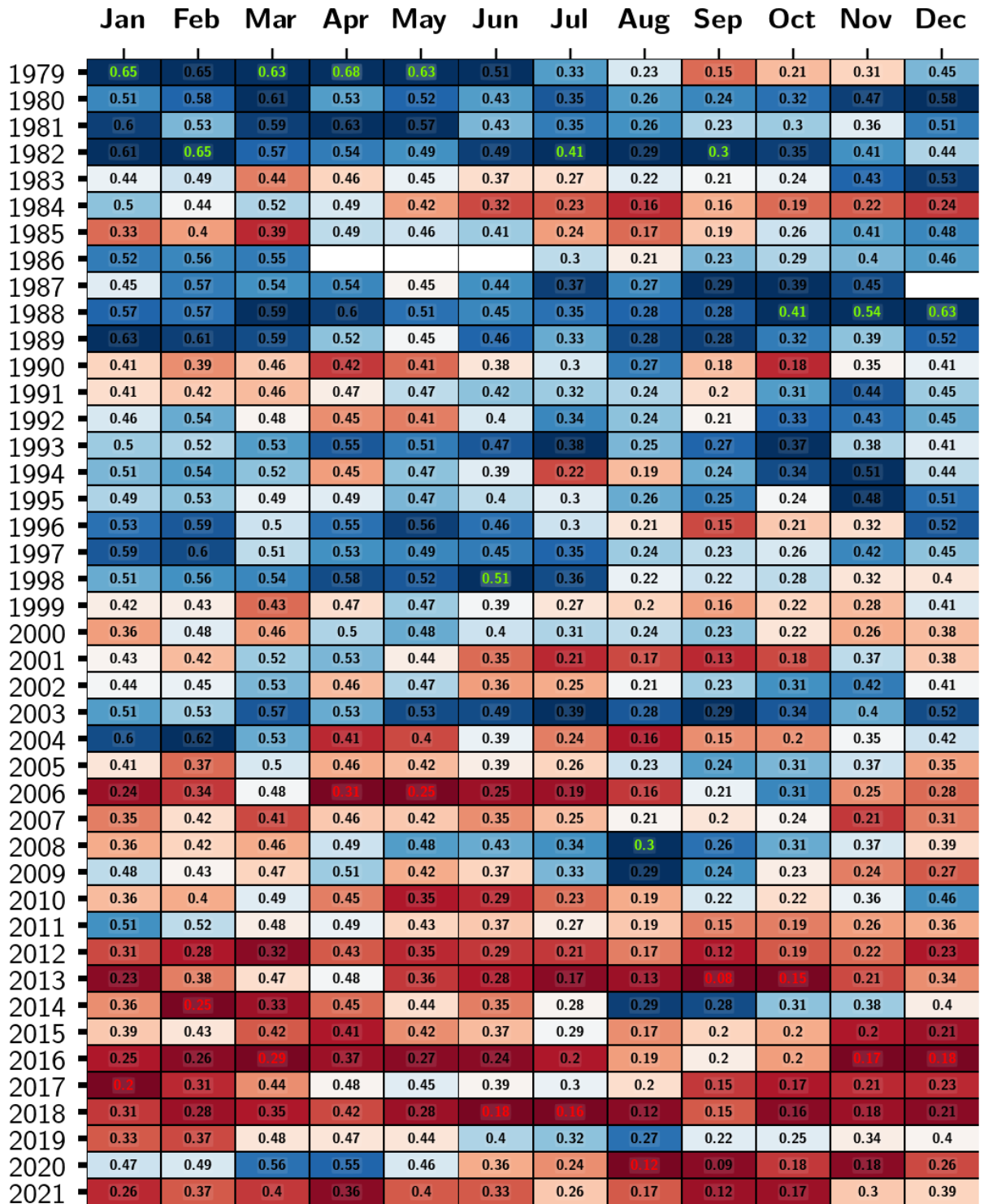
Station	Bin	PCMean	PCSD	PCSE	TempMean	TempSD	TempSE	SalMean	SalSD	SalSE
FRE	1	0.053	0.726	0.037	2.222	0.019	0.009	34.010	0.025	0.012
FRE	2	0.091	1.128	0.048	2.351	0.041	0.009	34.056	0.014	0.003
FRE	3	0.079	0.891	0.079	2.146	0.036	0.008	34.101	0.013	0.003
FRE	4	1.563	5.992	0.474	1.990	0.089	0.012	34.139	0.021	0.003
FRE	5	4.046	14.021	1.225	2.255	0.009	0.004	31.264	6.526	2.919
GLA	1	9.700	16.109	1.611	1.705	0.007	0.002	33.974	0.017	0.005
GLA	2	15.787	23.714	1.777	1.571	0.038	0.006	34.002	0.013	0.002
GLA	3	24.908	25.836	2.546	1.610	0.012	0.002	34.023	0.011	0.002
GLA	4	12.000	21.872	2.526	1.635	0.013	0.002	34.039	0.059	0.009
GLA	5	44.672	35.330	3.199	1.946	0.115	0.016	34.143	0.042	0.006
ICE	1	16.667	15.343	2.671	1.788	0.010	0.001	33.885	0.019	0.003
ICE	2	9.750	11.433	1.808	1.762	0.041	0.003	33.916	0.018	0.001
ICE	3	6.087	10.641	1.569	1.904	0.113	0.010	33.974	0.099	0.009
ICE	4	6.182	16.832	2.270	2.699	0.154	0.014	33.996	1.509	0.136
ICE	5	11.077	20.473	2.539	2.989	0.036	0.004	34.208	0.027	0.003

Station	Bin	TurbMean_	TurbSD_	TurbSE_	TurbMean_full	TurbSD_full	TurbSE_full
FRE	1	3.073	0.087	0.043	1.908	0.583	0.044
FRE	2	3.624	4.032	0.880	2.313	1.528	0.082
FRE	3	3.762	0.270	0.062	1.842	3.293	0.148
FRE	4	3.656	0.762	0.105	1.696	0.906	0.034
FRE	5	3.478	0.331	0.148	1.916	2.342	0.084
GLA	1	1.366	0.029	0.009	9.608	62.280	4.616
GLA	2	1.586	0.051	0.008	15.094	94.880	4.829
GLA	3	2.226	0.079	0.011	5.607	35.112	1.499
GLA	4	2.485	0.155	0.023	7.097	48.610	1.845
GLA	5	2.518	0.153	0.022	5.105	30.054	1.036
ICE	1	0.927	0.056	0.008	5.832	34.141	2.281
ICE	2	0.885	0.041	0.003	4.890	31.102	1.430
ICE	3	2.255	16.119	1.387	5.106	41.484	1.662
ICE	4	0.745	0.059	0.005	2.258	20.977	0.766
ICE	5	0.579	0.031	0.003	3.072	31.782	1.074

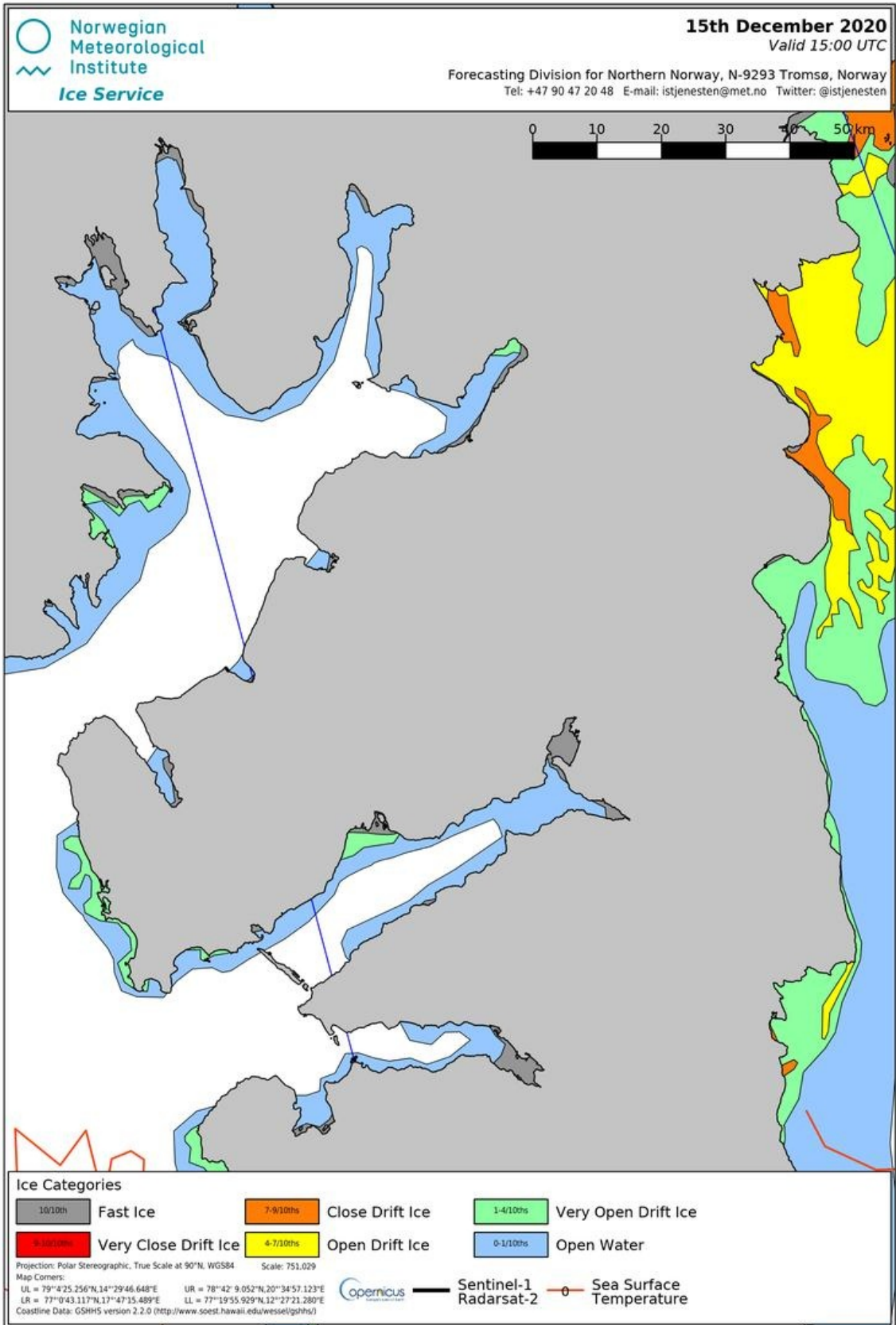
  

<b>PC</b>	Plant coverage [%]
<b>Temp</b>	Temperature [°C]
<b>Sal</b>	Salinity [psu]
<b>Turb</b>	Turbidity [ntu]
<b>Turb_full</b>	Turbidity of full water column [ntu]
<b>Mean</b>	Mean value
<b>SD</b>	Standard deviation
<b>SE</b>	Standard error



SEA ICE AREA (Mill. km<sup>2</sup>)  
 [ OSI SAF, v2.1, Svalbard ]

Figure 25: Rank of monthly sea-ice extent on Svalbard. Colour coding is relative to the respective months recorded maximum and minimum values. (source: Norwegian Meteorological Institute)



**Figure 26:** Sea-ice chart for Isfjorden from the 15 December, 2020. (source: Norwegian Meteorological Institute)

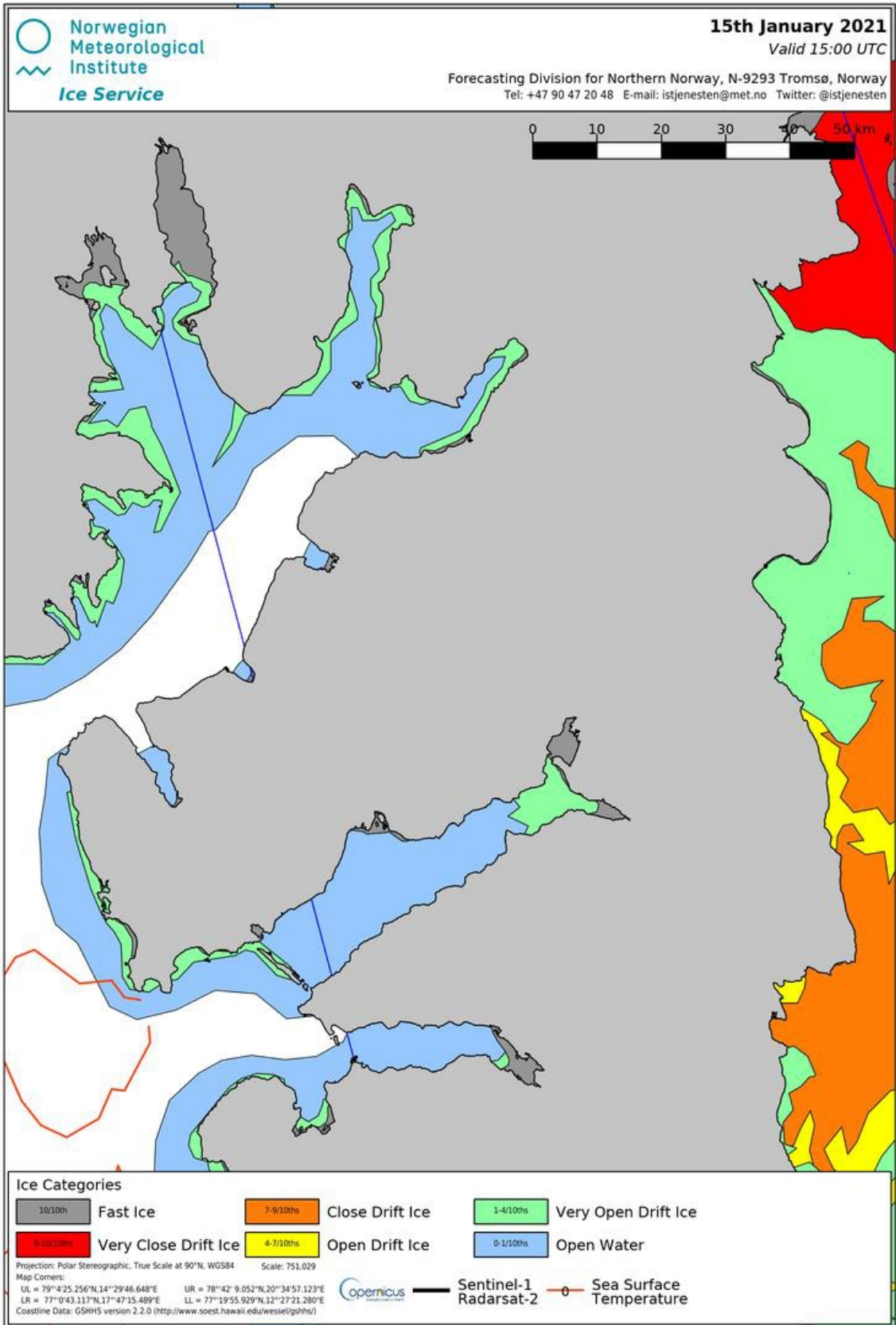


**Figure 27:** Sea-ice chart for Isfjorden from the 15 January, 2021. (source: Norwegian Meteorological Institute)

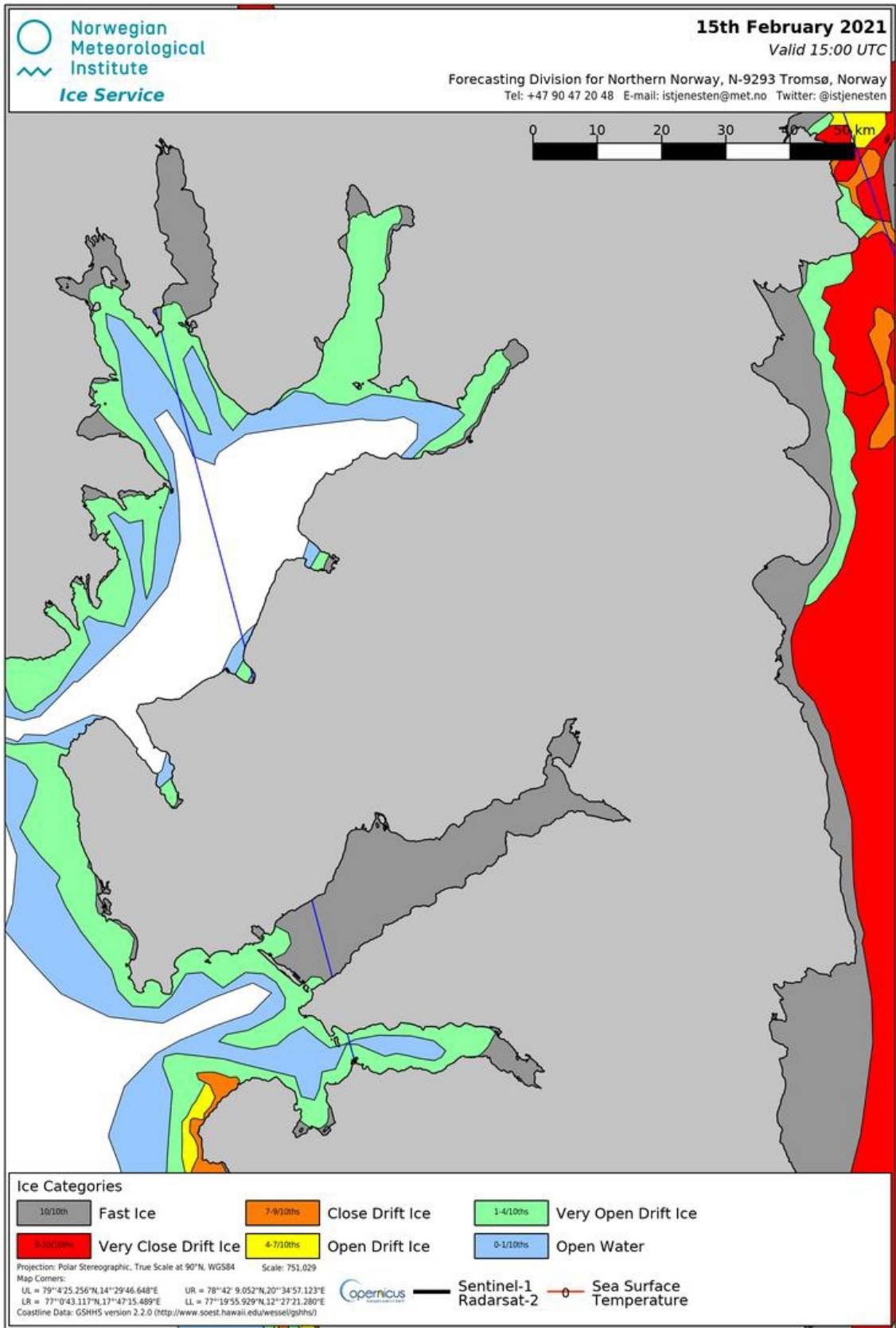


**Figure 28:** Sea-ice chart for Isfjorden from the 15 February, 2021. (source: Norwegian Meteorological Institute)

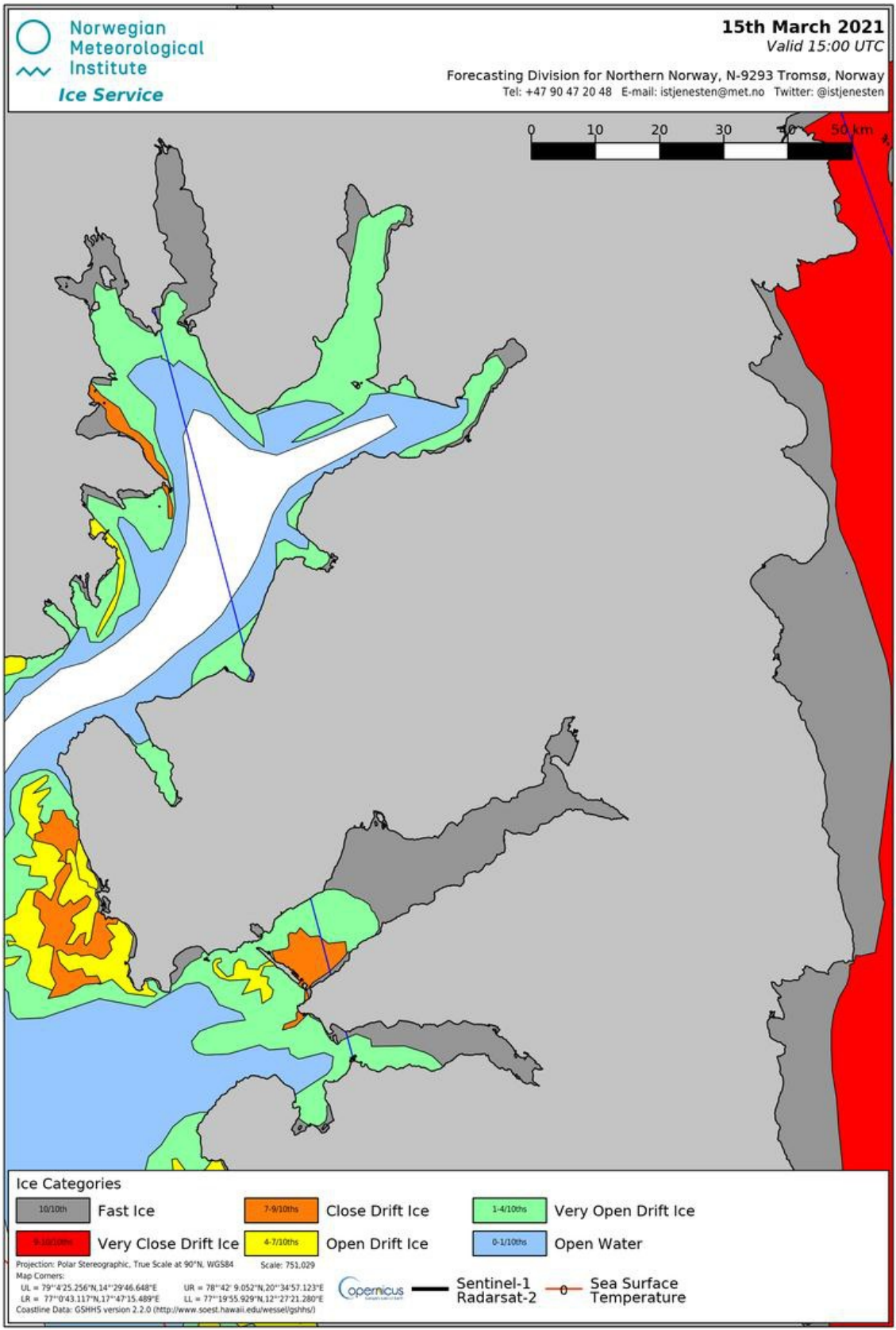
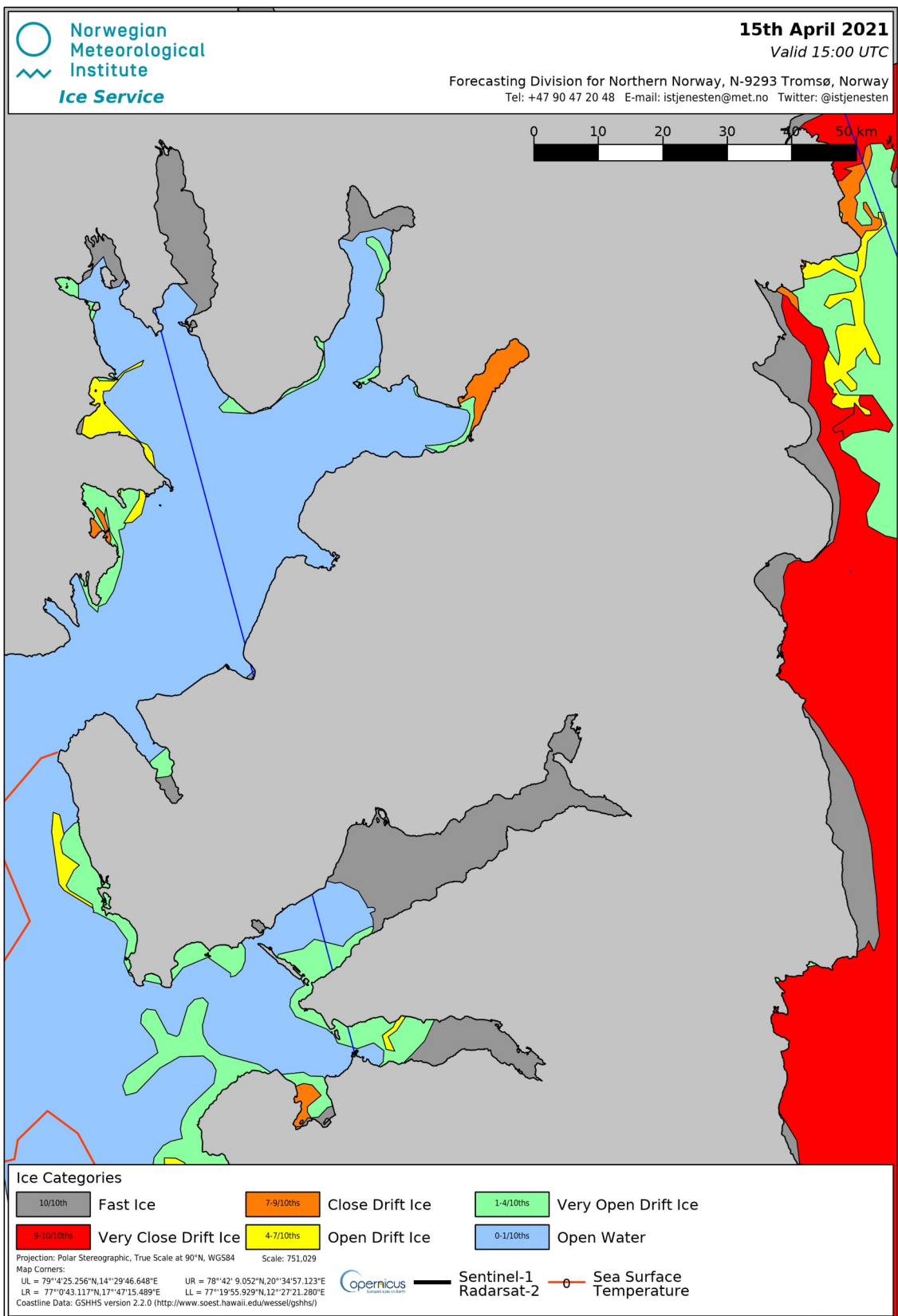


Figure 29: Sea-ice chart for Isfjorden from the 15 March, 2021. (source: Norwegian Meteorological Institute)



**Figure 30:** Sea-ice chart for Isfjorden from the 15 April, 2021. (source: Norwegian Meteorological Institute)



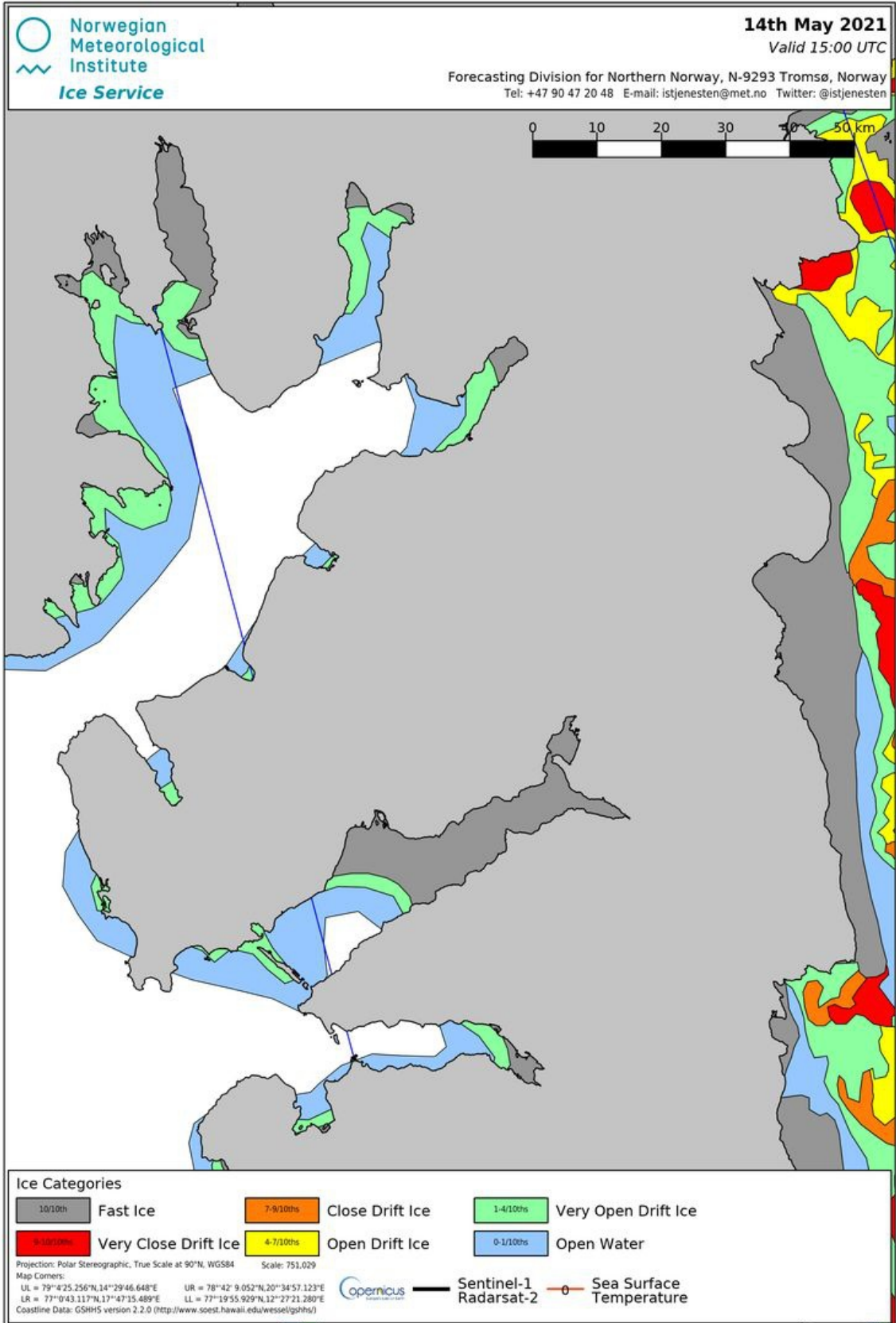


Figure 31: Sea-ice chart for Isfjorden from the 14 May, 2021. (source: Norwegian Meteorological Institute)

**Table 10:** Tide predictions for the day and location of bathymetric survey at the sea-ice station.

August 2021				August 2021				August 2021													
Time	Obs	Pre	Wea	For	Time	Obs	Pre	Wea	For	Time	Obs	Pre	Wea	For	Time	Obs	Pre	Wea	For		
24	0000	135	149	-13	24	1150	91	109	-18	24	2340	91	111	-20							
Tu	0010	142	155	-13	Tu	1200	97	115	-18	Tu	2350	98	117	-20							
	0020	149	162	-13		1210	104	122	-18		0000	104	124	-19							
	0030	155	168	-13		1220	110	129	-18	25											
	0040	161	174	-13		1230	117	135	-18	We											
	0050	165	179	-14		1240	124	142	-18												
	0100	170	184	-14		1250	130	148	-18												
	0110	174	188	-14		1300	136	154	-18												
	0120	177	191	-14		1310	141	159	-18												
	0130	180	193	-13		1320	146	164	-18												
	0140	182	195	-13		1330	150	168	-18												
	0150	183	196	-13		1340	153	171	-18												
	0200	183	196	-13		1350	156	174	-19												
	0210	183	196	-13		1400	157	176	-19												
	0220	181	195	-14		1410	158	177	-19												
	0230	180	193	-14		1420	159	178	-19												
	0240	177	191	-14		1430	159	178	-19												
	0250	175	189	-14		1440	158	177	-19												
	0300	172	186	-14		1450	158	176	-18												
	0310	168	183	-14		1500	156	174	-18												
	0320	164	179	-15		1510	153	172	-18												
	0330	160	175	-15		1520	150	169	-19												
	0340	156	171	-15		1530	147	166	-20												
	0350	152	167	-15		1540	143	163	-20												
	0400	148	163	-15		1550	139	160	-20												
	0410	144	158	-15		1600	136	156	-20												
	0420	139	154	-15		1610	132	152	-20												
	0430	134	149	-14		1620	128	148	-20												
	0440	129	143	-14		1630	124	144	-20												
	0450	124	138	-14		1640	120	140	-20												
	0500	117	132	-14		1650	116	136	-20												
	0510	111	126	-15		1700	112	131	-19												
	0520	104	119	-15		1710	107	126	-19												
	0530	97	112	-16		1720	102	121	-18												
	0540	90	105	-16		1730	97	115	-18												
	0550	82	98	-16		1740	91	110	-19												
	0600	75	91	-16		1750	84	104	-19												
	0610	67	84	-16		1800	77	98	-20												
	0620	60	76	-17		1810	71	91	-21												
	0630	53	70	-16		1820	64	85	-21												
	0640	47	63	-16		1830	57	79	-21												
	0650	41	57	-16		1840	51	72	-21												
	0700	35	51	-16		1850	45	66	-21												
	0710	30	46	-16		1900	40	60	-20												
	0720	26	42	-16		1910	35	55	-20												
	0730	22	38	-16		1920	31	50	-20												
	0740	18	35	-17		1930	27	46	-19												
	0750	16	33	-17		1940	23	42	-19												
	0800	15	31	-17		1950	20	39	-19												
	0810	14	31	-16		2000	17	37	-20												
	0820	14	31	-16		2010	16	36	-20												
	0830	15	31	-16		2020	15	35	-20												
	0840	16	32	-16		2030	15	36	-20												
	0850	18	34	-16		2040	16	36	-20												
	0900	20	36	-16		2050	18	38	-20												
	0910	22	38	-16		2100	20	40	-20												
	0920	25	41	-16		2110	22	43	-21												
	0930	28	44	-16		2120	25	46	-20												
	0940	31	47	-16		2130	29	49	-20												
	0950	34	51	-17		2140	33	53	-20												
	1000	37	54	-17		2150	37	57	-19												
	1010	41	58	-17		2200	42	61	-19												
	1020	45	62	-17		2210	46	65	-19												
	1030	49	66	-17		2220	50	70	-20												
	1040	54	70	-16		2230	55	74	-20												
	1050	58	75	-16		2240	59	79	-20												
	1100	63	80	-16		2250	64	84	-20												
	1110	68	85	-17		2300	69	89	-20												
	1120	74	90	-17		2310	74	94	-20												
	1130	79	96	-17		2320	79	100	-20												
	1140	85	102	-17		2330	85	105	-20												

Time is given in Central European Time (UTC + 1 hour). Daylight saving time from last Sunday in March to last Sunday in October. In that time interval the time of day has to be increased by one hour. Levels are in cm above Chart Datum which is reference level for depths in navigational charts and heights in tide tables.

**Table 11:** Tide predictions for the day and location of bathymetric survey at the freshwater station.

August 2021				August 2021				August 2021													
Time	Obs	Pre	Wea	For	Time	Obs	Pre	Wea	For	Time	Obs	Pre	Wea	For	Time	Obs	Pre	Wea	For		
24	0000	135	149	-13	24	1150	91	109	-18	24	2340	91	111	-20							
Tu	0010	142	155	-13	Tu	1200	97	115	-18	Tu	2350	98	117	-20							
	0020	149	162	-13		1210	104	122	-18		0000	104	124	-19							
	0030	155	168	-13		1220	110	129	-18	25											
	0040	161	174	-13		1230	117	135	-18	We											
	0050	165	179	-14		1240	124	142	-18												
	0100	170	184	-14		1250	130	148	-18												
	0110	174	188	-14		1300	136	154	-18												
	0120	177	191	-14		1310	141	159	-18												
	0130	180	193	-13		1320	146	164	-18												
	0140	182	195	-13		1330	150	168	-18												
	0150	183	196	-13		1340	153	171	-18												
	0200	183	196	-13		1350	156	174	-19												
	0210	183	196	-13		1400	157	176	-19												
	0220	181	195	-14		1410	158	177	-19												
	0230	180	193	-14		1420	159	178	-19												
	0240	177	191	-14		1430	159	178	-19												
	0250	175	189	-14		1440	158	177	-19												
	0300	172	186	-14		1450	158	176	-18												
	0310	168	183	-14		1500	156	174	-18												
	0320	164	179	-15		1510	153	172	-18												
	0330	160	175	-15		1520	150	169	-19												
	0340	156	171	-15		1530	147	166	-20												
	0350	152	167	-15		1540	143	163	-20												
	0400	148	163	-15		1550	139	160	-20												
	0410	144	158	-15		1600	136	156	-20												
	0420	139	154	-15		1610	132	152	-20												
	0430	134	149	-14		1620	128	148	-20												
	0440	129	143	-14		1630	124	144	-20												
	0450	124	138	-14		1640	120	140	-20												
	0500	117	132	-14		1650	116	136	-20												
	0510	111	126	-15		1700	112	131	-19												
	0520	104	119	-15		1710	107	126	-19												
	0530	97	112	-16		1720	102	121	-18												
	0540	90	105	-16		1730	97	115	-18												
	0550	82	98	-16		1740	91	110	-19												
	0600	75	91	-16		1750	84	104	-19												
	0610	67	84	-16		1800	77	98	-20												
	0620	60	76	-17		1810	71	91	-21												
	0630	53	70	-16		1820	64	85	-21												
	0640	47	63	-16		1830	57	79	-21												
	0650	41	57	-16		1840	51	72	-21												
	0700	35	51	-16		1850	45	66	-21												
	0710	30	46	-16		1900	40	60	-20												
	0720	26	42	-16		1910	35	55	-20												
	0730	22	38	-16		1920	31	50	-20												
	0740	18	35	-17		1930	27	46	-19												
	0750	16	33	-17		1940	23	42	-19												
	0800	15	31	-17		1950	20	39	-19												
	0810	14	31	-16		2000	17	37	-20												
	0820	14	31	-16		2010	16	36	-20												
	0830	15	31	-16		2020	15	35	-20												
	0840	16	32	-16		2030	15	36	-20												
	0850	18	34	-16		2040	16	36	-20												
	0900	20	36	-16		2050	18	38	-20												
	0910	22	38	-16		2100	20	40	-20												
	0920	25	41	-16		2110	22	43	-21												
	0930	28	44	-16		2120	25	46	-20												
	0940	31	47	-16		2130	29	49	-20												
	0950	34	51	-17		2140	33	53	-20												
	1000	37	54	-17		2150	37	57	-19												
	1010	41	58	-17		2200	42	61	-19												
	1020	45	62	-17		2210	46	65	-19												
	1030	49	66	-17		2220	50	70	-20												
	1040	54	70	-16		2230	55	74	-20												
	1050	58	75	-16		2240	59	79	-20												
	1100	63	80	-16		2250	64	84	-20												
	1110	68	85	-17		2300	69	89	-20												
	1120	74	90	-17		2310	74	94	-20												
	1130	79	96	-17		2320	79	100	-20												
	1140	85	102	-17		2330	85	105	-20												

Time is given in Central European Time (UTC + 1 hour). Daylight saving time from last Sunday in March to last Sunday in October. In that time interval the time of day has to be increased by one hour. Levels are in cm above Chart Datum which is reference level for depths in navigational charts and heights in tide tables.

**Table 12:** Tide predictions for the day and location of bathymetric survey at the glacier station.



**GLA 20210825 Tides**  
**Observations, predictions, weather effect and forecast.**

78°40' N 16°56' E

August 2021					August 2021					August 2021									
Time	Obs	Pre	Wea	For	Time	Obs	Pre	Wea	For	Time	Obs	Pre	Wea	For	Time	Obs	Pre	Wea	For
25	0000	104	124	-19	25	1150	68	89	-21	25	2340	78	93	-16					
We	0010	111	130	-19	We	1200	74	95	-21	We	2350	83	99	-15					
	0020	117	137	-19		1210	79	100	-21		0000	89	104	-15					
	0030	124	143	-19		1220	84	106	-22	26									
	0040	130	150	-20		1230	90	112	-22	Th									
	0050	137	156	-20		1240	96	118	-22										
	0100	143	163	-20		1250	102	124	-22										
	0110	149	169	-20		1300	109	131	-22										
	0120	154	175	-20		1310	115	137	-21										
	0130	159	180	-20		1320	121	143	-21										
	0140	164	184	-21		1330	127	149	-21										
	0150	168	188	-21		1340	133	154	-21										
	0200	171	192	-20		1350	138	159	-21										
	0210	174	194	-20		1400	143	164	-21										
	0220	176	196	-20		1410	146	168	-21										
	0230	177	197	-20		1420	149	171	-22										
	0240	177	197	-20		1430	151	174	-22										
	0250	177	197	-20		1440	153	176	-23										
	0300	175	196	-20		1450	154	177	-23										
	0310	174	194	-20		1500	154	177	-23										
	0320	171	192	-20		1510	154	177	-23										
	0330	169	189	-20		1520	154	176	-23										
	0340	165	186	-20		1530	152	175	-23										
	0350	162	182	-20		1540	150	173	-23										
	0400	157	178	-21		1550	148	170	-23										
	0410	153	174	-21		1600	145	167	-23										
	0420	148	170	-21		1610	141	164	-23										
	0430	144	165	-21		1620	138	161	-23										
	0440	139	161	-21		1630	134	157	-23										
	0450	135	156	-21		1640	131	153	-23										
	0500	130	151	-21		1650	127	149	-23										
	0510	125	146	-21		1700	123	145	-22										
	0520	119	140	-21		1710	119	141	-22										
	0530	114	135	-21		1720	115	137	-21										
	0540	108	129	-20		1730	112	132	-20										
	0550	103	123	-20		1740	108	127	-19										
	0600	96	117	-20		1750	104	123	-19										
	0610	89	110	-21		1800	99	118	-19										
	0620	82	103	-21		1810	93	112	-19										
	0630	74	96	-22		1820	87	107	-20										
	0640	67	89	-22		1830	80	101	-21										
	0650	60	83	-23		1840	74	96	-22										
	0700	53	76	-22		1850	67	90	-22										
	0710	47	69	-22		1900	62	84	-22										
	0720	41	63	-22		1910	56	78	-22										
	0730	35	57	-22		1920	50	72	-22										
	0740	29	51	-22		1930	45	66	-21										
	0750	25	46	-22		1940	40	61	-21										
	0800	21	42	-21		1950	36	56	-20										
	0810	17	38	-21		2000	33	51	-18										
	0820	15	36	-21		2010	30	47	-17										
	0830	12	33	-21		2020	27	44	-17										
	0840	11	32	-21		2030	24	41	-17										
	0850	10	31	-22		2040	21	39	-19										
	0900	10	32	-22		2050	18	38	-20										
	0910	10	32	-22		2100	17	38	-20										
	0920	12	34	-22		2110	18	38	-20										
	0930	14	36	-22		2120	19	39	-19										
	0940	16	38	-21		2130	22	40	-19										
	0950	19	41	-21		2140	24	43	-19										
	1000	22	44	-21		2150	27	45	-19										
	1010	26	47	-21		2200	30	49	-19										
	1020	29	50	-21		2210	34	52	-19										
	1030	33	54	-21		2220	38	56	-18										
	1040	36	58	-21		2230	43	60	-17										
	1050	40	62	-22		2240	48	65	-17										
	1100	44	66	-22		2250	53	69	-16										
	1110	48	70	-22		2300	58	74	-16										
	1120	53	75	-22		2310	63	79	-16										
	1130	58	79	-22		2320	68	83	-16										
	1140	63	84	-21		2330	73	88	-16										

Time is given in Central European Time (UTC + 1 hour). Daylight saving time from last Sunday in March to last Sunday in October. In that time interval the time of day has to be increased by one hour. Levels are in cm above Chart Datum which is reference level for depths in navigational charts and heights in tide tables.

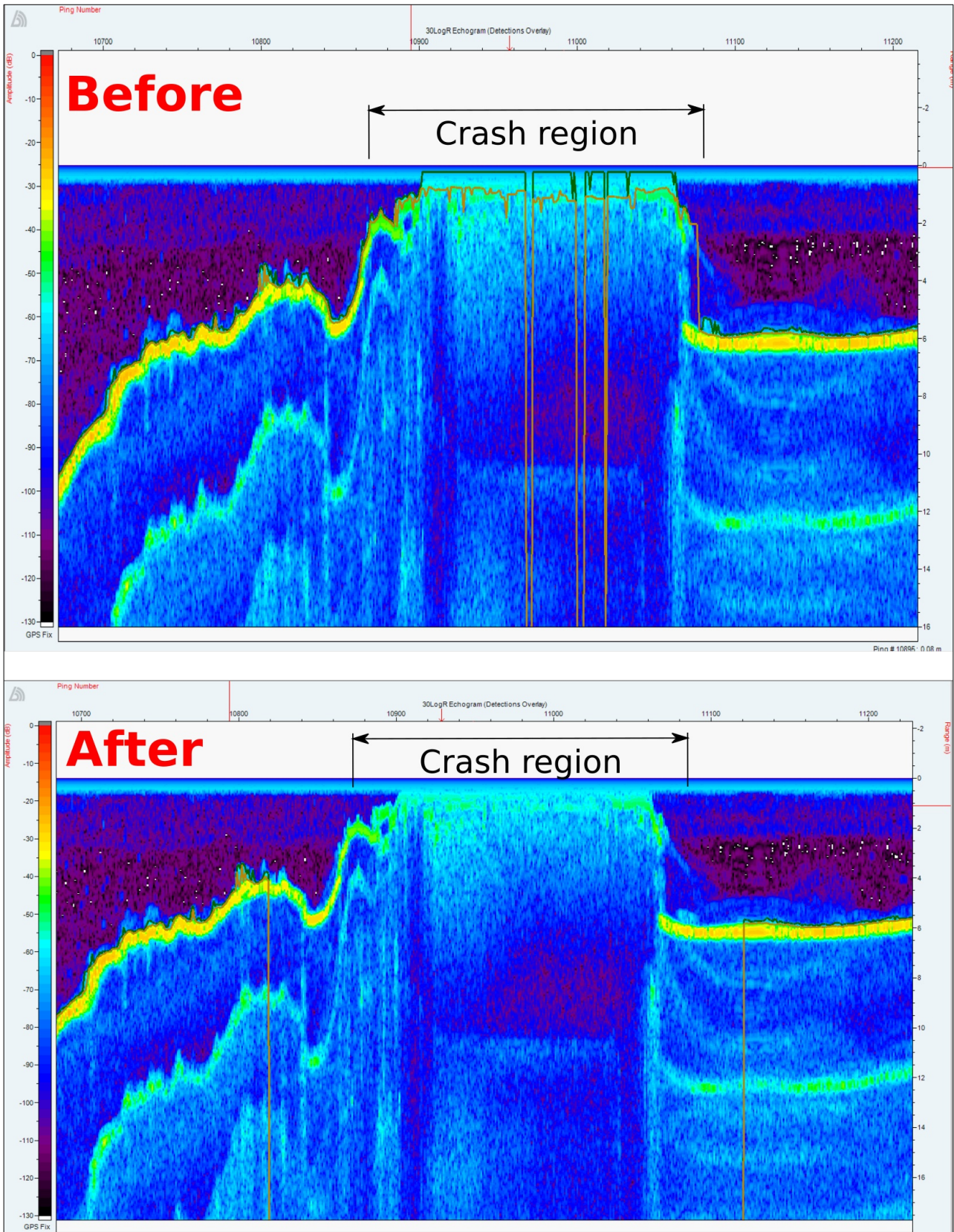


**Figure 32:** Example for manual editing of the "crash-signal" of the echogram in Visual Aquatics at the glacier station between ping 10870 and 11070. The bottom and plant signal was cut off 50 pings before and after the region.

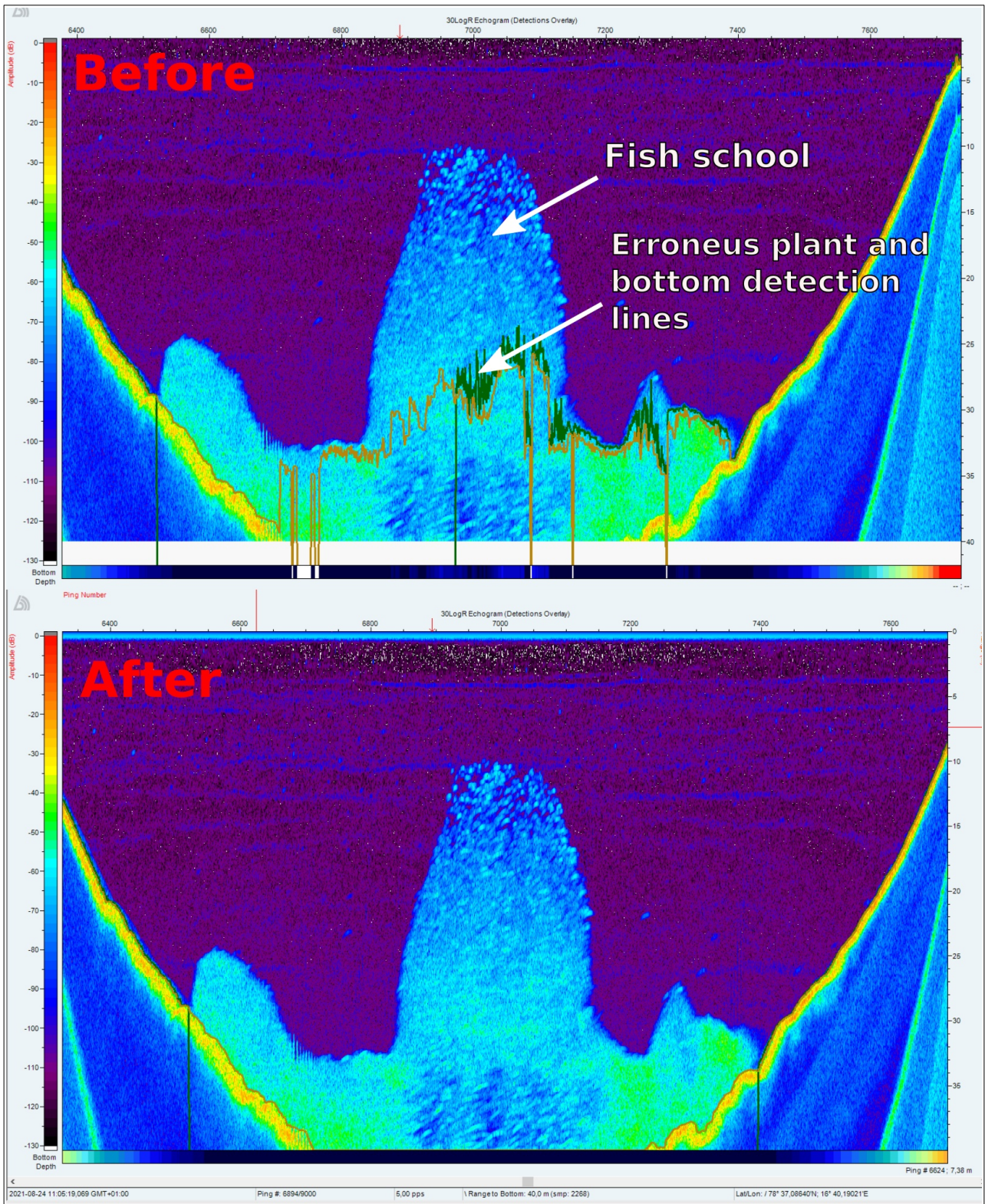


**Figure 33:** Echogram example for false bottom and plant detection by the algorithms in Visual Aquatics due to a dense fish school positioned in the water column and close to the sea floor. This echogram stems from the sea-ice station measurements

**Table 13:** Underwater camera validation table. Validation served the purpose of testing the accuracy of plant detection by the echosounders algorithms. The drops were conducted on 12 August, 2012 in Adolfbukta. The exact GPS coordinates and referenced data files for the echosounder (DT-X) and the camera (Paralenz) can be found in the digital appendix.

Paralenz Drop	Bottom ca. Depth (m)	Camera algae coverage (y/n)	DT-X algae coverage (y/n)
1	7.5	y	y
2	7.9	y	y
3	6.1	y	y
4	8.8	y	y
5	7.5	y	y
6	5.8	y	y
7	8.3	y	y
8	4.2	y	y
9	6.7	y	y
10	4.8	y	y
11	5.4	y	y
12	7.8	y	y
13	7.9	y	y
14	4.8	n	n
15	4.5	y	y
16	6	y	y
17	5.1	y	y
18	5.2	y	y

Paralenz File	Time stamp (mm:ss)	DT-X File	DT-X Ping
PARA0001	00:00	20210812_100542.rptx	2010
PARA0001	02:50	20210812_100542.rptx	2880
PARA0001	05:52	20210812_100542.rptx	3790
PARA0002	00:00	20210812_100542.rptx	3790
PARA0002	02:40	20210812_102042.rptx	4640
PARA0003	00:40	20210812_102042.rptx	5880
PARA0003	04:10	20210812_102042.rptx	6890
PARA0004	05:50	20210812_103542.rptx	9190
PARA0005	00:00	20210812_103542.rptx	9190
PARA0006	00:00	20210812_103542.rptx	11070
PARA0006	05:17	20210812_103542.rptx	12670
PARA0008	00:40	20210812_105042.rptx	15030
PARA0008	05:47	20210812_105042.rptx	16510
PARA0009	00:00	20210812_105042.rptx	16510
PARA0009	05:00	20210812_110542.rptx	18050
PARA0009	05:34	20210812_110542.rptx	18240
PARA0010	03:40	20210812_110542.rptx	19470
PARA0011	02:53	20210812_110542.rptx	21060
PARA0012	01:44	20210812_112042.rptx	22530
PARA0014	00:00	20210812_112042.rptx	24120
PARA0015	00:00	20210812_112042.rptx	25580

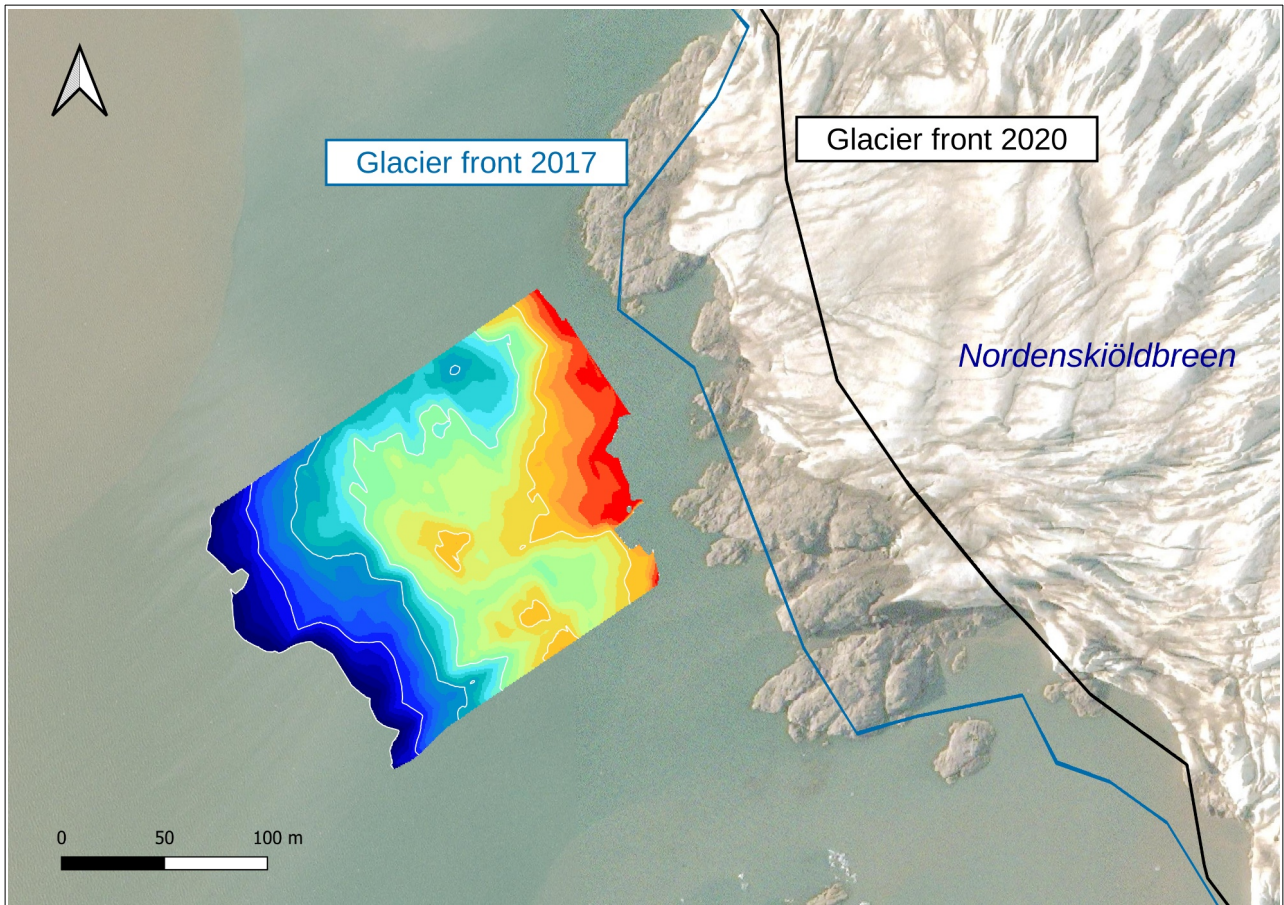


**Figure 34:** Glacier fronts in 2020 and 2017 at the glacier station (GLA) in front of Nordenskiöldbreen. Central coordinates of glacier station: 78.667902°N, 16.928750°E. Glacier front data: Norwegian Polar Institute's geographical map services. Basemap data: Esri, HERE, Garmin, METI/NASA, USGS